Investigating Patterns of Growth and Development in Subadults from the 10th-13th Century Cemetery of St. Étienne de Toulouse, France

Investigating Patterns of Growth and Development in Subadults from the 10th-13th Century Cemetery of St. Étienne de Toulouse, France

By: Hayley Welsh, B.A. Hon.

A Thesis Submitted to the School of Graduate Studies in Partial Fulfillment of the Requirements for the Degree Master of Arts

McMaster University MASTER OF ARTS (2021), Hamilton, Ontario (Anthropology)

TITLE: Investigating Patterns of Growth and Development in Subadults from the 10th-13th Century Cemetery of St. Étienne de Toulouse, France

AUTHOR: Hayley Welsh, B.A. Hon.

SUPERVISOR: Dr. Megan Brickley

NUMBER OF PAGES: 177

ABSTRACT

Growth and growth disruption are highly influenced by environmental factors such as nutritional intake, disease, and activity level. The purpose of this thesis is to investigate growth disruption in a medieval French subadult collection using femoral growth data as well as to examine developmental changes in midshaft geometry and cortical porosity. The femora of 94 subadults (fetal-12.49 years of age) from the 10th-13th century cemetery of Toulouse, France, were analyzed using macroscopic, radiographic, and microscopic techniques. Individuals were examined for growth disruption using endochondral and appositional growth, body mass estimates, cortical thickness, cortical pore volume, and Harris line data. Additionally, femoral cross-sectional geometry was used to examine ontogenetic changes in midshaft shape. Significant growth deficits were observed in the youngest individuals of this sample, especially in children 2.0-3.99 years of age. The prevalence of disrupted growth in the youngest individuals of this sample suggests that many children were likely born to malnourished mothers and provided nutritionally inadequate complementary foods during early development. These growth deficits, however, were largely ameliorated in older children and adolescents, indicating an improvement in nutrition and disease load. Ontogenetic changes in femoral midshaft geometry follow that of previous research, with young children (<4 years of age) having a more mediolaterally reinforced midshaft shape, indicative of an immature waddling gait. Increased midshaft porosity was experienced almost exclusively by infants and young children 0.5-1.49 years of age and was observed to be largely the result of trabecularized bone at the endosteal surface. The increased porosity likely results from the reorganization of bone stimulated by the onset of weight-bearing activity and increased growth velocity. This thesis contributes to the bioarchaeological literature by providing insight into the growth and development of children from medieval Toulouse and evidence of transient periods of increased cortical porosity during infancy.

ACKNOWLEDGMENTS

First and foremost I would like to thank my Master's thesis Supervisor Dr. Megan Brickley for her guidance and patience throughout this process. Due to COVID-19, the focus of this thesis changed numerous times, but I truly appreciate that Dr. Brickley always had a new plan of action ready. Her reassurance and endless determination meant that I never felt hopeless or incapable of completing my thesis on time. I would also like to thank Bonnie Kahlon for teaching me how to use the equipment necessary for completing my research; her knowledge has been invaluable. I am also grateful to my committee member, Dr. Tina Moffat, and third reader, Dr. Tracy Prowse, for providing their input on this thesis.

Thanks and gratitude are extended to everyone in the department of Anthropology at McMaster, all of whom made me feel welcome and accepted from my first day onward. I would also like to thank Dr. Christopher Ruff and Karen Swan for providing data used in this thesis. Additionally, thanks to Michal Kulus for providing me with his Harris line aging tool. Furthermore, I appreciate the generous funding I received from the Harry Lyman Hooker Sr. Fellowship and the Social Science and Humanities Research Council (SSHRC).

I would like to thank my fiancé, Zuber Ahmed, for supporting me throughout this process. He has been there for my highs and lows and yet still proposed to me. Finally, I would also like to thank my friends and family for their assistance, reassurance, and positive energy. I would especially like to thank my step dad Dr. Henry Vandelinde for reading over drafts of my work throughout this degree. A special thank you also needs to go to Mady Lamer who has supported and encouraged me throughout my time at McMaster and who kept me sane last summer with pizza dates at Bayfront Park.

TABLE OF CONTENTS

LIST OF FIGURES

Chapter 3 – Materials & Methods

Chapter 4 – Results

Chapter 5 – Discussion

LIST OF TABLES

Chapter 2 – Background

Chapter 3 – Materials & Methods

Chapter 4 – Results

LIST OF EQUATIONS

Chapter 3 – Materials & Methods

DECLARATION OF ACADEMIC ACHIEVEMENT

The research contained in this thesis dissertation was completed by Hayley Welsh under the supervision of Dr. Megan Brickley and Dr. Tina Moffat. Research questions and methodology were developed in consultation with Dr. Brickley and Dr. Moffat. Permission to access the skeletal collection was provided by Patrice Courtaud, *Research ingenior CNRS* at PACEA (from Prehistory to Today: Culture, Environment, and Anthropology), University of Bordeaux. Data collection and analysis was conducted by Hayley Welsh, and diaphyseal measurements and skeletal aging was conducted by Dr. Shelley Saunders' research team. Funding for this project was provided by the Harry Lyman Hooker Sr. Fellowship and the Social Science and Humanities Research Council (SSHRC).

Chapter 1: Introduction

1.1 Introduction

Growth and growth disruption can be influenced by genetics as well as environmental factors such as nutrition, illness, and physical activity (Mays et al., 2009; Ruff et al., 2013). When considering growth disruption in the past, human skeletal remains are an important primary source of evidence, especially when historical sources are unavailable; as the skeleton can embody an individuals' lived environment and culturally constructed experiences (Gowland, 2015; Zuckerman et al., 2014). The degree of growth disruption can therefore act as a proxy for environmental conditions experienced by past populations (Temple, 2008). The current thesis looks to evaluate the growth and development of a sample of medieval subadults from the South of France. The study sample comprises subadult femora from the 10th to 13th century cemetery of St. Étienne de Toulouse, France. One-hundred and fifteen subadults from fetal age to 12.49 years were assessed to determine if they could be used for this study. Of the 115 individuals assessed, 94 subadults could provide the necessary data. Femoral growth and body size were evaluated using macroscopic, radiographic, and microscopic techniques.

The under-representation of children in historical literature and archaeological research has left a gap in our understanding of children in past populations (Kamp, 2015; Lewis, 2007; Orme, 2009). The osteological collection housed at McMaster provides material to directly assess aspects of growth and development from individuals who lived in medieval Toulouse, France. During the period in which the individuals analyzed in the current research would have lived, France was engaging in numerous wars, such as the

crusades, and suffered from numerous famines and disease epidemics (Graves, 1917; Russel & Russel, 2000; Slavin, 2010; Trachant, 2012; Walford, 1878). Famines in particular have complex sociopolitical, ecological, and economic origins and may refer to a variety of situations including mass starvation, nutritional stress, food shortages, and ecological disasters, all of which may increase the risk of malnutrition and disease (Horocholyn & Brickley, 2017). Analyzing the subadult skeletal remains from the St. Étienne cemetery, therefore, has the potential to provide insight into how sociopolitical manifestations of war, malnutrition, and disease may have affected childhood growth and development in medieval Toulouse. Additionally, we may consider how their environmental conditions might have contributed to their early deaths.

Indicators of growth disruption such as long bone growth stunting, body mass, and Harris lines are commonly used in both contemporary and archaeological studies (e.g Dittmann & Grupe, 2000; Dobrova-Krol et al., 2008; Gooderham et al., 2019; Ives & Humphrey, 2017; Mays et al., 2009; McEwan et al., 2005; Spiller et al., 2020). This thesis will use the presence of growth stunting, Harris lines, body mass estimates, cortical thinning, and relative pore volume to aid in understanding the cultural and societal conditions in which children from 10^{th}-13^{th} century Toulouse lived. The indicators of growth disruption analysed, supported by available historical and archaeological data, are expected to provide evidence for nutritional and/or disease stress within the subadult population. Aging the observed Harris lines can provide timings for when periods of growth cessation and resumption took place for each individual as well as establish common patterns of growth stunting within the population. However, the relationship

between indicators of growth disruption, such as linear growth stunting and Harris lines, has been debated as the results of bioarchaeological and contemporary studies have been inconsistent (Blanco et al., 1974; Geber, 2014; Mays, 1995). Ontogenetic cross-sectional changes to long bones, such as the femur, can also provide information regarding the locomotor development and behaviour of subadults in the past, and exploring the mechanisms contributing to increased cortical porosity may aid in understanding transient periods of skeletal fragility (Cowgill & Johnson, 2018; Cowgill et al., 2010; Gosman et al., 2013; Swan et al., 2020). Cortical pore volume has only recently been quantified in infants (i.e Robbins Schug & Goldman, 2014). The current work therefore contributes to the literature by examining whether cortical porosity is an acceptable measure of infant and childhood stress using a larger sample population than previously published research. When interpreting the results of this study, an emphasis will be placed on the complex relationship between mothers and their offspring, the mother-infant nexus, and how this connection relates to growth disruption in infants and young children.

The five key aims of this thesis are to: (1) Identify growth disruption in the St. Étienne subadult sample using endochondral and appositional growth as well as body mass and relative cortical bone; (2) Examine ontogenetic changes in femoral cross-sectional geometry; (3) Determine the frequency of Harris line formation in this sample and the relationship between Harris lines and skeletal development; (4) Explore the etiology of cortical porosity among infants and children; (5) Use the results to discuss how this study contributes to the understanding of subadult health at this site as well as

consider how the sociocultural and environmental contexts may have affected subadult health.

1.2 Thesis Organization

This thesis is organized into six chapters with data gathered contained in Appendices I-VI. Chapter two contains the background information relevant to this thesis including information regarding the historical context of medieval France, femoral growth variables, cross-sectional geometry, and the mother-infant nexus. The third chapter presents the materials and methodology used for data collection, as well as statistical analyses used to determine significance. The results for linear growth, body mass, cross-sectional geometry, Harris lines, cortical porosity, and statistical analyses can be found in chapter four. Chapter five sets out and interprets the results based on previous historical, clinical, and bioarchaeological research. The final chapter, chapter six, provides a summary of the findings for this study and sets out the overall conclusions.

Chapter 2: Background

2.1 Historical Context of Medieval France and Medieval Toulouse

2.1.1 Political History

The sample examined in this thesis was excavated from the St. Étienne cemetery in Toulouse, France, which was estimated to have been in use between approximately the 10th and 13th century CE (De Filippo et al., 1988 in Kacki, 2016; Grolleau-Raoux et al., 1997; Murail, 1991). During the time period in which the cemetery was in use France was suffering from political unrest, as the country was involved in numerous wars, such as the Holy Crusades, and existing Feudal structures provided an institutional basis for the taxation of French subjects (Blaydes & Paik, 2016). The Crusades stimulated trade and economic growth across Western Europe, including France (Blaydes & Paik, 2016). Prior to the Crusades, feudal France had been cut off from Mediterranean trade (Thompson, 1959, p. 306). Collection of property and income tax also became prominent during this time period, especially during the 12th century, where funds from taxation were used to support the numerous Crusades (Blaydes & Paik, 2016). King Philip II of France even attempted to collect a steep levy of 10% on all income and nonessential goods, known as the Saladin Tithe, to support the reconquest of Jerusalem in the 12th century; however, this tax was abandoned due to protests from the people. Though the Crusades stimulated trade and urbanization within France (Blaydes & Paik, 2016; Kibler et al., 1995), the ongoing crusades also contributed to the suffering of the French people. Political unrest and war often result in resource insecurity and food shortages (Horocholyn & Brickley, 2017). This is evident in medieval France, as the country suffered from numerous insults

of famine and disease during the Crusades, with approximately 100,000 French men, women, and children perishing due to the plague and famine during the first Crusade of the 11th century alone (Graves, 1917).

While most of France, especially northern regions, was still under feudal Frankish rule, the County of Toulouse itself was an independent territory of Southern France from the 9th to 13th century (Duby, 1991, p. 26-27). Additionally, during the 12th century the inhabitants of the City and Bourg of Toulouse worked to limit the political power of their Count, by limiting his activities and forming a municipal governing council with 24 members (Chisholm, 1911; Jenkins, 2008). Throughout the 11th and 12th centuries multiple Toulousian Counts participated in the ongoing Crusades, during this time Toulousians also engaged in many territorial battles, as they frequently suffered invasions from neighboring regions (Benjamin, 2017; Chisholm, 1911; Mundy, 1954). As a result of the Toulousian Counts often taking part in the Crusades, the town was left to largely rely on its own resources and initiatives for many of these invasions (Mundy, 1954). While engaging in multiple political and physical battles, Toulouse also grew economically. Stimulated by the ongoing Crusades, Toulouse became the largest urban nucleus in Southern France during the late 11th and early 12th century, as it was strategically positioned along trade routes (Mundy, 1954). Therefore, individuals buried at St. Étienne would have lived during a time of both political and economic developments in France and more specifically political and economic developments in the County of Toulouse.

2.1.2 Agricultural Staples & Diet

Few sources detail the diet of individuals who lived in medieval Toulouse; however, archaeological and historical data provide evidence for agricultural staples in other parts of medieval Mediterranean France. Ruas (2005) examined archaeobotanical remains from medieval sites in the Mediterranean area of Southern France. The study yielded a variety of species of cereal grains and pulses such as wheat, barley, beans, peas, lentils, and chickpeas (Ruas, 2005). Additionally, the study found evidence of fruit species such as figs, olives, peaches, and grapes (Ruas, 2005). Other archaeobotanical studies examining sites in Southern France (Pyrénées-Orientales) have similarly found cereals, pulses, and fruits (Ros & Ruas, 2013). These results are supported by medieval and historical texts which indicate the cultivation of cereal crops such as wheat and barley in coastal areas (Bourin-Derruau, 1987 in Ruas, 2005; Duby & Mandrou, 1964; Durand, 1998 in Ruas, 2005). Historical texts also suggest that cereal grains were usually consumed as gruel and formed the basis of the diet at the time (Duby & Mandrou, 1964, p. 7). Historical information also suggests that children in medieval France were often breastfed by their mother or wet-nurse and fed gruel until approximately 2 years of age, after which they were weaned and fed an adult diet (Kibler et al., 1995, p. 409). The results of the archaeobotanical studies as well as the historical literature suggests that cereal grains formed a major part of the medieval French diet. Having a diet primarily focussed on cereal based food and pulses can lead to iron and zinc deficiencies due to high phytate levels, which can interfere with the bioavailability and absorption of these nutrients (Brnić et al., 2017; Hurrell, 2003; Schlemmer et al., 2009; Thacher et al., 2009).

Therefore, micronutrient deficiencies may have been prevalent in the medieval French population due to high consumption of cereals and pulses.

2.2 The Archaeological Child

2.2.1 Importance of Children in Bioarchaeology

The recent focus on children within anthropology and archaeology developed in the 1990s after the conception of feminist and gender archaeology, which sought to provide voices to individuals who had been largely excluded from narratives of the past (Gowland & Halcrow, 2020, p. 1). As previously, the focus of historians and bioarchaeologists had mainly been on the lives of adult men in the past (Lillehammer, 2015; Orme, 2009).

Children can be studied in terms of material culture and contribution of work, as researchers have attempted to identify young artists by examining finger prints on artifacts (Kamp, 2001). Children can also be studied in terms of health and disease through the study of their osteological remains, which will be the main focus of this thesis. Previously, subadult skeletal remains were thought to succumb to the burial environment and that because of this their sample sizes would be too small to reach statistical significance (Lewis, 2007, p. 20). Therefore, the perceived lack of subadults in the archaeological record is often interpreted as the result of preservation bias. However, recent improvements in excavation techniques, such as the routine sieving of grave soils, have seen excavations yielding larger numbers of subadult remains (Lewis, 2007; Mays, 2013, p. 5). Therefore, the common perception that infant and child remains do not survive in the archaeological record is unfounded (Lewis, 2007, p. 37).

Though infant remains can, and do, survive in the archaeological record, infants and children younger than two years of age are often excluded from paleopathological studies due to the difficulty in differentiating normal healthy new bone growth from pathological new bone formation (Hodson & Gowland, 2020; Lewis, 2017). When subadult lesions are studied in bioarchaeology and paleopathology, the focus often falls to periostitis, porotic hyperostosis, linear enamel hypoplasias (LEH), and stunted linear growth (Mays, 2013; Mays et al., 2017). Metabolic diseases stemming from nutrient deficiencies in childhood, such as rickets from vitamin D deficiency, have also been a recent focus of bioarchaeological studies (Mays, 2018a; Mays & Brickley, 2018; Peacock et al., 2019; Snoddy et al., 2016). Understanding nutrient deficiencies, such as vitamin D deficiency, in children can aid in understanding cultural factors, such as clothing choices, time spent outdoors, and infant and child feeding behaviours (Brickley et al., 2014). However, because it may be difficult to accurately identify pathological lesions in children, other indicators of growth and health status can be employed. Diaphyseal linear and appositional growth, as examined in the current thesis, are two useful proxies for growth disruption. Infants and young children should not be excluded from linear and appositional growth studies, as infants can provide important information regarding environmental stress and growth disruption (Halcrow, 2020) and represent one of the most vulnerable groups in society (Mays, 2013).

2.2.2 The Medieval French Child

The French historian Philippe Ariès has been credited for pioneering the historical study of childhood, with the French edition of his work *Centuries of Childhood* published

in 1960 (Ariès, 1962; Lewis, 2007; Turner, 1988). In his book, Ariès claims that in the medieval period childhood as a concept did not exist as it does today, as there was no separate language used to distinguish individuals at different stages of life (Ariès, 1962, p. 128). The author also makes the claim that once children could live without the "solicitude" of their mothers, they belonged to adult society (Ariès, 1962, p. 128). Life for medieval children of France was difficult as approximately 33% of children died before the age of five (Kibler et al., 1995, p. 409). Ariès interpreted high infant mortality as a lack of warmth or disconnect between parents and children (Ariès, 1962). However, since its publication, historians and archaeologists have questioned the validity of Ariès' claims and revised our understanding of childhood in the past (Lewis, 2007). Riché and Alexandre-Bidon combined pictorial and archaeological evidence to demonstrate that children did play with toys, dolls, and games (Riché & Alexandre-Bidon, 1994 in Hanawalt, 2002). Additionally, clothing styles could be used to differentiate life stages, as infants were known to be swaddled or naked, children often wore long loose gowns, and the transition to wearing adult style clothing usually did not occur until individuals entered adolescence (Hanawalt, 2002). The lack of distinguishing language has also be contended, as Lett (1997 in Hanawalt, 2002) analyzed medieval stories which clearly differentiate children based on age, with the term *enfant* used to refer to girls aged 0-7 and boys aged 0-12. Therefore, there is clearly more nuance to the experiences of children and the relationships between children and adults in medieval France than was previously described by Ariès.

2.3 Skeletal Growth

2.3.1 Endochondral Growth

Endochondral growth occurs at the growth plates of long bones. This process is responsible for the longitudinal growth of the skeleton. The growth plate can be divided into different developmental zones, which include: the resting zone, proliferative zone, hypertrophic zone, and ossification zone (Lampl & Schoen, 2017; Rolian, 2020; Scheuer & Black, 2004). The *resting zone* contains newly differentiated chondrocytes and can be found closest to the epiphysis (Lampl & Schoen, 2017; Rolian, 2020). In this zone the chondrocytes are small and randomly distributed (Scheuer & Black, 2004). Subjacent to the *resting zone* is the *proliferative zone* where flat proliferating chondrocytes stack in parallel longitudinal rows (Rolian, 2020; Scheuer & Black, 2004). In this zone the chondrocytes become mitotically active and increase in size as they accumulate glycogen (Lampl & Schoen, 2017; Scheuer & Black, 2004). In the *hypertrophic zone* chondrocytes begin to hypertrophy (enlarge) as they prepare to be replaced by bone (Scheuer & Black, 2004). Some of the chondrocytes transform into an osteoblast phenotype (Rolian, 2020; Scheuer & Black, 2004). In the last zone, the *ossification zone*, osteoblasts mineralize the cartilage and bone is reorganized through both osteoblastic and osteoclastic activity (Lampl & Schoen, 2017; Scheuer & Black, 2004). This process ceases when the growth plates senesce as the diaphysis and the epiphyses fuse and final adult height is attained (Lampl & Schohen, 2017; Rolian, 2020).

While long bones generally follow a prescribed growth trajectory, variation and delays in growth can occur. Variation in growth rates can be influenced by age, sex,

genetics, and environment (Bogin, 2020). Delays in longitudinal growth can occur due to external environmental influences on growth such as malnutrition and disease, which can severely impact an individual's ability to attain their predetermined adult stature. These delays can be especially apparent in fast growing bones such as the femur (Cardoso & Magalhães, 2011; Smith & Buschang, 2004). The distal end of the femur can be especially sensitive to growth disruption as approximately 70% of endochondral growth occurs in the distal epiphysis of this element (Scheuer & Black, 2004). Growth disruption and stunting occurs when skeletal growth halts in order to redirect energy to other areas of the body (Leonard et al., 2012, p. 410), such as the brain which utilizes approximately 87% of the resting metabolic rate in infants (Bogin, 2020; Said-Mohamed et al., 2018). Another example of energy redirection resulting in stunting is the body's response to infection (both with and without the association to malnutrition) (Assis et al., 2004; Checkley et al., 1998; Millward, 2017; Shang et al., 2010). Infections can lead to growth delays and stunting, as energy is redirected from skeletal growth in order to heighten immune response and function (Miller, 2020). Therefore, impaired endochondral growth can provide insights into childhood stress in the past.

2.3.2 Appositional Growth and Cortical Thickness

Appositional growth occurs when bone is deposited underneath the periosteum (Mays et al., 2009; Mays, 2018b). This type of growth occurs in tandem with endochondral growth, however, while endochondral increases bone length, appositional growth increases bone width. Appositional growth has been thought to be partially dependent on mechanical stimuli, while endosteal apposition and cortical thickness are

suggested to be more sensitive to nutritional and hormonal outcomes (Mays et al., 2009; Ruff et al., 1994; Ruff et al., 2013).

Cortical thickness has been shown to be a skeletal indicator of nutritional stress and growth disruption in both living and past populations (Eleazer & Jankauskas, 2016; Garn, 1964; Hummert, 1983; Huss-Ashmore et al., 1982; Mays, 2001; Mays, 2009; Ruff et al., 2013; van Gerven et al., 1985). The metacarpals are often used to measure cortical thickness due to minimal morphological variability (Garn et al., 1969; Rewekant, 2001), however other long bones such as the femur and tibia can also be used (Mays et al., 2009). Malnutrition related cortical thinning is marked by an increase in the dimensions of the medullary cavity relative to overall bone dimensions, leading to a decrease in cortical area and thinning appearance (Ives & Brickley, 2004; Ruff et al., 2013; Thompson, 1980). Interestingly, in cases where cortical thickness has been found to be reduced, appositional growth remains relatively stable (Garn et al., 1964; Garn et al., 1969; Mays et al., 2009). Therefore, while appositional growth is thought to be stable throughout life, even during periods of stress, cortical thickness is more strongly influenced by stress events and environmental variables (Mays, 1999; Mays et al., 2009; Ruff et al., 2013). In certain populations, however, appositional growth has been shown to be restricted, resulting in small-for-age total areas and bone widths (Himes et al., 1975; Gooderham et al., 2019). Restricted appositional growth has been interpreted as resulting from significant disruption to the normal remodelling process (Gooderham et al., 2019), potentially caused by malnutrition (Himes et al., 1975). While nutritional stress has been

associated with cortical thickness it is important to note that genetics and activity level may also influence the accrual of cortical bone (Hatch et al., 1983; Ruff, 1994).

While appositional growth increases linearly throughout development, cortical thickness begins to decline for the first few months after birth (van Gerven et al., 1985) and then increases in thickness until peak bone mass is reached in adulthood (Rauch & Schoenau, 2001a). The loss of cortical bone observed during infancy is thought to reflect the redistribution of endosteal bone tissue to the periosteal surface (Rauch & Schoenau, 2001a; Swan et al., 2020). Hormonal changes accompanied by the onset of puberty are related to increased endosteal deposition of cortical bone (Ruff, 1994; Wang et al., 2006). Therefore, cortical thinning observed during mid to late childhood or adolescence likely results from growth disruption. However, we cannot discount the possibility that a similar redistribution of bone may also occur during the adolescent growth spurt (Hummert, 1983; van Gerven et al., 1985; Wang et al., 2010). Adult cortical thickness can also serve as a proxy for earlier growth disruptions as deficiencies observed in peak cortical bone may indicate less than favourable conditions during skeletal growth and development (Mays, 2001).

2.4 Body Mass

Body mass can be an important indicator of health status and is commonly used for assessing health in modern subadult populations (Abarca-Gómez et al., 2017). However, methods for estimating body mass in subadult skeletal remains have only recently been established. Ruff (2007) and Robbins et al. (2010) are the first researchers to identify key measurements and formulae for estimating subadult body mass using the

femur. The three main femoral measurements identified for body mass estimations include: femoral metaphyseal breadth, femoral head breadth, and polar second moments of area (*J*) calculated using midshaft cross-sectional geometry (Robbins et al., 2010; Ruff, 2007). The adoption of these methods broaden the potential insights of bioarchaeological subadult growth and development studies, as previously, skeletal measurements such as long bone lengths were the only methods for assessing subadult body size.

When considering the implications of subadult body mass it is usually in terms of weight-for-age and/or weight-for-height (body mass index). However, body mass index (BMI) does not take into account differences in body proportions or body composition (Bogin, 2020). Additionally, body mass and fat distribution can vary based on population (genetics) and climate (Hadley & Hruschka, 2014) and may be more clearly exhibited during adolescence (Ruff et al., 2013). Therefore, population-specific growth curves are ideal when considering the health implications of body mass in both present and past populations.

2.5 Effect of Locomotor Stages on Skeletal Ontogeny

Bone size and shape change drastically during ontogeny through a process of modelling and remodelling based on mechanical, hormonal, nutritional, and phylogenetic inputs (Pearson & Lieberman, 2004; Ruff et al., 1994; Wallace et al., 2012). Bone modeling and remodeling, characterized by bone deposition and resorption (Enlow, 1963; Enlow, 1976; Frost, 1973), are essential for skeletal growth and changes to bone shape. This process begins in utero and continues at varying rates throughout the life course (Briana et al., 2008). Through using the Beam Model, which considers long bone

diaphyses as engineering beams, researchers have been able to interpret biomechanical effects of locomotor behaviour on cross-sectional geometry (Ruff, 2019; Swan et al., 2020). This model allows researchers to understand the strength and rigidity of bone based on the volume and distribution of cortical bone (Ruff, 2019).

Midshaft shape has previously been used within bioarchaeology to infer mobility trends in past adult populations. Increased antero-posterior (AP) reinforcement and loading is considered evidence of increased mobility (Cameron & Stock, 2018; Pomeroy, 2013; Shaw & Stock, 2009; Stock & Macintosh, 2016). Physiological differences, such as bi-iliac breadth have also been demonstrated to affect femoral midshaft shape in adults (Shaw & Stock, 2011). While few studies have documented changes in subadult femoral midshaft shape (See Table 2.1), similar ontogenetic transformations of the midshaft resulting from changes in locomotor behaviour have been noted. These studies have found that femoral midshaft shifts from a more mediolaterally (ML) reinforced shape during infancy and early childhood to a more AP reinforced shape during later childhood and adolescence due to transitions in locomotor behaviour (Cowgill et al., 2010; Swan et al., 2020). Studies have also examined how the relative humeral and femoral bending strength are related during the mechanical transition from crawling to walking (Cowgill & Johnston 2018).

Table 2. 1 *Studies Examining Ontogenetic Changes in the Femoral Midshaft Through July 2020*

Citation	Sample size	Age Range Examined	Imaging Modality Used
Swan et al. (2020)	110	0.0-8.5 years of age	Micro-CT
Eleazer & Jankauskas, (2016)	30	1.0-6.99 years of age	Light Microscopy
Robbins Schug & Goldman (2014)	11	2.0-13.0 months of age	Light Microscopy
Gosman et al. (2013)	46	0.0-17.9 years of age	X-rat Computed Tomography
Cowgill et al. (2010)	521	0.0-17.9 years of age	X-ray
Goldman et al. (2009)	14	2.0-19.0 years of age	Light Microscopy
Ruff (2003)	20	0.5-17.0 years of age	X-ray
Sumner & Andriacchi, (1996)	83	0.0-29.0	X-ray Computed Tomography
Trinkaus & Ruff (1996)	1	6.0 years of age	X-ray
Ruff et al. (1994)	46	14.0-39.0 years of age	X-ray

Geometric changes at the midshaft have been studied in children using both destructive methods such as light microscopy (Eleazer & Jankauskas, 2016; Goldman et al., 2009; Robbins Schug & Goldman, 2014) as well as non-destructive methods such as x-ray (Cowgill et al., 2010), x-ray computed tomography (CT) (Gosman et al., 2013), and micro-CT (Swan et al., 2020). While studies of the midshaft are most common, others have taken to examining multiple areas of the shaft in order to provide a whole-bone perspective of ontogenetic changes (Gosman et al., 2013; Swan et al., 2020). These types of ontogenetic studies are important for understanding what is considered *normal* subadult bone, a crucial step for recognizing how diseased bone differs from what is expected (Goldman et al., 2009). Additionally, understanding the ontogenetic changes of the long bones during childhood can aid in assessing locomotor behaviour as well as potential health risks in adulthood, as based on the current evidence, bone acquired during early childhood and adolescence affect bone strength later in life (Cooper et al., 2006a; Oliver et al., 2007).

2.6 Porosity

2.6.1 Biochemical Mechanisms

Cortical porosity consists of a network of vascular canals that supply living bone with blood and nutrients (Cooper et al., 2016). These canals can either be *primary* canals which are formed during the initial formation of bone or they are the product of bone turnover (remodelling) and are referred to as *secondary* canals (Pratt et al., 2018). Secondary canals are associated with layers of bone surrounding them and are also referred to as secondary osteons or Haversian systems (Cooper et al., 2016). The cells responsible for bone remodelling are collectively referred to as the Basic Multicellular Unit (BMU) (Cooper et al., 2006b). The BMU consists of osteoclasts, osteoblasts, blood supply, and connective tissue (Jilka, 2003; Sims & Martin, 2014). Bone remodelling is a healthy process that occurs to remove and replace old or damaged bone (Sims & Martin, 2014). The remodelling of bone is often initiated by osteoclastic cutting cones, which create tunnel-like resorption spaces that are then filled by osteoblastic closing cones (Cooper et al., 2006b; Cooper et al., 2016). The osteoclastic and osteoblastic activity must be balanced in order to properly replace bone that has been removed; the co-ordination and relationship between these two processes is referred to as *coupling* (Sims & Martin, 2014). An average remodelling cycle takes approximately 6 months to complete (Recker & Moreira, 2019)

2.6.2 Causes and Consequences of Increased Cortical Porosity

Uncoupling of osteoclastic and osteoblastic activity can lead to increased cortical porosity. This occurs when more bone is removed than is replaced by the BMU (Zebaze

et al., 2010). Increased cortical porosity can be the result of increased vascular canal size, an increase in the number of canals, or a combination of both of these processes (Cooper et al., 2016). The primary cause of increased cortical porosity is advancing age (Andreasen et al., 2018; Zebaze et al., 2010). Although transient periods of increased cortical porosity can occur during periods of rapid growth, such as adolescence (Wang et al., 2010), it is in individuals over the age of 50 that largely demonstrate decreased cortical bone and increased cortical porosity related to osteoporosis (Farr & Khosla, 2015). Increased cortical porosity is especially pronounced in peri- and post-menopausal women (Bjørnerem et al., 2018). Other factors that have also been demonstrated to increase cortical porosity include height (Bjørnerem et al., 2013) as well as metabolic diseases such as type two diabetes (Paccou et al., 2016; Wölfel et al., 2020), vitamin D deficiency (Sundh et al., 2016), and hyperparathyroidism (Osima et al., 2018; Vu et al., 2013). It has also been suggested that small stature and low BMI-for-age may lead to increased cortical porosity and skeletal emaciation in infants (Robbins Schug & Goldman, 2014).

The main consequence of increased cortical porosity is the heightened risk of skeletal fragility and fracture due to bone loss and structural decay (Cooper et al., 2016). Approximately 80% of non-vertebral fractures that arise in old age occur in skeletal areas primarily composed of cortical bone and are the result of increased cortical porosity (Cooper et al., 2016; Zebaze et al., 2010). Minimizing fracture risk is important as fractures can increase morbidity and mortality, especially in older adults (Borah et al., 2009; Brickley et al., 2020a; Cooper et al., 2006b).

2.7 Harris Lines

2.7.1 History of the Investigation of Harris Lines

The presence of transverse lines in the sub-epiphyseal region of long bones, also commonly known as Harris lines (HLs), growth recovery lines, and growth arrest lines (Zapala et al., 2016), were first discovered in dry bone by Wegner in 1874 (Wegner, 1874 in Harris, 1931). Since their discovery, numerous researchers have had their own ideas of what the etiology of these transverse striations may be. Fromme (1922 in Harris, 1931) described the HLs as remnants of calcium bands that are pushed into the diaphysis during the healing of rickets, a process that he compared to annual tree rings. Harris (1931) was the first to describe the transverse striations as general indicators of stress, referring to them as "tombstones" to the past illnesses, and is the researcher after which they are now named (Harris, 1931; Hughes et al., 1996, p. 115). Since their discovery many researchers have examined HLs experimentally, clinically, and archaeologically, in an attempt to determine their histological process of formation and etiology.

2.7.2 Mechanism of Line Formation and Detection

While not visible macroscopically, HLs are visible through radiography, electron microscopy, histology, and magnetic resonance imaging (Alfonso-Durruty, 2011; Miszkiewicz, 2015). Radiography is the most common method of detecting HLs, which appear on radiographs as radio-opaque lines (Mays, 1995). The radio-opaque line is a structure of dense horizontally-oriented trabeculae (Mays, 1995). HLs can also be microstructurally distinguished from normal bone, as histological sections of HLs display

a non-lamellar structure, irregularly distributed tubular structures, and are devoid of osteocyte lacunae (Miszkiewicz, 2015).

HLs are generally the most visible at the ends of bones which grow most rapidly, such as anterior rib ends, distal femora, as well as proximal and distal tibiae and fibulae (Mays, 1985; Mays, 1995; Piontek et al., 2001). HLs can appear from birth until approximately 15-16 years of age, when the epiphyseal fusion of long bones is complete (Alfonso et al., 2005). Lines are gradually removed by bone modeling and remodeling in childhood as well as bone remodeling in adulthood (Mays, 1995). It has also been suggested that the rate of HL resorption is also likely affected by the thickness of the HL (Piontek et al., 2001).

The uncoupling of osteoblastic and chondroblastic activity is what results in the HL, where osteoblastic activity continues and chondroblastic activity slows or halts (Alfonso et al., 2005; Fiscella et al., 2008). The function of the cartilage cells is to provide a template for the osteoblasts to deposit bone material (Mays, 1985; See Section 2.3.1). After a period of growth arrest there is an initial thickening of the primary stratum and bone growth resumes when mature chondrocytes become available (Mays, 1985). The thickened stratum is what produces the radio-opaque lines (Mays, 1985). Therefore, there are two factors required for the formation of the HL, the first being the growth arrest and the second being the recovery (Park, 1964). The recovery factor is primarily responsible for giving the stratum its thickness, without it the stratum may never acquire the density required to appear as a linear opacity in x-ray film (Park, 1964).

2.7.3 Experimental and Clinical studies of Harris lines

In an effort to uncover the etiology of HLs many researchers have attempted to study them experimentally and clinically. Many of the HL experiments occurred during the 20th century using a wide range of animal specimens including: rabbits, pigs, and dogs (Mays, 1995). Asada (1924 in Harris, 1931) was the first to use experiments to reproduce transverse lines through starvation studies on rats and pigs. Asada believed that Harris lines were the result of a disturbance in the homeostasis between the proliferation of the cartilage and formation of osteoblasts, a process now confirmed by subsequent studies (See Section 2.7.2). Similarly, Park and Richter performed starvation experiments on rats (Park, 1964). The experimenters fed the rats single food diets; one diet consisted of glucose with the addition of a B1 vitamin and the second diet consisted of olive oil supplemented with vitamin A. The rats in both diet groups experienced a halt in linear bone growth after approximately 4-5 weeks (Park, 1964). During the starvation period, linear growth stopped and the epiphyseal cartilage was reduced to a thin plate, creating a stratum of bone (Park, 1964). Once the rats were placed on an *ad lib* stock diet their bone growth resumed and the stratum thickened, creating a radiographically visible line on their long bones (Park, 1964).

Clinical studies have demonstrated that Harris lines may result from a variety of disturbances in growth such as dietary deficiencies or illness (Harris, 1931; Lempicki et al., 2017), ethanol consumption (Gonzalez-Reimers et al., 2007), vaginal child birth (Teele et al., 1999), as well as physical child abuse and neglect (Spiller et al., 2020; Zapala et al., 2016). Harris (1931) documented a child who suffered three successive

episodes of acute illness and had corresponding transverse lines on the tibia. He documented several other cases of children experiencing acute bouts of disease or poisoning with corresponding transverse lines on their long bones. Harris (1931) also found that the rate at which an HL disappears (remodels) is proportional to the functional usage of the element displaying the HL, as elements experiencing continual stresses and strains remodel faster than more inactive elements (Harris, 1931). Therefore, there is a significant correlation between periods of malnutrition/infection and the formation of HLs but not necessarily a simple 1:1 association (Mays, 1985).

While illness and malnutrition related growth disruption are often considered for the etiology of HLs, their presence has also been found in children at high risk for physical child abuse and neglect. Zapala et al. (2016) found that Harris lines were more common (71%) in infants at high risk for physical abuse compared to (38%) infants at low risk for abuse. The authors interpret the higher prevalence of Harris lines in the high risk group as periodic episodes of growth delay resulting from the increased stress associated with child abuse. High risk infants also displayed the presence at a younger average age (5 months) when compared to low risk infants (6.3 months). Similar results were described by Spiller et al. (2020) who found that children in the neglect and abuse groups had nearly 2x more HLs compared to the low-risk groups (Spiller et al., 2020). Based on their results Spiller et al. (2020) suggest that, in the absence of a major illness or medical condition, the presence of ten or more HLs by approximately two years of age could be considered evidence for child abuse or neglect.

Therefore, both experimental and clinical studies have found that various forms of physiological stress may result in the halting of skeletal growth. When interpreting the etiology of archaeological cases of Harris lines, other types of evidence such as the presence of growth stunting, multiple abuse related fractures, and metabolic illness should be considered.

2.7.4 Bioarchaeology of Harris lines

HLs are prevalent in both adult and subadult archaeological collections (Ameen et al., 2005; Hughes et al., 1996; Geber, 2014; Mays, 1985; Mays, 1995; Nowak & Piontek, 2002; Papageorgopoulou et al., 2011; Piontek et al., 2001; Ribot & Roberts, 1996). Many bioarchaeological studies have interpreted the high prevalence of HLs as resulting from increased rates of environmental stress in the past (Dittmann & Grupe, 2000; Geber, 2014; Goodman & Clark, 1981; Mays, 1995); this interpretation has been supported by studies that have found the prevalence of HLs in archaeological populations to be higher than contemporary populations (Ameen et al., 2005). Studies that interpret HLs as resulting from environmental stress follow the traditional, pathological thesis for HL formation (Alfonso-Durruty, 2011). However, other studies have interpreted HLs as resulting from normal patterns of growth, which is considered the physiological thesis for HL formation (Alfonso-Durruty, 2011). These researchers interpret the formation of HLs as occurring due to accelerated growth, rather than result of pathology (Alfonso et al., 2005; Piontek et al., 2001).

Harris lines, which are commonly considered indicators of growth disruption and environmental stress, have been compared with other stress indicators such as linear

enamel hypoplasias (LEHs) and endochondral bone growth in bioarchaeological studies. When considering the HLs and LEHs the majority of studies have found little to no correlation between the two in terms of timing of formation (Alfonso et al., 2005; Clark, 1982; McHenry & Schulz, 1976; Papageorgopoulou et al., 2011; Ribot & Roberts, 1996). The lack of correlation between HLs and LEHs suggests that different physiological mechanisms influence their development or that the different tissues have different thresholds for line formation. When considering the relationship between HLs and endochondral growth, both Mays (1995) and Geber (2014) found individuals with the presence of HLs to be slightly shorter than individuals without HLs. However, both of these studies failed to find a statistically significant correlation between Harris lines and growth delay (Geber, 2014; Mays, 1995). One of the only studies to find an association between HLs and stature was a study of 1,412 living Guatemalan children (Blanco et al., 1974). Therefore, it is possible that difference in significance could be related the type of the population being studied (i.e living vs. archaeological); however, the relationship between HL formation and endochondral growth requires further research due to inconsistent findings.

2.8 Mother-Infant Nexus and Weaning Stress

When considering infants in any discipline it is important not to completely separate them from their mothers. The infant and mother are intertwined socially and physically (Gowland & Halcrow, 2020). As such, the health of infants can potentially inform anthropologist and archaeologists about the health and well-being of their mothers.

2.8.1 Intrauterine Environment

The intrauterine stage is a critical period for mammalian growth and development. Improper maternal nutrition can lead to altered placental nutrient availability and affect the fetal endocrine system leading to epigenetic changes, which can affect the offspring's subsequent growth and adult health (Cetin et al., 2013). Alterations in fetal nutrition and endocrine status can lead to permanent adaptations in fetal homeostatic mechanisms, known as fetal programming, that can produce long-term changes in physiology and lead to a higher susceptibility to metabolic diseases later in life (Barker et al., 2002; Bloomfield et al., 2003; Chadio et al., 2007; de Rooij et al., 2006; Gardner et al., 2006; Johnsen et al., 2013; Manuel-Apolinar et al., 2014; Vieau, 2011). Even minor dietary insufficiencies can cause adverse effects, especially during important stages of development (Lucassen et al., 2013). The first 1000 days of life (conception until approximately 2 years of age) is considered a critical period of developmental plasticity (Barker et al., 2002; Martorell, 2017; Said-Mohamed et al., 2018). While the examination of fetal development most often considers contemporary mother-infant pairs, fetal growth can also be examined in past communities through examining fetal and perinatal remains.

Over the last few decades, bioarchaeologists have become more interested in the infant remains and the information they can provide in regards to infant and maternal health. When considering the intrauterine environment, fetal and neonatal body size are often used as proxies. Adverse intrauterine environments relating to poor maternal health, genetics, and placental abnormalities can lead to intrauterine growth restriction (IUGR) and infants that are small-for-gestational age (SGA) (Sharma et al., 2016). This

designation is given to infants who fall below the 10th percentile for gestational age (Lausman et al., 2013; Wollman, 1998). Fetuses that are found in utero (still within the abdominal cavity of their mothers) are quite rare in the archaeological record, however, they provide direct evidence of fetal health in the past (Halcrow, 2020). Since in utero fetuses are rare, infants aged less that 37 weeks "gestation" are often considered fetal, regardless if they are found in utero or not (Halcrow et al., 2017; Halcrow, 2020, p.20). Additionally, fetal remains recovered during excavation often represent fetuses that died during the third trimester, as they are larger and more likely to preserve compared to less developed fetuses (Halcrow, 2020, p. 20). Fetal and neonatal remains demonstrating IUGR can provide important information regarding malnutrition and disease, as IUGR is associated with neonatal morbidity, metabolic disturbances, and mortality (Salam et al., 2014). While IUGR provides evidence for non-specific growth disruption, infants have also demonstrated evidence for specific diseases such as vitamin D deficiency and scurvy both in clinical and archaeological cases (Besbes et al., 2010; Brickley & Ives, 2006; Brickley et al., 2020a; Snoddy et al., 2017). Metabolic disease in infants suggests maternal micronutrient insufficiency during pregnancy and lactation. Through examining pre- and neonatal remains bioarchaeologists can more closely investigate maternal and infant health status in the past as well as interpret acute and chronic disease within a community or population.

2.8.2 Breastfeeding, Complementary Feeding, and Associated Stress

Breastmilk is an important resource during early development as it provides vital nutrients and immunity. While immunity provided by breastmilk if often described as

being solely passive, recent research has demonstrated the potential for collaborative immunity. Collaborative immunity is the retrograde flow of infant saliva into the mammary gland, which has been shown to increase immunological components in breastmilk, such as white blood cells, in response to infant specific infections (Moossavi et al., 2019; Riskin et al., 2012). Furthermore, studies have demonstrated that direct breastfeeding is more protective compared to indirect bottled fed breastmilk and formula feeding (Klopp et al., 2017). The immuno-protective factor of breastmilk is important during infancy as independent production of immunoglobulin A (IgA) in children is not thought to reach adult levels until approximately 4-6 years of age (Burgio et al., 1980; Weemaes et al., 2003). IgA is a predominant antibody type for secretory surfaces and the mucosal immune system, and can be found in the respiratory and gastrointestinal tracts, the middle ear, and colostrum (Kaur et al., 2012; Li et al., 2020). Therefore, the secretory IgA delivered through exclusive and complementary breastfeeding has been shown to be especially protective against infant diarrheal, respiratory, and ear infections (Bener et al., 2011; Fisk et al., 2011; Hajeebhoy et al., 2014; Hanson & Korotkova, 2002; Hanson et al., 2003; Hanson et al., 2009; Lamberti et al., 2011). Reduced incidence of morbidity and mortality have also been associated with exclusive breastfeeding for the first six months of life and complementary breastfeeding until approximately two years of age (Sankar et al., 2015; Victora et al., 2016; WHO, 2009). Complementary foods, often introduced around six months of age, that provide inadequate nutrition can lead to growth disruption and stunting in young children (6-24 months of age) (Black et al., 2008; Dewey & Adu-Afarwuah, 2008). Additionally, because full immunological competence normally does

not occur until later childhood, children will be at the greatest risk for an unbuffered disease load after the cessation of breastfeeding (Kendall et al., 2021), potentially contributing to growth disruption and mortality in infants.

According to historical records, women in medieval France were encouraged to breastfeed, however, colostrum was thought to be a *bad* substance and was often discarded before the onset of breastfeeding (Fildes, 1995). Colostrum contains vital nutrients and maternal antibodies that are essential to neonatal health (Kuralkar & Kuralkar, 2010; Palmquist, 2017). When considering breastfeeding patterns they appear to be in line with current WHO suggestions, as historical information suggests that caretakers and infants and young children engaged in complementary breastfeeding until approximately 2 years of age (See Section 2.1.2; Kibler et al., 1995, p. 409). However, typical complementary foods, such as gruel, were often inadequate, as cereal based porridges and gruel are high in antinutrients (phytates) and low in energy and nutrient density (Michaelsen & Friis, 1998).

When examining the mother-infant nexus, teeth are one of the most important tissues to consider as they form throughout growth and do not remodel like bone (Veselka et al., 2019). They can, therefore, reveal periods of stress experienced during pre- and postnatal life. Stable carbon and nitrogen isotope analyses from both subadult and adult dentine as well as infant bone is considered a reliable method for examining breastfeeding patterns in the past (Bourbou et al., 2013; Dupras & Tocheri, 2007; Kendall, 2021; Mays, 2013; Nitsch et al., 2011). Nitrogen is especially important when considering breastfeeding patterns, as it is approximately 2-4‰ higher in breastfeeding infants than

adults due to consuming a by-product of their mother, thereby increasing their trophic level (Mays, 2013). Temporal comparisons between infant feeding and later childhood diets can be achieved using incremental dentine sampling (Mays et al., 2017). Additionally, methods such as analysis of interglobular dentin (IGD) in the first permanent molar and deciduous teeth can provide evidence for maternal vitamin D deficiency (Brickley et al., 2020b). New methodological techniques have also allowed for LEHs, which developed in utero, to be identified in deciduous canines and incisors (Adams et al., 2021). In utero LEH formation is suggested to be evidence for maternal and fetal stress (Adams et al., 2021). LEHs are suggested to be highly related to the stress experienced during the weaning process, especially when combined with isotopic data (Adams et al., 2021; Corruccini et al., 1985; Sandberg et al., 2014; Temple, 2018). Understanding breastfeeding patterns in the past cannot only aid in understanding infant health but also in estimating birth spacing and family size in past communities (Mays, 2013). However, bioarchaeologists should be cautious when discussing infant feeding patterns. Many bioarchaeological papers describing "weaning" and "weaning stress" are often ambiguous and unclear; as some researchers use the term to refer to the introduction of complementary foods, while others refer to the cessation of breastfeeding or even the transitional period in between (Kendall et al., 2021, p. 60). The inconsistency in terminology in bioarchaeological studies may lead to poorly framed interpretations.

While infant and early childhood health can be interpreted from adult remains, they only give us the perspective of individuals who survived into adulthood. Infant and child remains can directly speak to the experiences and life histories of children in past

societies and are particularly useful when examining infant and child mortality, growth disruption, and disease. Though archaeological children represent the non-survivors in their respective communities, bioarchaeologists should continue to examine both child and adult remains as they can both provide nuanced perspectives regarding childhood health and life in the past.

Chapter 3: Material & Methods

3.1 Materials

3.1.1 St. Étienne

The skeletal material used in this study comes from the St. Étienne cemetery of Toulouse, France (Figure 3.1). The St. Étienne cemetery is estimated to have operated between the 10th and 13th century, based on stratigraphic dating and available burial materials (De Filippo et al., 1988 in Kacki, 2016; Grolleau-Raoux et al., 1997; Murail, 1991). The cemetery was excavated between August 1986 and August 1987 due to the construction of an underground parking garage (Kacki, 2016; Telmon et al., 1993). The excavation uncovered 142 burials (De Filippo et al., 1988); however, the number of excavated individuals (n=243) surpasses the number of individual graves (Grolleau-Raoux et al., 1997; Murail, 1991; Telmon et al., 1993). The discrepancy between the number of burials and excavated individuals was due to overlapping and superimposed burials, which led to the comingling of some of the remains (See Figure 3.2). As a result of time constraints enforced during the initial excavation, only approximately 150 m^2 of the western part of the cemetery was excavated, which unfortunately did not cover the entire surface area of the cemetery (De Filippo et al., 1988; Kacki, 2016). While the site could not be excavated in its entirety, the portion that was excavated has good skeletal preservation and a high percentage of subadults (Grolleau-Raoux et al., 1997; Murail, 1991), making this collection an ideal sample for bioarchaeological research regarding children and childhood.

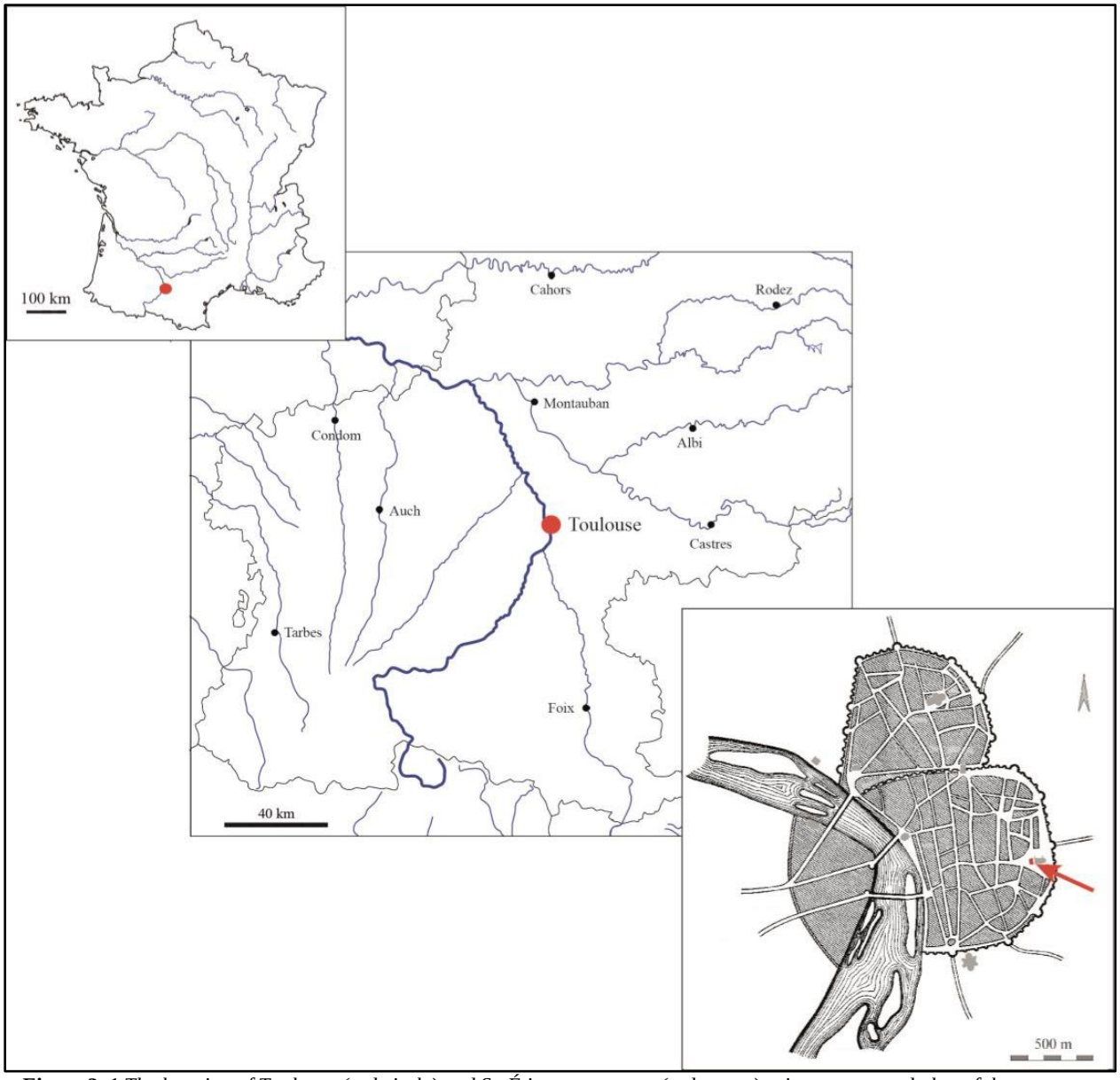

Figure 3. 1 *The location of Toulouse (red circle) and St. Étienne cemetery (red arrow) using a recreated plan of the city in 1200 CE, image retrieved from Kacki (2016, Figure 21, p. 119)*

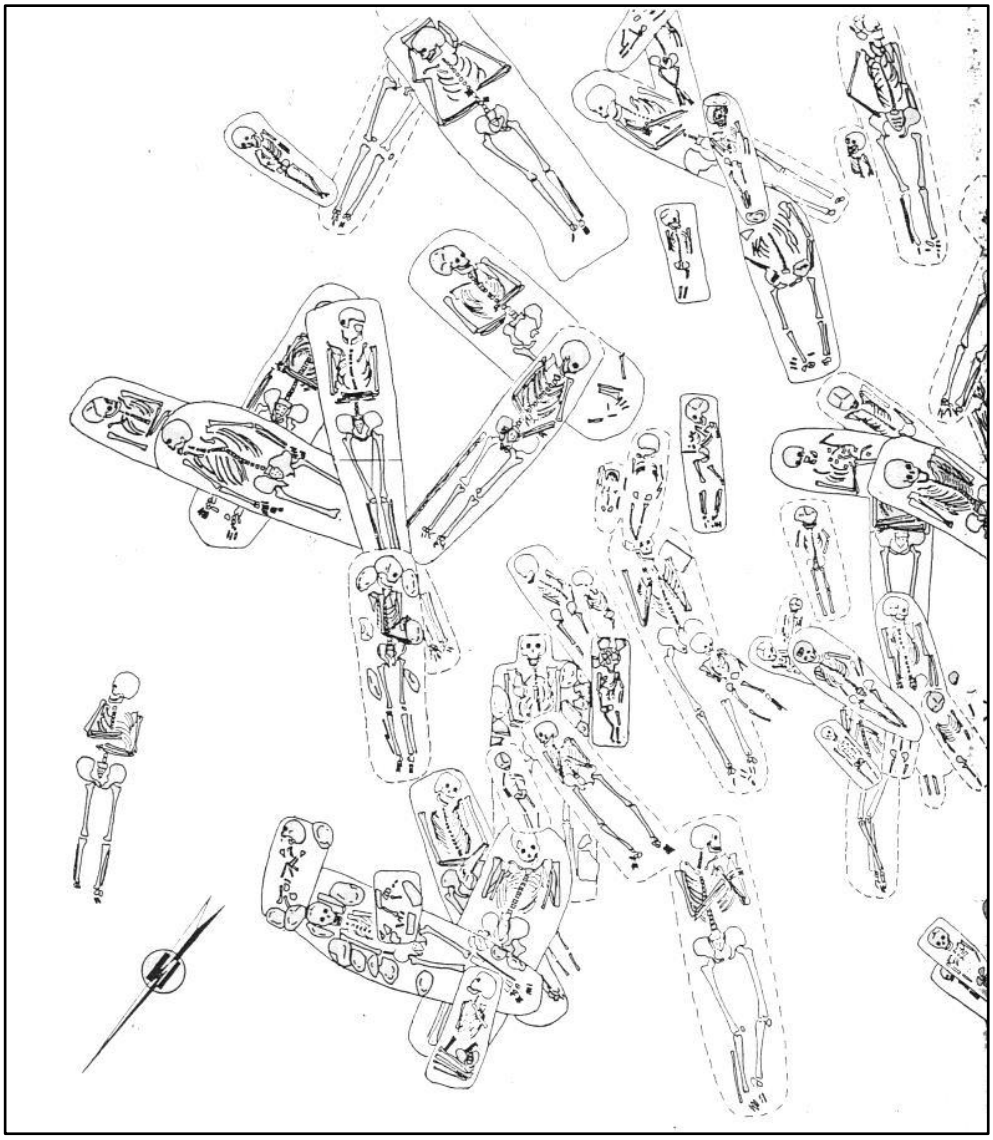

Figure 3. 2 *This illustration provides a visual representation of the density of the burials and the variability of grave orientation at St. Étienne (image retrieved from Kacki, 2016, Figure 24, p. 124).*

The St. Étienne sample was deemed appropriate for answering the research questions of this thesis, based on previously collected data by Dr. Shelley Saunders. Saunders et al. (1994) plotted femoral lengths against dental ages for those who could be aged dentally (n=96). According to the Saunders et al. (1994) report, the subadults from St. Étienne have shorter femoral lengths when compared to modern standards and the 19th

century Belleville collection. Therefore, because many of the individuals from this sample are small for their dental age, this sample presents the opportunity to evaluate whether these individuals were "small but healthy" (Seckler, 1980, p. 219) or if these individuals were suffering from skeletal emaciation (Robbins Schug & Goldman, 2014). This sample was examined at McMaster University and made available by the University of Bordeaux. The sample examined is comprised of left and/or right femora from 115 individuals aged fetal-12.49 years. Twenty-one individuals were excluded from analysis due to inadequate information provided in recording documents or extensive post-depositional damage which limited the collection of necessary measurements, leaving the femora of 94 individuals available for analysis. All individuals had unfused proximal and distal epiphyses.

3.2 Methods

3.2.1 Age estimation

The ages used for this study are based on the age estimates formulated by Dr. Shelley Saunders' research team (See Appendix I). X-rays of all available subadult mandibles and maxillae were previously taken by Dr. Saunders' research team, from these x-rays subadult age was estimated based on tooth formation using the standards of Moorrees et al. (1963a; 1963b; in Saunders et al., 1994). Dental scoring was primarily used for age estimation, as tooth formation is less susceptible to environmental effects compared to skeletal growth and maturation (Cardoso, 2007; Conceição & Cardoso, 2011; Elamin & Liversidge, 2013), making it a more reliable method for age estimation. The distribution of diaphyseal lengths from the dentally aged sample were then used to

create age estimates for the individuals without ageable dentition (Saunders et al., 1994). See Table 3.1 and Table 3.2 for a sample breakdown by age and assigned age categories.

Table 3. 1 *Age Breakdown for Individuals Analysed in Thesis*

Age (years) :	Number of Individuals
Fetal	3
0.0-0.99	28
1.0-1.99	13
2.0-2.99	15
3.0-3.99	10
4.0-4.99	3
5.0-5.99	2
6.0-6.99	3
7.0-7.99	3
8.0-8.99	2
9.0-9.99	6
10.00-10.99	4
11.0+	2
Total:	94

Table 3. 2 *Individuals Analysed in this Thesis by Age Category*

Age Category:	Age (years):	Number of Individuals
1	Fetal-0.99	31
2	1.0-1.99	13
3	2.0-3.99	25
4	4.0-8.99	13
5	9.0-12.49	12

3.2.2 Midshaft Embedding

Of the 94 individuals included in this study, 91 had previously cut midshaft sections. Five individuals have a midshaft section for both their left and right femora,

totaling 96 midshaft sections. Seventy-seven of the 96 midshaft section were previously embedded by Shelley Saunders' research team and 19 were unembedded sections. The 19 samples were embedded for the purpose of this thesis, as embedding is an important process required for creating thin sections for light microscopy. A mixture of Buehler EpoThin Epoxy Resin and Buehler EpoThin 2 Epoxy Hardener were used to create the epoxy. The epoxy was mixed, following the instructions provided by Buehler, in three batches of 50g resin and 22.5g hardener, 72.5g total (See Table 3.3 for mixing guide). The epoxy resin and hardener were manually mixed using a stir stick for approximately 1-2 minutes until the mixture was uniform. A Buehler release agent was used to coat the inside of circular epoxy moulds prior to adding the midshaft sections, to aid removal of the epoxy blocks from the moulds after they have hardened. The midshaft sections were then added to the moulds and the epoxy mixture was poured onto them, enough mixture was added to cover the samples completely. The samples were then placed into a glass vacuum chamber for approximately 30-35 minutes to extract bubbles. After hardening for 48 hours the epoxy blocks were removed from the moulds. Of the 19 sections, thirteen were embedded on their own (one sample per mould), while the remaining six samples were embedded in three moulds using a divider to separate them (two samples per mould).

Table 3. 3 *EpoThin 2 Mixing Guide*

Resin (gram)	Hardener (gram)	Resin + Hardener (gram)
100	45	145
50	22.5	72.5
25	11.25	36.25
12.5	5.63	18.13
6.25	2.81	9.06
3.13	1.41	4.54
1.56	0.7	2.26
0.78	0.35	1.13
0.39	0.18	0.57

3.2.3 Radiography

The femora of 93 individuals were x-rayed using the portable Vidisco FlashX Pro digital radiograph system in the Department of Anthropology at McMaster University. Individual BN-314 was excluded from femoral radiographs due to extensive post-depositional damage. The number of pulses (exposure time) used while conducting radiographs ranged from 19-36 depending on density of bones imaged and duration of use, with a photo energy of 150 kVp. The images were then saved and converted to tiff files.

All femoral diaphyses and midshaft sections were radiographed with a tube to film height of 120cm. The femoral diaphyses were imaged in the anteroposterior (AP) and mediolateral (ML) position. The diaphyses were stabilized using egg crate foam to prevent movement during the scan. Egg crate foam was used because of its low density, which prevents it from being visualized in the radiograph scans, similar to using florist

foam in micro-CT scans (du Plessis et al., 2017; Welsh et al., 2020). Diaphyses of a similar length/width were radiographed on the same plate, each plate held a minimum of three and maximum of 11 diaphyses. Midshaft sections were also radiographed. Midshaft sections were radiographed in the AP, ML, and disto-proximal (DP) positions. A minimum of eight and maximum of 17 midshaft sections were radiographed per plate. Previously unembedded midshaft sections (n=19) were radiographed both before and after embedding. A 2.54cm lead calibration ball was radiographed with all femoral diaphyses and midshafts sections to provide a reference scale and 0.64cm lead numbers were used for labelling purposes (See Figure 3.3).

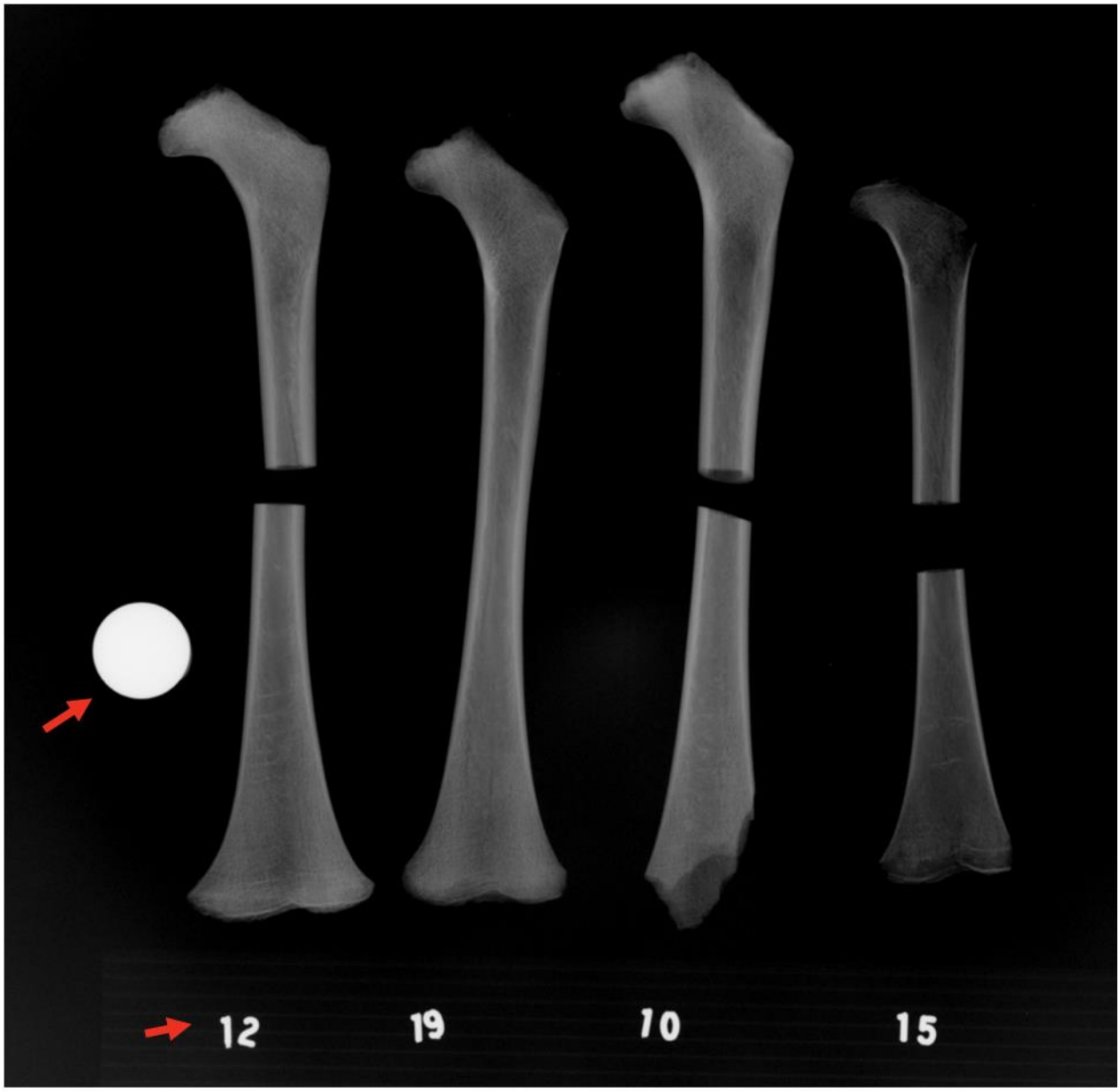

Figure 3. 3 *This image displays plate 2 in the Anteroposterior (AP) position, radiographed using 27 pulses. The red arrows indicate the 2.54cm lead ball and the lead numbers.*

3.2.4 Growth and Femoral Length Assessment

Endochondral growth (femoral length; See Section 2.3.1) was previously recorded by Dr. Saunders' research team (See Appendix II). Midshaft appositional growth (See Section 2.3.2) was assessed using the total subperiosteal area (TA; See Section 3.2.6) from midshaft cross-sections.

To determine if growth stunting occurred in the St. Étienne sample, z-scores were calculated using the femoral length means from the modern Denver Cohort reference sample (Cardoso, 2005). The Denver sample has been found to be similar to the WHO International Reference Standard, and therefore suitable for comparative human growth studies (Schillaci et al., 2012). The FL means created by Cardoso (2005) were used in place of the original Maresh (1970) FL means, as Maresh (1970) did not correct the data for the magnification of the radiographs. The original uncorrected Maresh (1970) data presents femoral length means that are larger than they should be (Cardoso, 2005), therefore, had the original data been used the individuals from St. Étienne would appear to be comparatively smaller than they really are. The Cardoso (2005) FL means and standard deviations (SDs) for males and females were averaged for each age category. Z-scores were then calculated by subtracting the long bone lengths (x) of St. Étienne individuals from the Cardoso (2005) long bone length mean of the same age cohort (μ), and then dividing the total by the corresponding Cardoso (2005) SD (σ):

Equation 3. 1: **Z-score**

$$Z = \frac{x - \mu}{\sigma}$$

Since the Denver Cohort reference sample increases in 6-month intervals (Cardoso, 2005; Maresh, 1970), the St. Étienne individuals were assigned to age categories in half year intervals starting from quarter year midpoints; for example, individuals aged 1.25-1.74 had z-scores created using the means from the 1.5-year old Denver age category. Individual BN-337 is the only exception as the Denver sample only provides means for individuals without epiphyses until age 12. After age 12 the FL means

created use the whole femoral length, including the epiphyses. Individual BN-337 (aged 12.42 yrs; See Appendix I) was not measured with epiphyses present, therefore, the age category of 12, rather than 12.5, will used for their z-score calculation.

3.2.5 Body Mass Estimation

Subadult body mass was estimated using the width of the femoral distal metaphysis (MET) (See Figure 3.4; Buiksta & Ubelaker, 1994, p.46 measurement 17b; Robbins et al., 2010; Ruff, 2007) and superior-inferior femoral head breadth (FH) (See Figure 3.5; Robbins et al., 2010; Ruff, 2007), measured from radiographs, as well as *J* (polar moment of inertia; See Equation 3.3, p. 49), calculated from midshaft (MS) histological images. The body mass measurement used was based on the age of the individual, available measurable areas (MS, FH, and MET), and percent standard error of the estimate (%SEE) for different formulae available. Each measurement and corresponding formulae has a %SEE, which is used to compare the precision of measurement and corresponding formulae across the different age categories (Robbins et al., 2010; See Table 3.4). Therefore, the available measurements and formulae with the lowest %SEE were used for body mass estimation (See Appendix II). Body mass was estimated using the equation tables provided in Ruff (2007, p. 703) and Robbins et al. (2010, p. 147) (See Figure 3.6 for equation and example). For individual BN-32 whose estimated skeletal age was provided as a range of 8.5-10.5 yrs (See Appendix I), the average age of 9.5 years was taken and used for the body mass calculation.

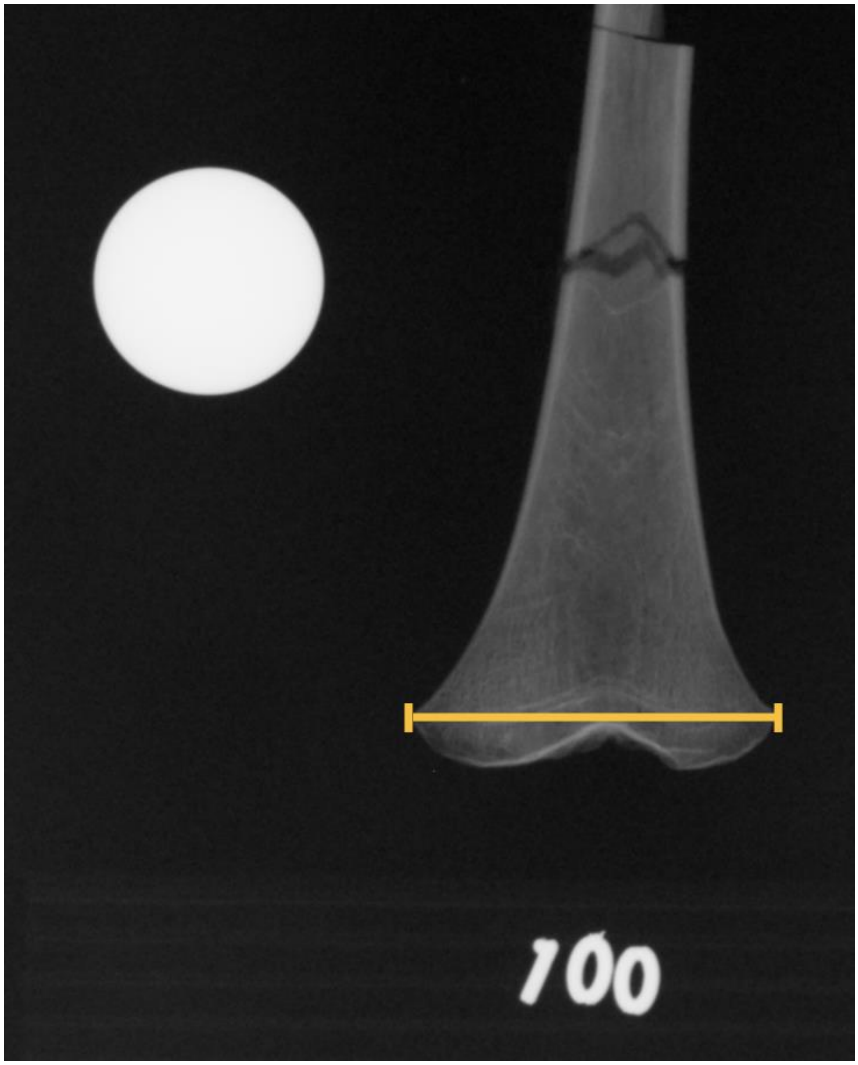

Figure 3. 4 *Femoral distal metaphysis (MET) Measurement. Lead ball = 2.54cm.*

Figure 3. 5 *Superior-inferior femoral head breadth (FH) measurement. Lead ball = 2.54cm*

Table 3. 4 *Body Mass Estimation Methods with the Lowest Standard Error of the Estimates (%SEE) by Age*.

Age (years)	Body estimate method with the lowest %SEE*
0	MS
1	MS
2	log MET
3	log MET
4	MS, log MET
5	MS, MET
6	MS
7	FH
8	MS
9	log FH
10	log FH
11	log FH
12	log FH

**Information from Robbins et al. (2010, p. 148). Legend – MS = Midshaft (J); MET = Distal Metaphyseal Breadth; FH = Femoral Head*

Body Mass Estimate (Kg) = (Measurement in mm X Slope) + Intercept
Example
Individual: BN-12
Age: 4.63
$J= I_x+I_y$
$J= 1095.54mm^4 + 1263.69mm^4$
$J= 2359.23mm^4$
Body Mass Estimate (Kg)= (2359.23 X 0.001) + 12.8
Body Mass Estimate (Kg)= 15.16

Figure 3. 6 *Body Mass estimation equation and example using BN-12. Age specific intercepts and slopes can be found in Robbins et al. (2010, p. 147) and Ruff (2007, p. 703).*

Body mass estimates were compared against the body mass data from the Denver Cohort sample (Hansman, 1970, p. 126-127). The BM means and SDs for males and females were averaged for each age category and used to create BM z-scores. Individuals with z-scores falling below -2 SDs from the mean are considered underweight for their age (Cogill, 2003, p. 8). See Section 3.2.4 for information regarding z-score calculations.

3.2.6 Histology

Of the 96 embedded midshaft sections, 14 were previously mounted onto petrographic microscopy slides by Dr. Saunders' research team (two samples per slide). Eight samples were excluded from histological analysis due to damage or incomplete (<95%) cross-sectional area. The total number of individuals with useable femoral cross sections for histological analysis is 84 and the total number of histological samples available for analysis is 88.

Embedded samples were prepared for light microscopy (LM) using de Boer et al.'s (2013) method and hand ground and polished following Frost's (1958) methods. The polished surface of each sample was mounted onto a slide using 0CON-186 UV resin and hardened under ultraviolet (UV) light. The mounted sections were then cut using the

Wafer blade Buehler Isomet 1000 precision saw leaving an approximately 1.5 mm thick section on each of the slides. Subsequently, the samples were hand ground and polished again using the Frost (1958) method to approximately 50-100 μm.

Thin sections were analyzed and imaged using the Keyence VHX-2000 Digital Microscope. Samples were analyzed under both plain and polarized light. The samples were imaged to capture the full cross sectional surface of the bone. Samples that were too large to be viewed at the minimum magnification (20x), were imaged using the *Stitch* option available with the Keyence. Disjointed sections that separated during the embedding process were rejoined using the free open-source image editing software Gimp 2.10 (The GIMP Developing Team, 2019, See Figure 3.7). Images were then imported to the free open-source image analysis tool Fiji (Schindelin et al., 2012) where they were binarized. Images were binarized by first creating a grey scale image using commands Image>Type>8-bit and then binarizing the grey scale image using commands Image>Adjust>Auto Threshold. Bone was given a value of "255" (black) and non-bone space (background, medullary space, and pore space) was given a value of "0" (white).

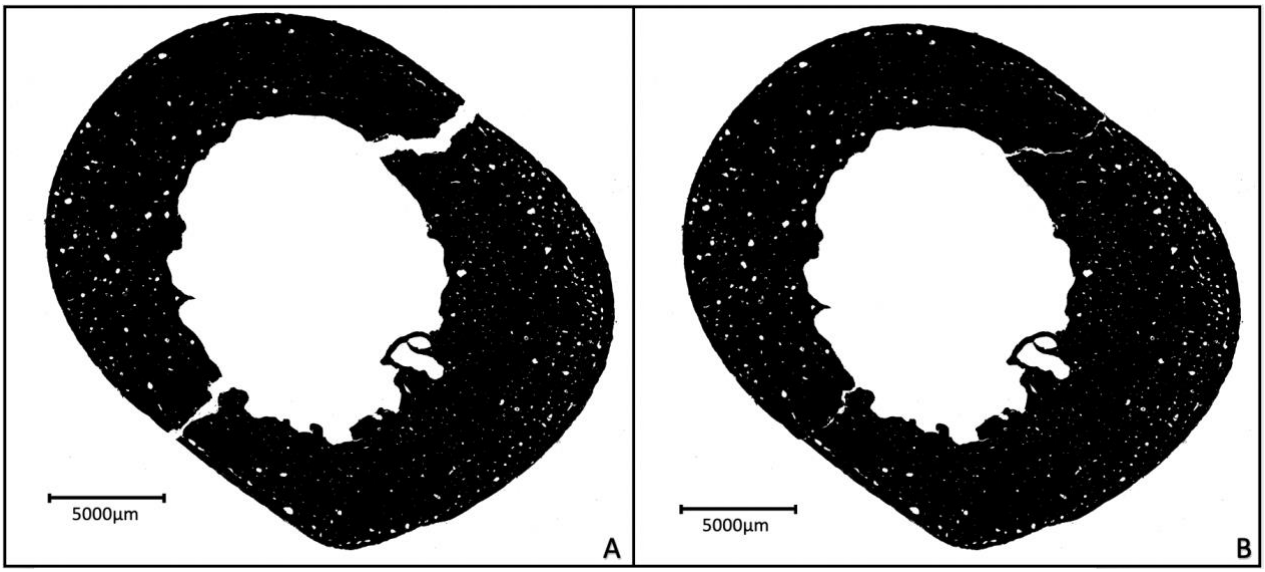

Figure 3. 7 *Example of rejoined image using GIMP 2.10 Software. A) Displays individual BN-367, midshaft separated during the embedding process B) Displays adjusted image of BN-367, which was used for cross-sectional geometry.*

The geometric properties that were calculated using these femoral cross sections are: Total Subperiosteal Area (total area; TA), Cortical Area (CA), Medullary Area (MA), Pore Area (PA), CA/MA, CA/TA (expressed as %CA), maximum and minimum second moments of area (I_{max} and $I_{min)}$ and second moments about the medio-lateral (I_x) and antero-posterior (I_y) axes, and polar moment of inertia (*J*). The TA is calculated by filling in the medullary cavity using the *Fill Holes* (Process>Binary> Fill Holes) command found in the BoneJ plugin in Fiji (Doube et al., 2010; Gosman et al., 2013). The area of the filled cross section was then calculated using the *Area/Fraction* command in the BoneJ plugin (Plugins>BoneJ>Fraction>Area/Volume Fraction). The CA was calculated using the *Slice Geometry* command (Plugins>BoneJ>Slice Geometry), which produces the cross-sectional area (as denoted in BoneJ), which measures the available cortical area. Pore area (PA) was calculated by manually filling in the pores within the cortical space, recalculating the cross-sectional area using the *Slice Geometry* command, and subtracting

the new figure from the original CA. Because it is not possible to accurately identify the edge of the endocortical surface when it is disrupted by trabecularization (Zebaze & Seeman, 2015), all enclosed pores were included in the PA calculation (See Figure 3.8). The MA is calculated using the equation:

Equation 3. 2: **Medullary Area**

$$Medullary\ Area = TA - (CA + PA)$$

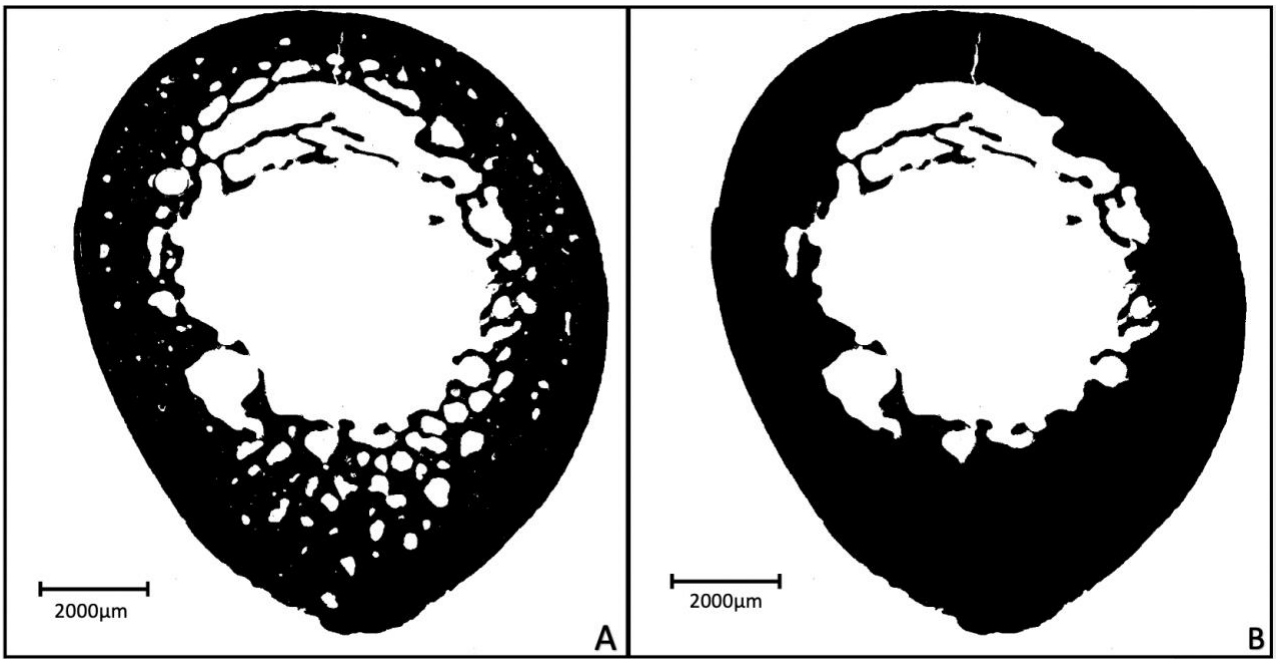

Figure 3. 8 *A) Binarized cross-sectional image of individual BN-321 B) Image of BN-321 with all closed Pores manually filled. All open pores remain unfilled and are considered a part of the medullary space.*

The ratios of CA/MA and %CA were used to examine the relative proportion of cortical bone, which can be more easily compared across age categories. The maximum and minimum second moments of area (I_{max} and I_{min}) and the second moments about the medio-lateral (I_x) and antero-posterior (I_y) axes were calculated using the BoneJ plug-in

(Doube et al., 2010). The ratios of I_{max}/I_{min} and I_x/I_y were used to examine differences in cross sectional shape (Cowgill et al., 2010; Goldman et al., 2009; Gosman et al., 2013; Robbins Schug & Goldman, 2014; Swan et al., 2020). Midshaft shape (I_x/I_y) was compared with the previously published data from Swan et al. (2020), made available by lead author Karen Swan. This data comprises 110 samples of individuals of documented age (birth-8.5 yrs) from the 18th to 19th century sites Bethnal Green and Christ Church Spitalfields, London, UK (Swan et al., 2020). The samples were analysed using the age categories considered by Swan et al. (2020) (i.e 0.0-0.49; 0.5-0.99; 1.0-1.99; 2.0-3.99; 4.0-8.5). The polar moment of inertia (*J*) was calculated using the O'Neil and Ruff (2004, p. 225) equation:

Equation 3. 3: **Polar moment of inertia (J)**

$$J = I_x + I_y$$

Pore volume (%pore) was calculated by dividing the PA by the CA (Robbins Schug & Goldman, 2014):

Equation 3. 4: **Pore Volume (%pore)**

$$\%pore = \frac{PA}{CA}$$

In samples where diagenesis obstructed pore visibility, %pore was not quantified and only TA, CA, MA, CA/MA, %CA, I_{max}/I_{min}, I_x/I_y, and *J* were calculated. For individuals without sectioned midshafts, geometric properties were calculated from radiographs using the methodology and equations of O'Neill and Ruff (2004, p. 225).

Z-scores were created for TA and %CA using unpublished geometric data from the Denver Cohort sample, which was made available by Dr. Christopher Ruff (Ruff,

n.d). Age cohort specific means and SDs were created from the unpublished Denver TA and %CA data. However, when comparing the cross-sectional variables it should be noted that the variables in the Denver sample were calculated from anteroposterior x-rays of living individuals (Ruff, Personal Communication), while the current study calculated these variables using measurements from the whole cross-section.

3.2.7 Harris line Assessment

This sample has previously been studied for Harris line (HL) frequencies using tibiae (Grolleau-Raoux et al., 1997); however, because the femur was the only element available for this thesis, femoral HL frequency was evaluated. A total of 85 individuals were evaluated for HLs, as individual BN-314 was excluded from radiography and eight individuals had damage to the distal femora which could interfere with adequate HL assessment. Anteroposterior radiographs of the left and/or right femora were used to assess the presence of HLs. The age of HL formation for each HL was estimated using a non-linear Harris Line age-at-formation calculation tool provided by Michal Kulus (Kulus et al., Submitted Manuscript). The calculator only requires two measurements: the total length of the diaphysis and the distance from the Harris line to the closest end (proximal or distal) (See Figure 3.9). The tool requires the input of whole ages; therefore, individual ages were rounded to the nearest whole number (i.e. an individual aged 3.7 was entered as 4.0). After, inputting the age of the individual and the two required measurements, the calculator provides the ratio of bone growth at time of HL formation expressed as a percentage, the ratio of estimated adult bone length expressed as a percentage, and estimated age-at-formation of the HL. Unfortunately, the calculator only allows ages 2-17

to be inputted. Therefore, individual BN-325-1 (aged 1.32 years) was inputted as 2 years of age rather than 1 year of age; thus overestimating the age at which the HLs formed in this individual. This age estimation system was chosen as it is more precise compared to Kulus and Dabrowski's (2019) Harris line age-at-formation estimation tables for subadult femora.

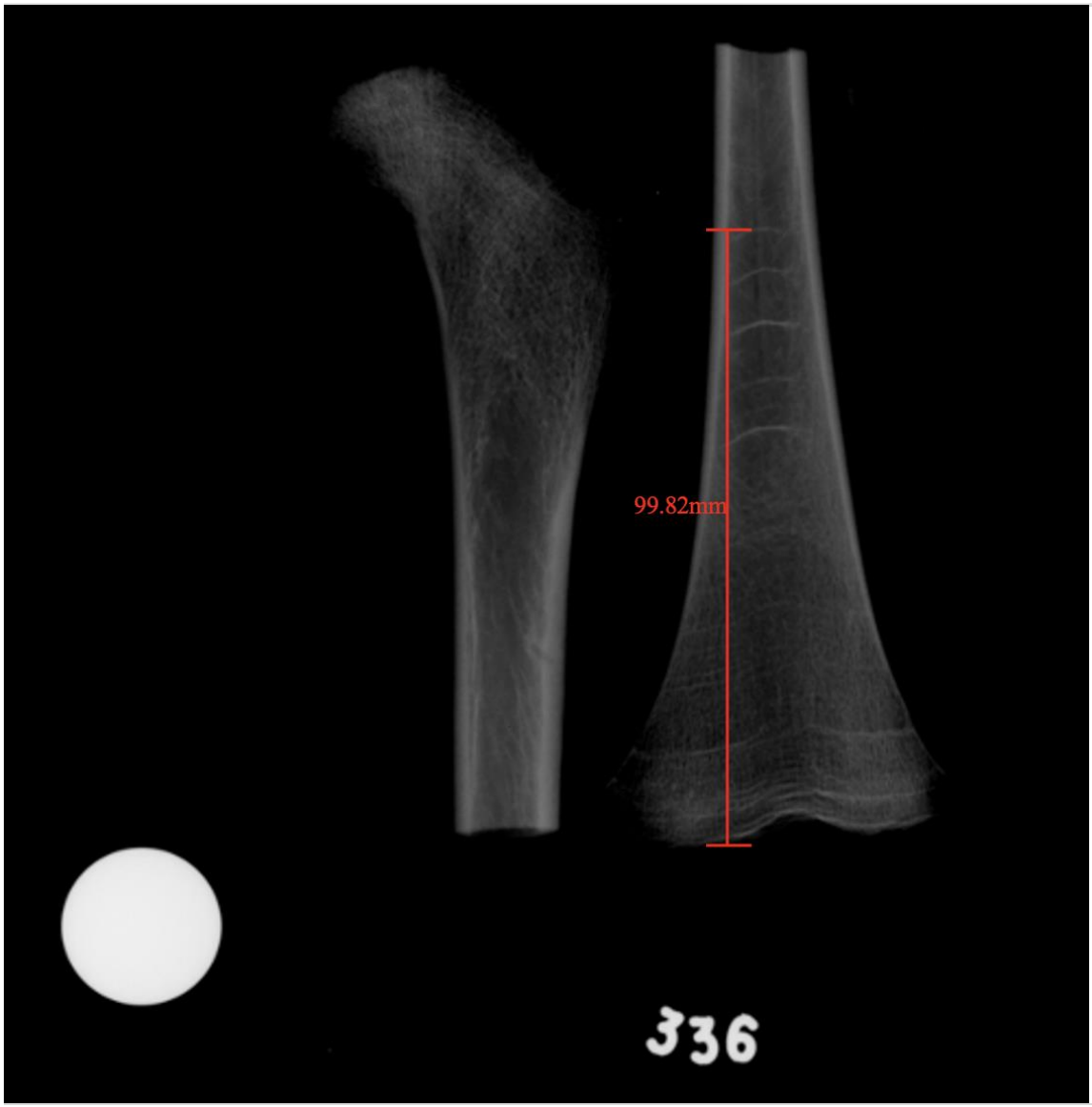

Figure 3. 9 *Displays 6.45 year old BN-336 with numerous HLs on the distal left femur. The oldest visible HL is measured from the distal end of the diaphysis. Lead ball = 2.54cm.*

3.2.8 Statistical Analyses

Statistical analyses were conducted using IBM SPSS Statistics 26 Software. Normality tests were used to determine whether parametric (normal distribution) or non-parametric (non-normal distribution) statistical tests should be used for each variable tested. When parametric testing was required, Independent T-tests were used when considering two groups and one-way analysis of variance (ANOVA) tests were used when considering more than two groups. When non-parametric testing was required, Mann-Whitney U tests were used in place of Independent T-tests and Independent-Samples Kruskal-Wallis tests were used in place of ANOVA tests. Chi-square tests were used to determine the relationship between Presence/Absence of Harris lines and whether an individual was classified as average/small using BM and FL z-scores. A Confidence Interval (CI) of 95% (α=0.05) was used to determine significance in parametric, non-parametric, and Chi-square tests. The Pearson's Correlation Coefficient bivariate test was used to determine linear relationships between variables examined. A CI of 95% (α=0.05) and 99% (α=0.01) were used to determine significance in correlational tests.

Chapter 4: Results

4.0 Introduction

This chapter presents the results for the femoral growth and development data from the medieval St. Étienne subadult sample. Femoral growth was assessed based on diaphyseal lengths as well as cross-sectional geometric properties such as total area, cortical area, and their relative relationship expressed as %CA. Body mass estimates were also used to determine if individuals were underweight-for-age. Comparisons were made between the healthy modern Denver sample and that of St. Étienne in order to establish growth disruption and stunting in the medieval population. Additionally, ontogenetic changes in femoral shape and cortical porosity were investigated.

4.1 Femoral Length

4.1.1 Pearson's Correlation Coefficient

Femoral length (FL) measurements were available for n=93 individuals (See Appendix II). In order to examine the relationship between femoral length and other growth variables a Pearson's Correlation Coefficient bivariate test was employed. The test was used to determine if FL is linearly correlated with the following variables: estimated age-at-death, total area (TA), cortical area (CA), medullary area (MA), CA/MA, CA/TA (%CA), body mass (BM), polar moments of inertia (*J*), I_x/I_y, and I_{max}/I_{min} (See Table 4.1). FL was found to have a statistically significant ($p<0.01$) positive linear relationship with age, TA, CA, MA, I_x/I_y, *J*, and BM. FL was found to have a significant ($p<0.01$) negative relationship with CA/MA. FL was also found to have a significant ($p<0.05$) negative relationship with I_{max}/I_{min}.

Table 4. 1 *Pearson's Correlation Coefficient Results for Femoral Length Vs Estimated Age-at-Death, Body Mass, and Geometric Variables*

		Age (yrs)	TA	CA	MA	CA/MA	I_{max}/I_{min}	I_x/I_y	J	Body Mass (kg)	%CA
Femoral Length	Pearson Correlation	.966**	.960**	.920**	.961**	-.338**	-.268*	.459**	.855**	.976**	-0.194
	Significance (2-tailed)	0.000	0.000	0.000	0.000	0.001	0.014	0.000	0.000	0.000	0.073
	N	93	86	86	86	86	83	86	86	93	86

Legend – N= Number of individuals analyzed; TA= Total Area; CA= Cortical Area; MA= Medullary Area; CA/MA= Cortical Area/Medullary Area; I_{max}/I_{min} = Maximum polar moment of Area/Minimum Polar moment of area; I_x/I_y= Polar moment of area about the mediolateral axis/Polar area about the Anteroposterior axis; J= I_x+I_y; %CA= Cortical Area/Total Area
***Correlation is significant at the 0.01 level*
**Correlation is significant at the 0.05 level*

4.1.2 Comparison to Modern and Archaeological Collections

To determine if there are differences between the growth trajectories of the medieval St. Étienne sample and that of expected modern standards, z-scores were created using the means from the Denver cohort study. The z-score results are used to determine if individuals from the St. Étienne sample experienced growth stunting during their life; as z-scores falling below -2 SDs from the mean are considered evidence of moderate to severe malnutrition and growth stunting (Cogill, 2003, p. 41-42). A z-score of < -1 to > -2 is considered evidence of mild malnutrition (Cogill, 2003, p. 42). Therefore, z-scores of < -1 are considered evidence of growth disruption in the current study. Z-score calculations were available for n=90 individuals (0.0-12.49yrs) (See Figure 4.1; See Appendix III). Fifty-one individuals fell below -2 SDs of the mean (51/90, 56.7%) (See Table 4.2 for breakdown by age category), indicating that the majority of individuals from St. Étienne suffered from linear growth stunting. Children aged 1.0-1.99 and 2.0-3.99 were the most affected by growth stunting with n=9 (69.2%) and n=21 (84%) of individuals falling below -2 SDs, respectively. Only six individuals exhibit

positive z-scores and only two individuals (BN-367 & BN-86) were above 2 SDs from the mean. Although 56.7% of individuals fell below -2 SDs of their respective means, an Independent T-test found that the femoral lengths of the St. Étienne individuals do not differ significantly ($p>0.05$) from the Denver Cohort sample (See Table 4.3). Therefore, while stunting was prevalent in the St. Étienne sample, FL did not significantly differ from modern expectations.

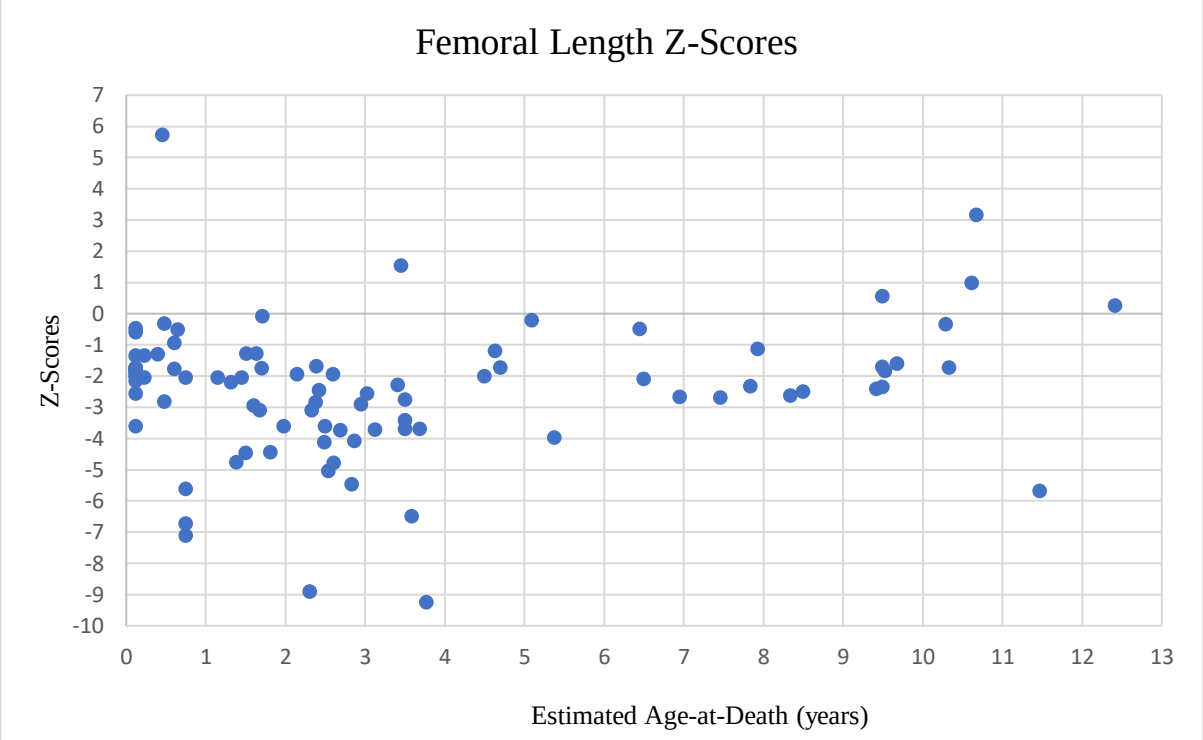

Figure 4. 1 *The scatter plot displays the distribution of Femoral Length z-scores for the St. Étienne sample.*

Table 4. 2 *Prevalence of Stunting in St. Etienne Subadult Sample*

Age Category (years)	*n*	Below -2 SDs	Below -3 SDs	Below -4 SDs
1 (0-0.99)	27	10 (37%)	4 (14.8%)	3 (11.1%)
2 (1.0-1.99)	13	9 (69.2%)	5 (38.5%)	3 (23.1%)
3 (2.0-3.99)	25	21 (84%)	15 (60%)	8 (32%)
4 (4.0-8.99)	13	8 (61.5%)	1 (7.7%)	0 (0%)
5 (9.0-12.49)	12	3 (25%)	1 (8.3%)	0 (0%)
Total	90	51 (56.7%)	26 (28.9%)	14 (15.6%)

Legend – n= number of individuals included; SD= Standard Deviation

Table 4. 3 *Independent T-test of Mean Femoral Length Between St. Étienne and the Denver Cohort Sample*

	St. Étienne		Denver			
	Mean	SD	Mean	SD	*t*-value	Significance (2-tailed)
Femoral Length	204.70	85.17	232.89	87.82	-1.08	0.29

Legend – Denver = Modern Denver Reference Sample (Cardoso, 2005); SD = Standard Deviation; t-value= T Statistic
**Significant at the 0.05 level; No Significant results*

To assess if the current sample differs significantly from other archaeological collections, the femoral lengths of the St. Étienne individuals were plotted against the means of three archaeological samples (See Figure 4.2). The archaeological samples include: St. Martin's Churchyard, Birmingham, England, which dates from the 18th to 19th century CE (Mays et al., 2008); Wharram Percy, North Yorkshire, England, which dates from the 10th to 19th century CE (Mays et al., 2008); and St. Thomas' Church, Belleville, Ontario, which dates to the 19th century CE (Saunders et al., 1993). An Independent T-test was performed to determine whether the FL means of St. Étienne individuals differ significantly from the Belleville sample and a One-way Anova test was used to determine if the FL means of St. Étienne individuals differ significantly from the St. Martin's Churchyard and Wharram Percy samples. Two separate statistical tests were performed due to differences in age categories used by Mays et al. (2008) and Saunders et al. (1993). The Independent T-test found that the FL means of St. Étienne did not differ significantly ($p>0.05$) from the Belleville sample (See Table 4.4). Similarly, the One-Way Anova did not find a significant difference ($p>0.05$) between the St. Étienne, St. Martin's, and Wharram Percy FL means (See Table 4.5). The results indicate that the growth trajectory

of St. Étienne most similarly resembles that of the European collections: Wharram Percy and St. Martin's.

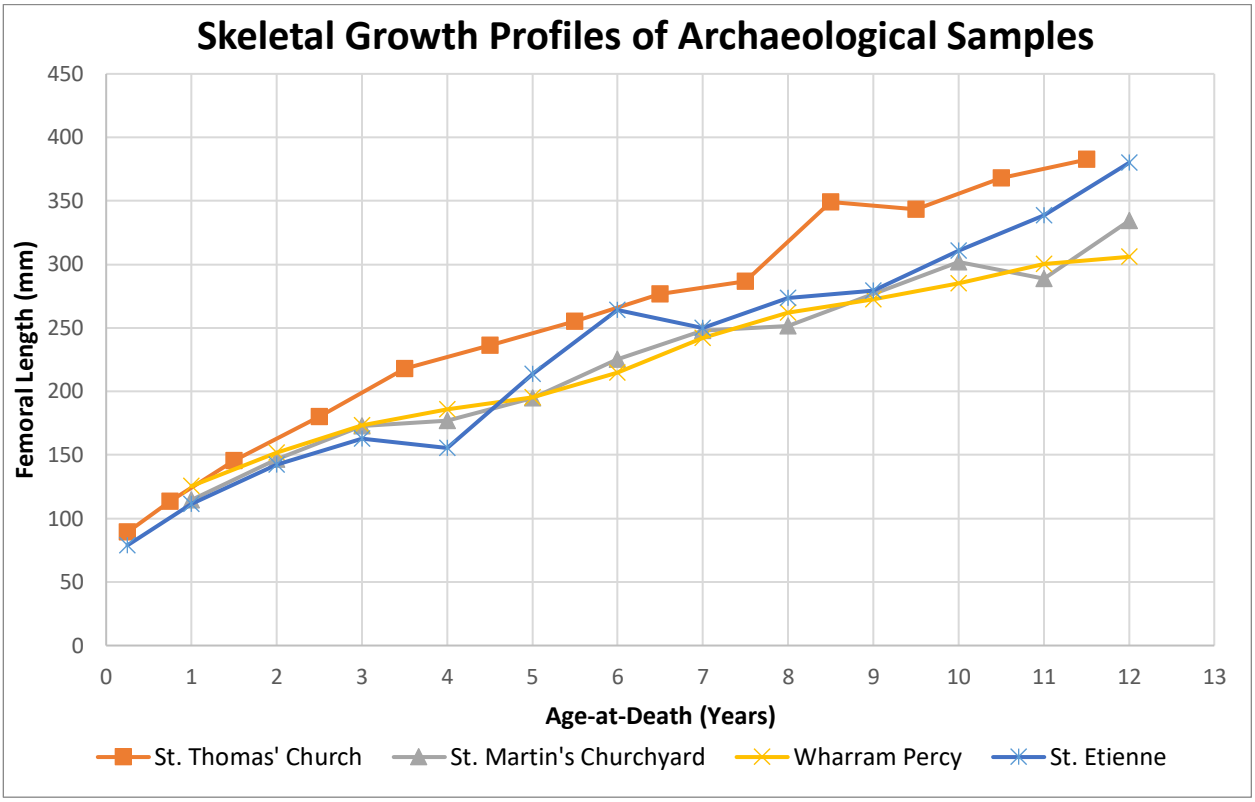

Figure 4. 2 *Femoral Length means vs Age-at-Death for four archaeological sites. Legend – St. Thomas' Church = 19th century St. Thomas' Church Belleville site (Saunders et al., 1993); St. Martin's Churchyard= 18th- 19th century St. Martin's Churchyard Birmingham site (Mays et al., 2008); Wharram Percy = 10th-19th century Wharram Percy North Yorkshire site (Mays et al., 2008).*

Table 4. 4 *Independent T-test of Mean Femoral Length Between St. Étienne and the St. Thomas' Church Sample*

	St. Étienne		St. Thomas' Church Sample			
	Mean	SD	Mean	SD	*t*-value	Significance (2-tailed)
Femoral Length	212.4	81.24	249.58	97.30	-1.06	0.30

Legend – St. Thomas' Church Sample = 19th century St. Thomas' Church Belleville site (Saunders et al., 1993); SD= Standard Deviation; t-value = T Statistic
**Significant at the 0.05 level; No significant results*

Table 4. 5 *One-Way Anova for Mean Femoral Lengths Between St. Étienne, Wharram Percy, and St. Martin's Churchyard*

		Mean Difference (mm)	Std. Error	Sig.	95% Confidence Interval	
					Lower Bound	Upper Bound
St. Étienne	Wharram Percy	13.95	29.33	0.88	-58.11	86.02
	St. Martin's Churchyard	16.89	29.99	0.84	-56.80	90.58
Wharram Percy	St. Étienne	-13.95	29.33	0.88	-86.02	58.11
	St. Martin's Churchyard	2.93	29.99	0.99	-70.75	76.62
St. Martin's Churchyard	St. Étienne	-16.89	29.99	0.84	-90.58	56.80
	Wharram Percy	-2.93	29.99	0.99	-76.62	70.75

Legend – Wharram Percy = 10th-19th century Wharram Percy North Yorkshire site (Mays et al., 2008); 18th- 19th century St. Martin's Churchyard Birmingham site (Mays et al., 2008); Mean Difference = Difference in Mean Femoral Lengths; Std. Error= Standard Error; Sig. = Sigificance
**Significant at the 0.05 level; No Significant results*

4.2 Body Mass Estimation

4.2.1 Pearson's Correlation Coefficient

Body mass (BM) estimations were available for all individuals in the present study (n=94) (See Table 4.6 for descriptive statistics of body mass estimates by age category; See Appendix II). A Pearson's Correlation Coefficient bivariate test was used to determine if BM is linearly correlated with the following variables: age-at-death, TA, CA, MA, CA/MA, %CA, FL, I_x/I_y, *J*, and I_{max}/I_{min} (See Table 4.7). BM was found to have a statistically significant ($p<0.01$) positive linear relationship with age-at-death, TA, CA, MA, FL, *J*, and I_x/I_y . The results were anticipated, because as individuals age they are expected to increase in all size parameters. BM was found to have a significant ($p<0.05$) negative linear relationship with CA/MA and I_{max}/I_{min}. Demonstrating that while the infants (fetal-0.99 yrs) have the largest CA/MA value of all life stages, the results indicate a statistically significant trend is apparent for older children and adolescents to have smaller medullary cavities relative to cortical area compared to younger children.

Table 4. 6 *Descriptive Statistics for Body Mass Estimates by Age Category*

Age Category (years)		Body Mass (kg)
1 (fetal-0.99)	Mean	5.38
	N	31
	Std. Deviation	1.85
	Minimum	3.86
	Maximum	10.22
2 (1.0-1.99)	Mean	9.15
	N	13
	Std. Deviation	0.76
	Minimum	8.06
	Maximum	10.46
3 (2.0-3.99)	Mean	11.09
	N	25
	Std. Deviation	1.43
	Minimum	8.76
	Maximum	14.52
4 (4.0-8.99)	Mean	19.49
	N	13
	Std. Deviation	3.46
	Minimum	14.81
	Maximum	25.72
5 (9.0-12.49)	Mean	29.54
	N	12
	Std. Deviation	4.14
	Minimum	23.91
	Maximum	38.77

Legend – N= Number of individuals analyzed; Std. Deviation = Standard Deviation

Table 4. 7 *Pearson's Correlation Coefficient Results for Body Mass (kg) Vs. Estimated Age-at-Death, Femoral Length, and Cross-Sectional Variables*

		Age (yrs)	TA	CA	MA	CA/MA	Imax/Imin	Ix/Iy	J	Femoral Length	CA/TA
Body Mass (kg)	Pearson Correlation	.980**	.981**	.957**	.940**	-.280**	-.271*	.450**	.907**	.976**	-0.140
	Significance (2-tailed)	0.000	0.000	0.000	0.000	0.009	0.013	0.000	0.000	0.000	0.196
	N	94	87	87	87	87	84	87	87	93	87

Legend – N= Number of individuals analyzed; TA= Total Area; CA= Cortical Area; MA= Medullary Area; CA/MA= Cortical Area/Medullary Area; I_{max}/I_{min} = Maximum polar moment of Area/Minimum Polar moment of area; I_x/I_y= Polar moment of area about the mediolateral axis/Polar area about the Anteroposterior axis; J= I_x+I_y; %CA= Cortical Area/Total Area
***Correlation is significant at the 0.01 level*
**Correlation is significant at the 0.05 level*

4.2.2 Comparison to Modern Data

Body mass z-scores were also available for all individuals in the study (See Figure 4.3). Nineteen (19/94, 20.2%) individuals fell below -2 SDs of their respective means (See Table 4.8; See Appendix III). Children aged 2.0-3.99 years were most commonly classified as underweight-for-age, with n=11 (44%) of individuals in this age category falling below -2 SDs from the mean. No individuals between the ages 4.0 and 12.49 years fell below -2 SDs of their respective means when considering body mass estimates. The majority of individuals who were classified as underweight-for-age were also classified at stunted (16/19; 84.2%). An Independent T-test found that the St. Étienne BM means do not differ significantly ($p>0.05$) from the Denver Cohort BM means (See Table 4.9). Therefore, similarly to FL (See Section 4.1.2) while nearly a quarter of individuals were classified as underweight-for-age, the mean body mass estimates for the sample do not significantly differ from modern expectations.

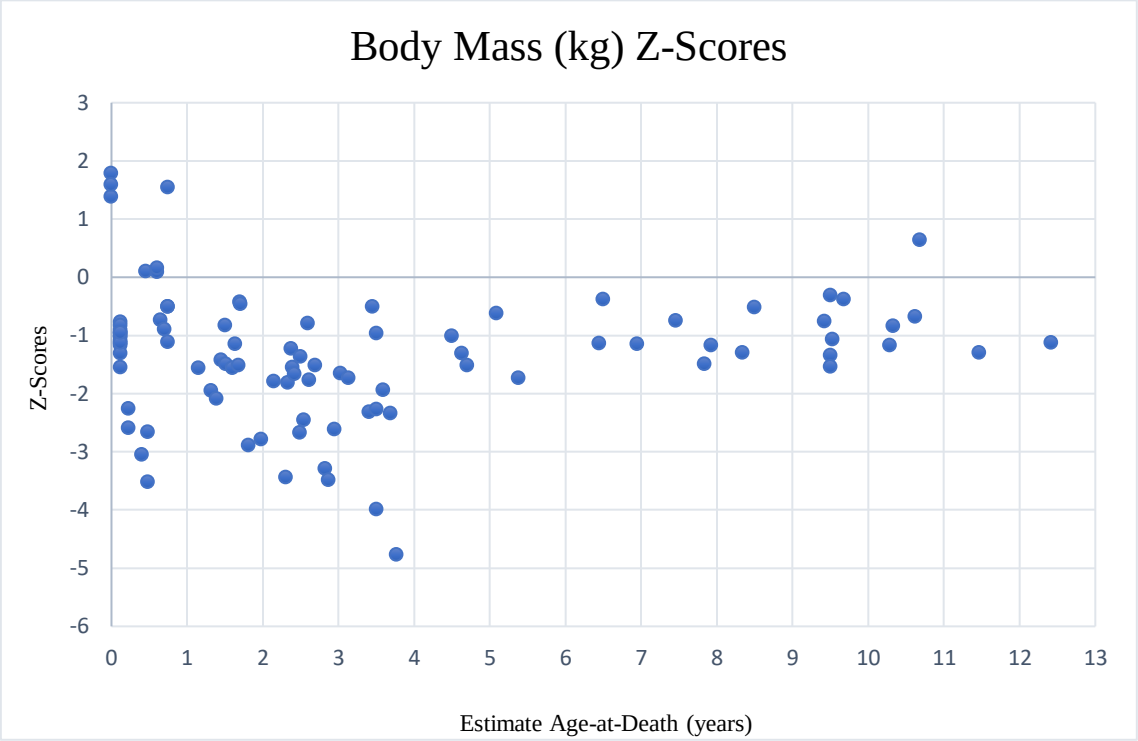

Figure 4. 3 *The scatter plot displays the distribution of Body Mass z-scores for the St. Étienne sample.*

Table 4. 8 *Prevalence of Underweight-for-Age Individuals in the St. Etienne Subadult Sample*

Age Category (years)	*n*	Below -2 SDs	Below -3 SDs	Below -4 SDs
1 (0-0.99)	31	5 (16.1%)	2 (6.5%)	0 (0%)
2 (1.0-1.99)	13	3 (23.1%)	0 (0%)	0 (0%)
3 (2.0-3.99)	25	11 (44%)	5 (20%)	1 (4%)
4 (4.0-8.99)	13	0 (0%)	0 (0%)	0 (0%)
5 (9.0-12.49)	12	0 (0%)	0 (0%)	0 (0%)
Total	94	19 (20.2%)	7 (7.4%)	1 (1.1%)

Legend – n= number of individuals included; SD= Standard Deviation

Table 4. 9 *Independent T-test of Mean Body Mass (kg) Between St. Étienne and the Denver Cohort Sample*

	St. Étienne		Denver			
	Mean	SD	Mean	SD	*t*-value	Significance (2-tailed)
Body Mass	15.27	9.38	18.2	10.8	-1.03	0.308

Legend – Denver = Modern Denver Reference Sample (Hansman, 1970); SD = Standard Deviation; t-value= T Statistic

**Significant at the 0.05 level; No Significant results*

4.3 Cross-Sectional Geometry

4.3.1 Pearson's Correlation Coefficient

The cross-sectional results of this study found that age-at-death estimates are positively linearly associated with the majority of the geometric variables including: TA, CA, MA, I_x/I_y, and *J*. This linear relationship was expected and is statistically significant ($p<0.01$). However, CA/MA ratio and I_{max}/I_{min} is shown to decrease with age; this result was found to be statistically significant ($p<0.05$). The correlational test did not identify a statistically significant ($p>0.05$) linear relationship between %CA and age, indicating that %CA may be more variable compared to the other cross-sectional geometric variables examined in the study. See Table 4.10 for statistics.

Table 4. 10 *Pearson's Correlation Coefficient Results for Estimated Age-at-Death Vs. Geometric Variables*

		TA	CA	MA	CA/MA	Imax/Imin	Ix/Iy	*J*	%CA
Age (years)	Pearson Correlation	.957**	.935**	.920**	-.261*	-.291*	.455**	.869**	-0.113
	Significance (2-tailed)	0.000	0.000	0.000	0.015	0.007	0.000	0.000	0.296
	N	87	87	87	87	84	87	87	87

Legend – N= Number of individuals analyzed; TA= Total Area; CA= Cortical Area; MA= Medullary Area; CA/MA= Cortical Area/Medullary Area; I_{max}/I_{min} = Maximum polar moment of Area/Minimum Polar moment of area; I_x/I_y= Polar moment of area about the mediolateral axis/Polar area about the Anteroposterior axis; J= I_x+I_y; %CA= Cortical Area/Total Area

**Correlation is significant at the 0.01 level

*Correlation is significant at the 0.05 level

4.3.2 Group Variability

Appositional growth and cortical thickness are inferred based on total midshaft areas and relative cortical area (CA/TA, %CA). The means for TA, CA, MA, CA/MA, %CA, *J*, I_x/I_y, and I_{max}/I_{min} were found to differ significantly ($p<0.05$) between the five age categories using a nonparametric Independent samples Kruskal-Wallis test

(See Figure 4.4). With TA, CA, and I_x/I_y increasing in each age category. Appositional growth is especially rapid in the first two years of life, as TA nearly doubles from a mean of 41.24mm^2 in infants aged fetal-0.99 years to 79.99mm^2 in children aged 1.0-1.99 years. Unlike the other geometric variables, %CA does not follow a clear linear trajectory. As can be seen in Figure 4.5, %CA is highest in infants aged fetal-0.99 years. Relative cortical area then rapidly declines after the age of one and maintains this decline until increasing again in children four years of age and older. The descriptive statistics for each geometric variable can be found in Table 4.11, See Appendix IV for all cross-sectional data collected.

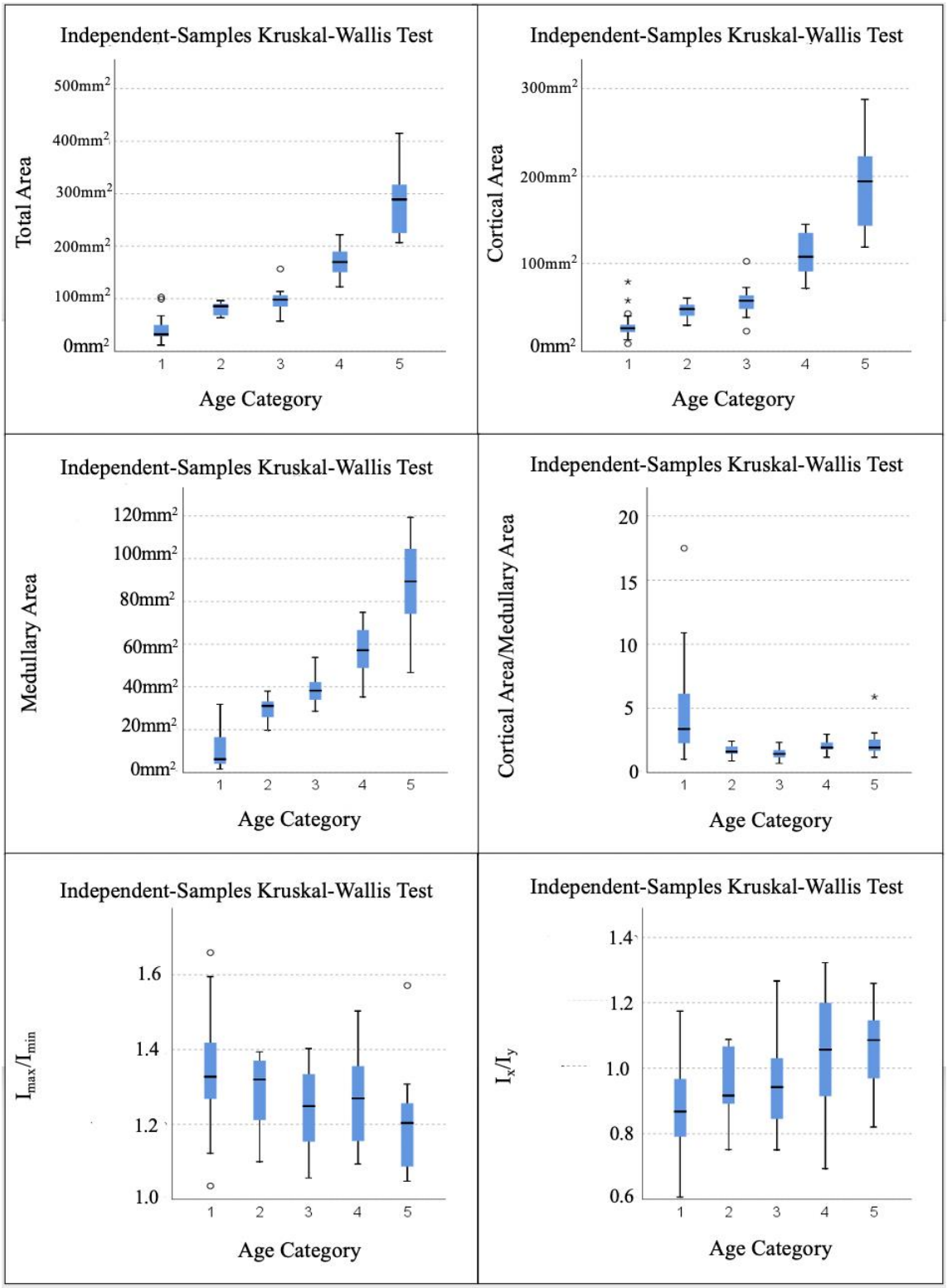

Figure 4. 4 *Box-and-whisker plots of midshaft cross-sectional variables: Total Area (TA), Cortical Area (CA), Medullary Area (MA), Cortical Area/Medullary Area (CA/MA), and Second Polar Moments of Area (Imax/Imin & Ix/Iy). Outliers are represented by circles and extreme outliers are represented by stars.*

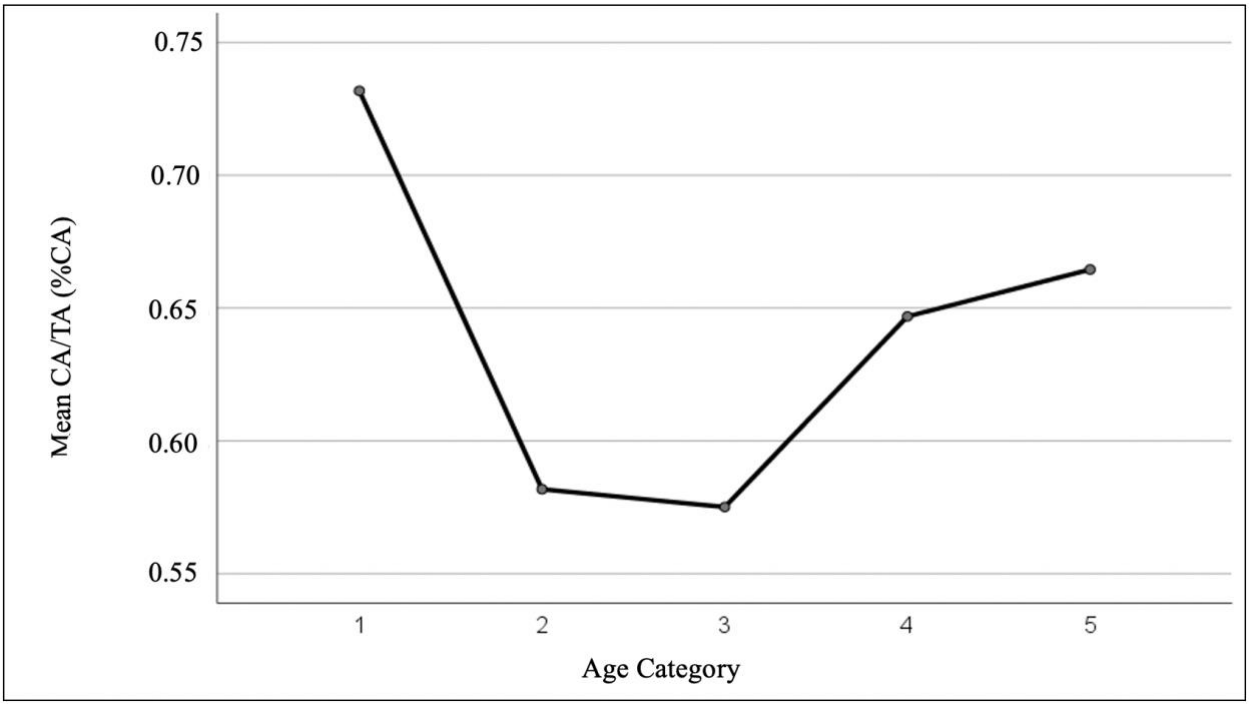

Figure 4. 5 *Graph presents the midshaft Cortical Area/Total Area (%CA) ratio means by age category.*

Midshaft shape can be inferred from I_x/I_y and I_{max}/I_{min} ratios (Cowgill et al., 2010; Swan et al., 2020). The means for I_x/I_y are less than 1.0 in children aged fetal-3.99 years of age, while the means for I_x/I_y are above 1.0 in older children and adolescents aged 4.0-12.49 years. A linear increase of I_x/I_y is due to the gradual change from a mediolaterally reinforced cross-sectional shape to a more anteroposteriorly reinforced cross-sectional shape. The I_{max}/I_{min} means are shown to decrease with age. The descriptive statistics for each geometric variable can be found in Table 4.11.

Table 4. 11 *Descriptive Statistics for Cross-Sectional Geometric Variables by Age Category*

Age Category		TA	CA	MA	CA/MA	Imax/Imin	Ix/Iy	J	%CA
1	Mean	41.24	28.56	10.19	4.56	1.34	0.88	291.56	0.73
	N	31	31	31	31	29	31	31	31
	Std. Deviation	21.74	13.35	8.13	3.58	0.13	0.13	337.28	0.13
	Minimum	11.71	8.63	1.50	1.02	1.04	0.61	20.14	0.47
	Maximum	103.01	79.30	31.86	17.49	1.66	1.17	1560.59	0.94
2	Mean	79.99	46.71	29.25	1.65	1.29	0.94	834.87	0.58
	N	13	13	13	13	13	13	13	13
	Std. Deviation	12.51	9.68	6.07	0.44	0.09	0.10	268.17	0.07
	Minimum	63.56	29.64	19.72	0.89	1.10	0.75	455.96	0.45
	Maximum	96.28	60.80	38.01	2.45	1.39	1.09	1180.30	0.67
3	Mean	97.62	56.96	38.84	1.47	1.24	0.96	1302.82	0.58
	N	18	18	18	18	18	18	18	18
	Std. Deviation	20.63	16.64	6.54	0.38	0.11	0.14	653.38	0.07
	Minimum	57.45	22.97	28.67	0.70	1.06	0.75	330.99	0.40
	Maximum	156.65	102.68	53.84	2.34	1.40	1.27	3480.46	0.69
4	Mean	171.97	111.76	57.19	2.00	1.27	1.04	4252.15	0.65
	N	13	13	13	13	12	13	13	13
	Std. Deviation	32.56	25.74	11.66	0.49	0.14	0.21	1656.79	0.06
	Minimum	122.70	71.79	35.29	1.19	1.09	0.69	2011.03	0.51
	Maximum	221.82	145.21	74.91	2.97	1.50	1.32	6854.22	0.72
5	Mean	284.33	191.31	88.58	2.34	1.20	1.06	11982.92	0.66
	N	12	12	12	12	12	12	12	12
	Std. Deviation	61.72	55.62	21.10	1.23	0.15	0.13	5647.23	0.07
	Minimum	207.01	118.91	46.68	1.19	1.05	0.82	5734.47	0.54
	Maximum	415.19	287.74	119.32	5.89	1.57	1.26	24987.64	0.82

Legend – N= Number of individuals analyzed; Std. Deviation= Standard Deviation; TA= Total Area; CA= Cortical Area; MA= Medullary Area; CA/MA= Cortical Area/Medullary Area; I_{max}/I_{min} = Maximum polar moment of Area/Minimum Polar moment of area; I_x/I_y= Polar moment of area about the mediolateral axis/Polar area about the Anteroposterior axis; J= I_x+I_y; %CA= Cortical Area/Total Area

4.3.3 Comparison to Reference sample

The Denver cohort study means and SDs were used to create z-scores for the St. Étienne individuals. Total Area (TA) z-scores were available for n=84 individuals (See Figure 4.6). Fifty-seven (56/84; 66.7%) individuals fell below -2 SDs (See Table 4.12).

Children aged 2.0-3.99 years had the highest proportion of individuals falling below -2 SDs (17/18; 94.4%). These children (2.0-3.99 years) also had the highest proportions of individuals falling below -3 and -4 SDs with n=13 (13/18; 72.2%) and n=6 (6/18; 33.3%), respectively. Relative cortical area (CA/TA; %CA) z-scores were also available for n=84 individuals (See Figure 4.7). Thirty-one (31/84; 36.9%) individuals fell below -2 SDs (See Table 4.13). Children aged 1.0-1.99 and 2.0-3.99 years had the highest proportions of individuals falling below -2SDs with n=9 (9/13; 69.2%) and n=9 (9/18; 50%), respectively. A normality test found that TA and /%CA do not follow a normal distribution within the population ($p<0.05$); therefore, Mann-Whitney U tests were employed. Results generated using the Mann-Whitney U test demonstrate that St. Étienne TA values were significantly ($p<0.05$) smaller compared to the Denver Cohort sample TA values (See Table 4.14). Similarly, a Mann-Whitney U test found that St. Étienne %CA ratios are significantly ($p<0.05$) smaller compared to the Denver Cohort sample %CA (See Table 4.15). These results indicate that while femoral length and body mass estimates do not significantly differ from modern expectations, appositional growth (represented by TA) and relative cortical thickness (%CA) do.

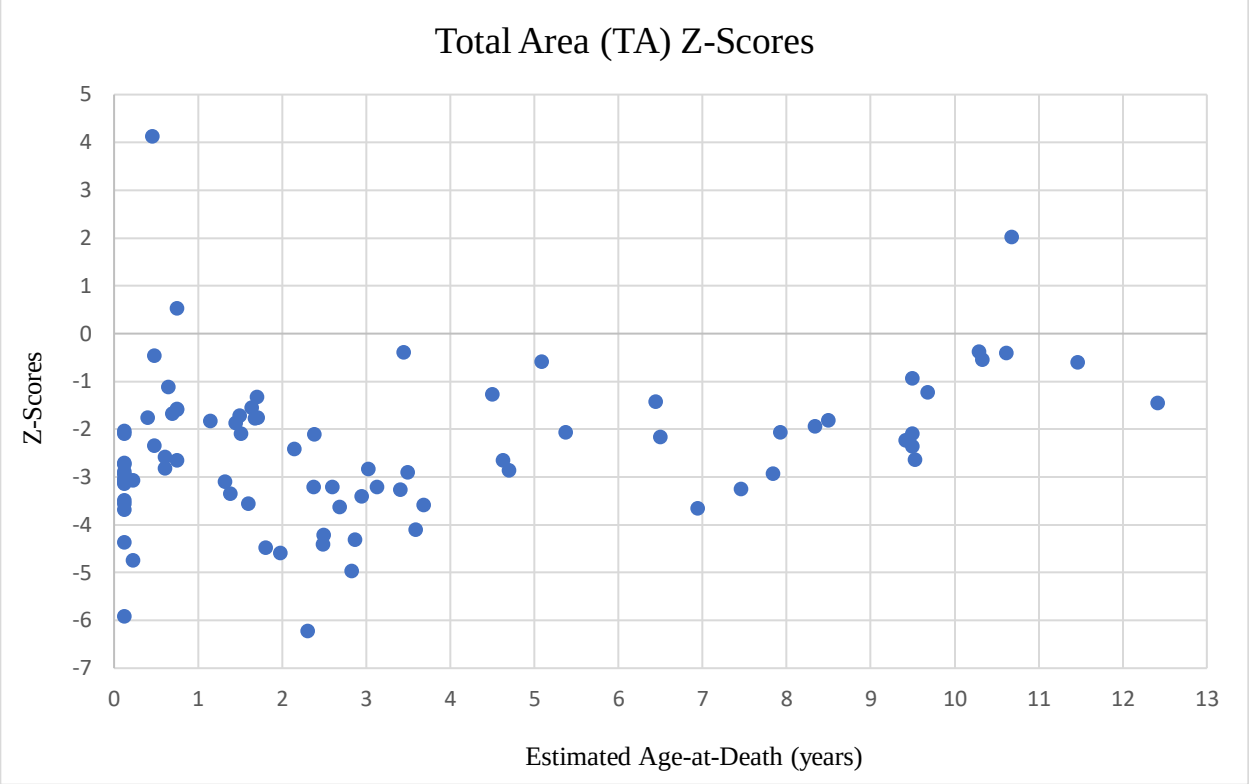

Figure 4. 6 *The scatter plot displays the distribution of midshaft Total Area z-scores for the St. Étienne sample.*

Table 4. 12 *Prevalence of Individuals with Small-for-Age Total Midshaft Areas in the St. Etienne Subadult Sample*

Age Category (years)	*n*	Below -2 SDs	Below -3 SDs	Below -4 SDs
1 (0-0.99)	28	20 (71.4%)	10 (35.7%)	3 (10.7%)
2 (1.0-1.99)	13	6 (46.2%)	5 (38.5%)	3 (23.1%)
3 (2.0-3.99)	18	17 (94.4%)	13 (72.2%)	6 (33.3%)
4 (4.0-8.9)	13	8 (61.5%)	2 (15.4%)	0 (0%)
5 (9.0-12.49)	12	5 (41.7%)	0 (0%)	0 (0%)
Total	84	56 (66.7%)	30 (35.7%)	12 (14.3%)

Legend – n= number of individuals included; SD= Standard Deviation

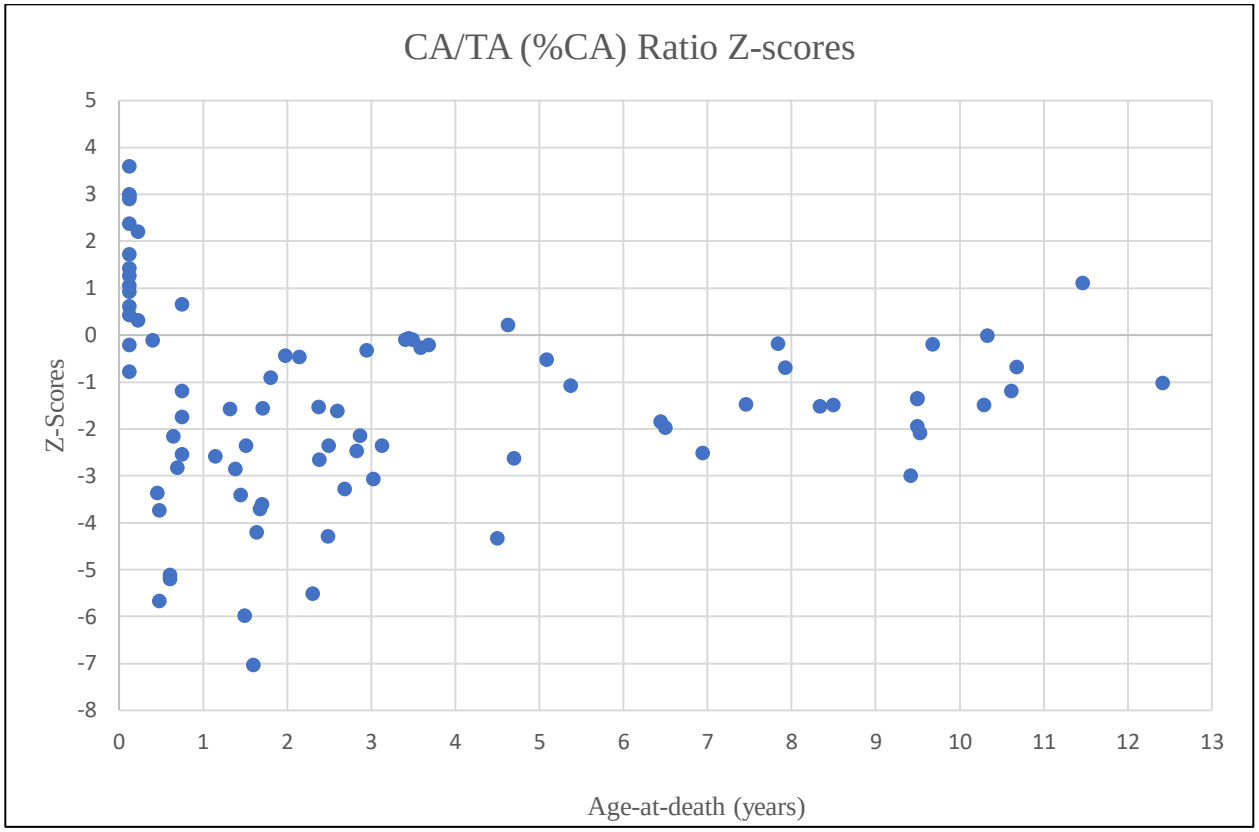

Figure 4. 7 *The scatter plot displays the distribution of midshaft Cortical Area/Total Area ratio (%CA) z-scores for the St. Étienne sample.*

Table 4. 13 *Prevalence of Individuals with Small-for-Age Cortical Area//Total Area (%CA) Ratios in the St. Etienne Subadult Sample*

Age Category (years)	*n*	Below -2 SDs	Below -3 SDs	Below -4 SDs
1 (0-0.99)	28	8 (28.7%)	5 (17.9%)	3 (10.7%)
2 (1.0-1.99)	13	9 (69.2%)	6 (46.2%)	3 (23.1%)
3 (2.0-3.99)	18	9 (50%)	5 (27.8%)	2 (11.1%)
4 (4.0-8.99)	13	3 (23.1%)	1 (7.7%)	1 (7.7%)
5 (9.0-12.49)	12	2 (16.7%)	1 (8.3%)	0 (0%)
Total	84	31 (36.9%)	18 (21.4%)	9 (10.7%)

Legend – n= number of individuals included; SD= Standard Deviation

Table 4. 14 *Mann-Whitney U Test Results for St. Étienne vs. Denver Cohort Sample Midshaft Total Area*

	St. Étienne	Denver	
	n=84	n=488	
	Mean Rank	Mean Rank	Z-Value
TA	149.01	310.17	-8.255*

Legend – Denver = Modern Denver Reference Sample (Ruff, n.d.); TA = Total Area; n= Number of individuals analyzed.
**Significant at the 0.05 level*

Table 4. 15 *Mann-Whitney U Test Results for St. Étienne vs. Denver Cohort Sample Cortical Area/Total Area (%CA) Ratios*

	St. Étienne	Denver	
	n=84	n=486	
	Mean Rank	Mean Rank	Z-Value
%CA	159.06	307.35	-7.620*

Legend – Denver = Modern Denver Reference Sample (Ruff, n.d.); %CA = Cortical Area/Total Area; n= Number of individuals analyzed.
**Significant at the 0.05 level*

4.3.4 Comparison to Archaeological Collection

Midshaft shape (I_x/I_y) results were compared with the results from Swan et al. (2020). Individuals aged 0.5-0.99 years and 2.0-8.5 years did not differ significantly between the two study samples ($p>0.05$) (See Table 4.16). However, individuals aged 0.0-0.49 years and 1.0-1.99 years did differ significantly between the two study samples ($p<0.05$). Individuals at St. Étienne present a more mediolaterally reinforced cross-sectional shape in infants 0.0-0.49 years of age and a more circular cross-sectional midshaft shape in children 1.0-1.99 years of age compared to the study sample examined by Swan et al. (2020) (See Table 4.16).

Table 4. 16 *Independent T-test for Ix/Iy Between St. Étienne and the Swan et al. (2020) Sample*

	St. Étienne		Swan et al. (2020)			
Age (years)	Mean	SD	Mean	SD	*t*-value	Significance (2-tailed)
0.0-0.49	0.85	0.14	0.98	0.12	-3.608	0.001*
0.49-0.99	0.94	0.10	1.01	0.16	-1.081	0.293
1.0-1.99	0.94	0.10	0.87	0.10	2.151	0.038*
2.0-3.99	0.96	0.14	0.91	0.10	1.187	0.244
4.0-8.50	1.04	0.21	1.07	0.13	-0.511	0.614

Legend – SD = Standard Deviation; t-value = T Statistic
**Significant at the 0.05 level*

4.4 Harris lines

Thirty-one of the 85 radiographed femora that could be assessed of Harris lines (HL) (31/85, 36.5%) displayed the presence of a least one observable HL (See Appendix V). Of the 31 individuals, a total of 120 HLs were counted. All HLs observed were located in the distal diaphysis of the femora. The mean age-at-death for individuals presenting observable HLs is 4.13yrs (SD 2.97) with an age range of 1.32-12.42 years. The number of HLs per individual ranged from 1-10 with a mean of 3.87 HLs (SD 2.91, median 3). No individuals below 1.0 year of age presented with observable HLs. The highest prevalence of HLs were found in young children aged 2.0-2.99 years, with n=12 individuals (38.7%) having at least one HL. Based on the calculations generated using Kulus et al. (Unpublished Manuscript)'s Harris line aging tool, the mean age at which HLs formed is 2.98 (SD 2.14). HLs formed most frequently (79/120, 65.8%) between the ages of 2.0-3.99 years. Older children and adolescents (7.0-12.49 years) exhibit a lack of HLs from early years of life, with no individuals displaying HLs with an age-of-formation estimated before five years of age. See Table 4.17 for the breakdown in age at HL formation by age category.

Table 4. 17 *Age-at-Death vs. Age-at-Harris line Formation*

Age-at-Death (years)	Age of Harris Line Formation (years)													
	n	0-1	1-2	2-3	3-4	4-5	5-6	6-7	7-8	8-9	9-10	10-11	11-12	12-13
0-1	0	-	-	-	-	-	-	-	-	-	-	-	-	-
1-2	6	2	13	-	-	-	-	-	-	-	-	-	-	-
2-3	12	4	22	24	-	-	-	-	-	-	-	-	-	-
3-4	3	1	2	4	5	-	-	-	-	-	-	-	-	-
4-5	2	-	3	7	1	6	-	-	-	-	-	-	-	-
5-6	1	-	-	-	-	1	-	-	-	-	-	-	-	-
6-7	2	1	3	1	-	3	2	1	-	-	-	-	-	-
7-8	1	-	-	-	-	-	-	-	1	-	-	-	-	-
8-9	0	-	-	-	-	-	-	-	-	-	-	-	-	-
9-10	2	-	-	-	-	-	-	1	1	2	4	-	-	-
10-11	1	-	-	-	-	-	1	2	-	1	-	-	-	-
11-12	0	-	-	-	-	-	-	-	-	-	-	-	-	-
12-13	1	-	-	-	-	-	-	-	1	-	-	-	-	-
Total	31	8	43	36	6	10	3	4	3	3	4	-	-	-

The left column displays estimated age-at-death for individuals displaying Harris lines. Column "n" represents the number of individuals with observed Harris lines per age category. The rows represent the frequencies for Harris line age-at-formation.

A Test of Normality was used to determine if the HLs followed a normal distribution. The results of the test found the distribution to be non-normal at the 95% CI. Therefore, a Mann-Whitney U test were used in place of an Independent T-test. The independent variable used for this test was the Presence/Absence of HLs, and the dependent variables examined include: TA, CA, MA, CA/MA, %CA, BM, and FL. Infants aged fetal-0.99 years were excluded from the statistical analyses due to the lack of Harris lines present within this age category. Including the infants ages fetal-0.99 years would have significantly reduced the values in the Absent category for each of the dependent variables. The Mann-Whitney U test did find that individuals without HLs had

higher mean values in each of the dependent variables; however, none of the results were found to be statistically significant (p>0.05) (See Tables 18-21 for Mann-Whitney U results). Interestingly, when considering only individuals aged 1.0-3.99 the results are shown to be reversed for BM and FL, with these variables being larger in the Present category (See Table 4.21). Chi-square tests were performed for FL and BM as they met the minimum sample size requirement of 50. All Chi-Square tests failed to produce statistically significant results (p>0.05) at the 95% CI. See Tables 4.22-4.23 for Chi-square results.

Table 4. 18 *Mann-Whitney U Test Results for Geometric Variables Based on the Presence/Absence of Harris Lines (Ages 1.0-12.49)*

	Present	Absent	
	n=26	n=22	
	Mean Rank	Mean Rank	Z-Value
TA	21.73	27.77	-1.490
CA	21.77	27.73	-1.469
MA	22.65	26.68	-0.993
CA/MA	21.73	27.77	-1.490
%CA	22.62	26.73	-1.014

Legend – Present = Harris line(s) present; Absent = Harris line(s) absent; n = Number of individuals analyzed; TA = Total Area; CA = Cortical Area; MA = Medullary Area; CA/MA = Cortical Area/Medullary Area; %CA = Cortical Area/Total Area
**Significant at the 0.05 level; No Significant Results*

Table 4. 19 *Mann-Whitney U Test Results for Body Mass and Femoral Length based on the Presence/Absence of Harris Lines (Ages 1.0-12.49)*

	Present	Absent	
	n=31	n=24	
	Mean Rank	Mean Rank	Z-Value
BM	25.55	31.17	-1.290
FL	26.53	29.90	-0.772

Legend – Present = Harris line(s) present; Absent = Harris line(s) absent; n = Number of individuals analyzed; BM = Body mass; FL = Femoral length
**Significant at the 0.05 level; No Significant Results*

Table 4. 20 *Mann-Whitney U Test Results for Geometric Variables Based on the Presence/Absence of Harris Lines (Ages 1.0-3.99)*

	Present	Absent	
	n=16	n=10	
	Mean Rank	Mean Rank	Z-Value
TA	13.19	14.00	-0.264
CA	13.00	14.30	-0.422
MA	13.75	13.10	-0.211
CA/MA	12.31	15.40	-1.001
%CA	13.31	13.80	-0.158

Legend – Present = Harris line(s) present; Absent = Harris line(s) absent; n = Number of individuals analyzed; TA = Total Area; CA = Cortical Area; MA = Medullary Area; CA/MA = Cortical Area/Medullary Area; %CA = Cortical Area/Total Area
**Significant at the 0.05 level; No Significant Results*

Table 4. 21 *Mann-Whitney U Test Results for Body Mass and Femoral Length based on the Presence/Absence of Harris Lines (Ages 1.0-3.99)*

	Present	Absent	
	n=21	n=12	
	Mean Rank	Mean Rank	Z-Value
BM	17.52	16.08	-0.412
FL	18.26	14.79	-0.993

Legend – Present = Harris line(s) present; Absent = Harris line(s) absent; n = Number of individuals analyzed; BM = Body mass; FL = Femoral length
**Significant at the 0.05 level; No Significant Results*

Table 4. 22 *Chi-square results for the Number of Small Body Mass and Average Body Mass individuals based on the Absence/Presence of Harris Lines*

	Number of Individuals	
Body Mass	With Harris Lines	Without Harris lines
Small	9	6
Average	22	18

Chi-square=0.111, P=0.739
Legend – Small = below -2 standard deviations; Average = Met growth expectations

Table 4. 23 *Chi-square results for the Number of Small Femoral Length and Average Femoral Length individuals based on the Absence/Presence of Harris Lines*

	Number of Individuals	
Femoral Length	With Harris Lines	Without Harris lines
Small	17	18
Average	14	6

Chi-square=2.376, P=0.123
Legend – Small = below -2 standard deviations; Average = Met growth expectations

4.5 Porosity

Cross-sections were evaluated for evidence of diagenesis, microbial tunnelling, and taphonomic damage (Robbins Schug & Goldman, 2014). Samples demonstrating diagenetic infilling, microbial tunnelling, or taphonomic damage which obscured or effected pore visibility were excluded from analysis as the inclusion of these individuals could potentially lead to an under- or overestimation of pore volume (pore area/cortical area; %pore) in the sample. Due to a higher prevalence of diagenetic inclusions and taphonomic damage in older children and adolescents, porosity was only calculated for individuals aged fetal-2.99 years who displayed sufficient preservation for pore analysis (n=44). Rather than separating these individuals into the age categories assigned for all other variables, individuals examined for porosity were divided into five new age categories (fetal-0.49; 0.5-0.99; 1.0-1.49; 1.5-1.99; 2.0-2.99). The final age category considered (2.0-2.99) represents individuals within a full year rather than half year due to small sample size. When considering the age categories in 0.5 and 1.0 year intervals, a clearer pattern is evident in the data, with individuals aged 0.5-0.99 years and 1.0-1.49 years having significantly higher mean pore volume (%pore) compared to all other age categories (See Figure 4.8).

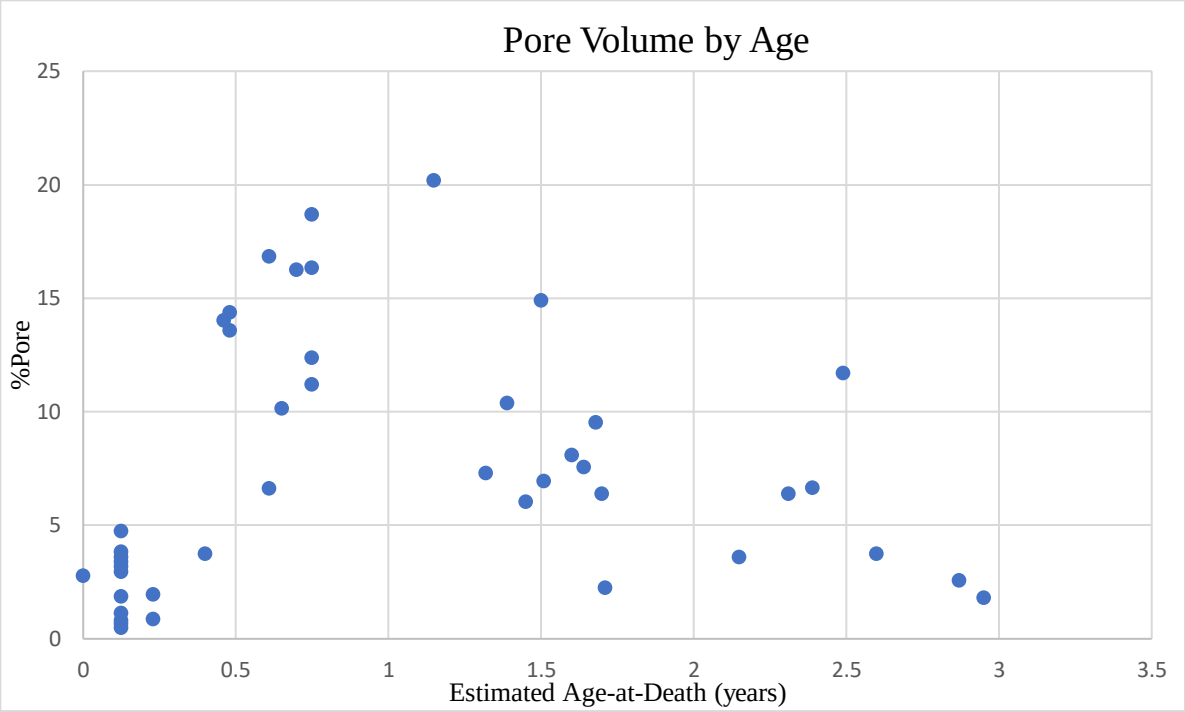

Figure 4. 8 *Scatter plot of estimated Age-at-Death vs. Pore Volume (%pore) in the St. Étienne sample.*

To analyze the statistical differences in %pore within the sample, individuals were assigned to one of two body size groups based on different variables including: BM and FL. Individuals who met body size expectations (above -2 SDs) will be hereafter referred to as "average" and individuals who did not meet these growth expectations (below -2 SDs) will be hereafter referred to as "small". A Test of Normality was used to determine if %pore was normally distributed in the BM and FL data sets. The results of the test found the distributions to be non-normal ($p<0.05$). Therefore, nonparametric Mann-Whitney U tests were used in place of Independent T-tests. The Mann-Whitney U tests were used to determine if there are significant differences in %pore between average and small individuals when examining BM and FL z-scores. The statistical test did not find a

significant (p>0.05) difference in %pore between average and small individuals when examining BM and FL. See Tables 4.24-4.25 for statistics.

Table 4. 24 *Mann-Whitney U Test Results Examining Pore Volume in Individuals with Small Body Mass and. Average Body Mass*

	Small	Average	
	n=12	n=32	
	Mean Rank	Mean Rank	Z-Value
Body Mass	21.33	22.94	-0.369

Legend – Small = below -2 standard deviations; Average = Met growth expectations; n = Number of individuals analyzed
**Significant at the 0.05 level; No Significant Results*

Table 4. 25 *Mann-Whitney U Test Results Examining Pore Volume in Individuals with Small Femoral Length and Average Femoral Length*

	Small	Average	
	n=20	n=22	
	Mean Rank	Mean Rank	Z-Value
Femoral Length	24.70	18.59	-1.612

Legend – Small = below -2 standard deviations; Average = Met growth expectations; n = Number of individuals analyzed
**Significant at the 0.05 level; No Significant Results*

While body size is not a statistically significant factor contributing to variation in %pore, age is (See Table 4.26 for descriptive statistics). Infants fetal-0.49 years of age have the lowest %pore with a mean of 4.33%. Pore volume (%pore) then greatly increases in the infant 0.5-0.99 and children 1.0-1.49 years of age with a mean %pore of 13.55% and 10.96% respectively. After the age of 1.5, %pore begins progressively decreasing with children 1.5-1.99 and 2.0-2.99 years of age having a mean %pore of 7.95% and 5.2% respectively. An Independent-Samples Kruskal-Wallis test found that the five age categories differed significantly (p<0.05) (Figure 4.9).

Table 4. 26 *Descriptive Statistics for Pore Volume (%pore) by Age Category*

Age Categories (years)	Mean	N	Standard Deviation	Minimum	Maximum
1 (Fetal-0.49)	4.33	18	4.62	0.48	14.37
2 (0.50-0.99)	13.55	8	4.12	6.61	18.67
3 (1.0-1.49)	10.96	4	6.41	6.02	20.17
4 (1.50-1.99)	7.95	7	3.81	2.24	14.90
5 (2.0-2.99)	5.20	7	3.38	1.80	11.68
Total	7.32	44	5.54	0.48	20.17

Legend – N = Number of individuals analyzed

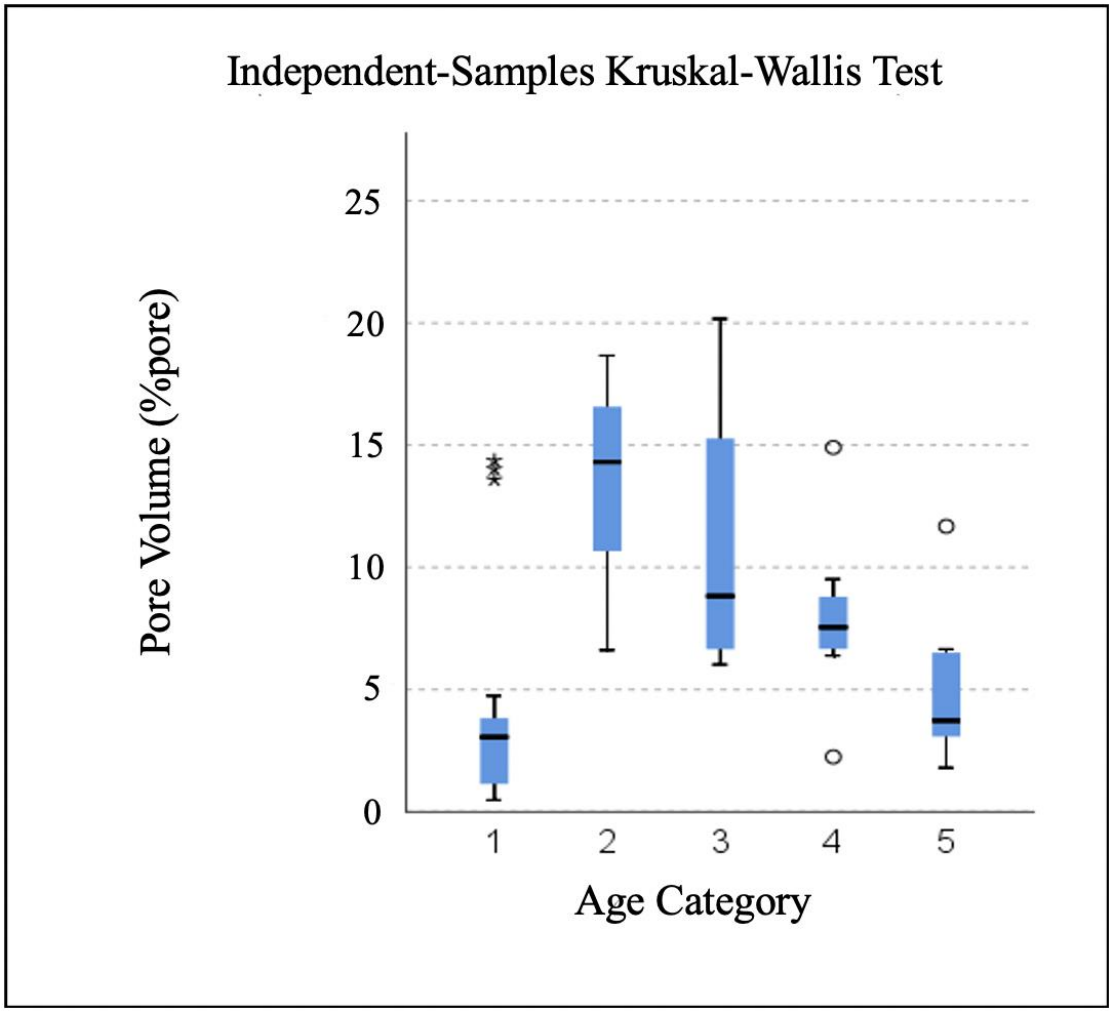

Figure 4. 9 *Box-and-whisker plots for Pore Volume (Pore Area/Cortical Area; %pore) based on age categories. Mean pore volume significantly differs between age categories at the 0.05 level. Outliers are represented by circles and extreme outliers are represented by stars.*

Chapter 5: Discussion

5.0 Discussion

In this chapter, the major findings from the explorations into femoral growth stunting, body mass estimates, midshaft geometric properties, Harris lines, and cortical porosity are discussed in relation to the medieval subadults from the St. Étienne cemetery of Toulouse, France. The interpretations and implications of the results will be placed in the context of previous research surrounding childhood growth and development.

5.1 Childhood Growth Disruption in Medieval Toulouse

5.1.1 Femoral Growth Disruption and Body Mass Estimates

Linear and appositional growth are an effective measure of growth disruption and environmental stress frequently used in bioarchaeological studies (Cardoso, 2005; Dori et al., 2020; Geber, 2014; Gooderham et al., 2019; Ives & Humphrey, 2018; Mays et al., 2009; Newman et al., 2019; Schillaci et al., 2011). The infants and young children (fetal-3.99 years) at St. Étienne underwent a considerable amount of growth disruption indicated by restricted linear and appositional femoral growth, when compared to the reference collection of modern healthy individuals. However, these growth deficits become progressively ameliorated in individuals that died after the age of four, with older children and adolescents attaining similar outcomes in terms of linear and appositional growth as those in the modern Denver sample. These results suggest that those who survived to a later stage of childhood either did not experience the same severity of growth disruption as those who died at a younger age or that they were able to achieve catch-up growth following earlier periods of growth disruption. Additionally, the

increased femoral means present in older children and adolescents likely skewed the femoral length results, thereby potentially preventing the Independent t-test from reaching statistical significance (See Table 4.3).

A significant proportion of the subadult population at St. Étienne likely suffered from various forms of malnutrition. Infants and young children (fetal-3.99 yrs) demonstrated the highest rates of stunting and being underweight-for-age; collectively, 61.5% were classified as stunted and 27.5% as underweight-for-age (See Tables 4.2 & 4.8). Individuals classified at stunted or underweight-for-age (< -2 SDs) are considered to be moderate-to-severely malnourished (Cogill, 2003, p. 41-42). Additionally, many individuals in this age category also fell between -1 and -2 SDs when considering femoral length (26.1%) and body mass estimates (39.1%) (See Appendix III). According to the WHO reference standards, falling between -1 and -2 SDs is evidence of mild malnutrition (Cogill, 2003, p. 42). Malnutrition may be caused by either one, or a combination of, the following factors: inadequate caloric intake, disease, or incorrect feeding practices (Cogill, 2003, p. 11-12). Malnutrition has also been associated with reduced %CA in children (Garn et al., 1969; Himes et al., 1975).

All aspects of growth and development assessed were found to be below expected levels in those who died in the youngest age categories (0.0-3.99 years), with lower than expected total areas and reduced %CA and CA/MA. Small-for-age total areas indicate that individuals are experiencing reduced periosteal deposition, which may be linked to both poor diet and reduced mechanical loading (Ruff, 1994). These results are especially apparent in the 2.0-3.99 age category, with individuals in this category experiencing the

highest rates of stunting, low body mass-for-age, and small-for-age total areas within the sample. The observed decline in %CA and CA/MA begins at approximately one year of age and continues until approximately four years of age. After the age of four, %CA and CA/MA increase significantly. Rather than a linear increase as can be observed in other growth variables such as femoral length, body mass, total area, medullary area, and cortical area (See Figure 4.2 and 4.4), %CA and CA/MA present more of a V- or U-shaped trajectory. This type of ontogenetic trajectory is also found by Swan et al. (2020) when considering the CA/MA ratio. However, in the sample examined by Swan et al. (2020) the CA/MA ratio begins to climb again for individuals aged 2.0-3.99 years, while in the current study the same age category experiences the lowest CA/MA ratio. Additionally, while the total areas and %CAs are significantly smaller than their modern counterparts (See Tables 4.14 & 4.15), the increased periosteal deposition and endosteal resorption, which results in an expanded medullary cavity and reduced %CA, is a pattern previously described in forensic and archaeological collections (Goldman et al., 2009; Gosman et al., 2013; Ruff et al., 1994; Swan et al., 2020).

Ruff (2003) observed a peak in femoral growth velocity in the first two years of life in nearly all individuals in the modern Denver sample. This acceleration in femoral diaphyseal growth is especially apparent after 1.5 years of age (Gasser et al. 1991) and begins to decline between approximately 2 to 3 years of age until puberty (Rogol & Hayden, 2014; Ruff, 2003; Smith & Buschang, 2004; Szulc et al., 2000). The expected acceleration in femoral diaphyseal growth that occurs during the first two years of life likely contributes to the heightened prevalence of growth disruption observed in this age

category, since critical periods of growth are most susceptible to disruption from environmental stressors such as malnutrition (Pinhasi et al., 2006). Growth disruption is especially apparent in rapidly growing long bones such as the femur (Cardoso & Magalhães, 2011).

Infants who are underweight-for-age and experiencing diaphyseal stunting in the first few months following birth, may have been born to malnourished mothers. Maternal malnutrition can restrict intrauterine growth, which is associated with increased perinatal morbidity and mortality (Belkacemi et al., 2010; Papathakis et al., 2016). Subsequently, if maternal nutritional status does not improve following birth, infants may receive a suboptimal amount of breastmilk (Khan et al., 2019) or nutritionally deficient breastmilk (Allen, 2005). Therefore, poor maternal nutrition could have contributed to the growth stunting, low body mass, and mortality of those that died at the youngest ages (fetal-0.99 years) in the St. Étienne collection. The current thesis only considers subadult individuals from the study population. However, health assessments of women of childbearing age as well as incremental dentine studies examining stable isotope data and mineralization defects in teeth that formed in utero can aid in understanding maternal health during pregnancy (Beaumont et al., 2015; Brickley et al., 2020b; Mays, 2010). By combining both the health assessments of infants and women of childbearing age from a population, a more holistic view of mother-infant health can be examined.

While maternal nutritional status likely contributed to the stunting in infants (0.0-0.99 years), weaning and cessation of breastfeeding likely exacerbated this effect in young children (1.0-3.99 years). Very little is known regarding the care practices of

children in medieval Europe (Saunders et al. 1994); however, historians have suggested that the commencement of weaning likely occurred during the first two years of life in medieval France (Fildes, 1986; Kibler et al., 1995, p. 409). Similarly, stable isotope data of individuals from the medieval (13^{th}-15^{th} century) archaeological site of Saint-Laurent in Grenoble, a city in Southeast France, finds that weaning occurred between the ages of 2.6 and 3.3 years (Herrscher, 2003). Reduced relative cortical area, femoral length, and body mass in the St. Étienne children aged approximately 2.0-3.99 years of age aligns with the previous historical and isotopic studies describing the onset of complementary feeding and cessation of breastfeeding in medieval France.

Malnutrition and disease are two of the most important factors that contribute to the slowing or stunting of growth (Cogill, 2003; Scheuer & Black, 2004, p. 3). Therefore, poor infant feeding practices may be a major contributor to growth disruption in developing infants as inadequate complementary feeding may increase the risk for malnutrition and disease (Ali et al., 2018; Miller, 2020; Mkhize & Sibanda, 2020). The onset of complementary feeding is a significant stressor for infants because as individuals rely less on breastmilk, their risk of exposure to food shortages and overreliance on nutritionally inferior foods, such as cereal grains, increases (Leonard et al., 2000; Rousham & Humphrey, 2002; Saunders et al. 1994). Additionally, WHO guidelines suggest that infants will often become iron deficient by 6-months of age, at this stage iron rich complementary foods are required (Pérez-Escamilla et al., 2019). The introduction of low protein and high phytate complementary foods, such cereals made into gruel, would

likely have contributed to micronutrient deficiencies, such as iron deficiency anemia, and reduced growth potential.

Once breastfeeding ceases, infants will no longer be receiving passive and collaborative immunity, thereby increasing their risk of various diseases as well as mortality (Bourbou et al., 2013; Dittmann & Grupe, 2000; McDade, 2003). Both bioarchaeological and modern studies also support the interpretation that inadequate infant feeding strategies can be associated with growth stunting (Espo et al., 2002; Gurven, 2012; Ives & Humphrey, 2017; Leonard et al., 2000; Padmadas et al., 2002; Wall, 1991). Therefore, inadequate nutrition and/or disease insults resulting from the onset of complementary feeding and cessation of breastfeeding are likely major contributing factors to the high levels of growth stunting and mortality in children aged approximately 2.0-3.99 years in the St. Étienne sample.

After the age of four, no individuals from St. Étienne are classified as underweight-for-age and the prevalence of diaphyseal stunting progressively decreases for individuals aged 4.0-8.99 years and 9.0-12.49 years (See Tables 4.2 & 4.8). The trend of ameliorating deficits similarly continues when considering variables such as total midshaft area and %CA. Older children (4.0-8.99 years) would have likely finished the process of weaning, but may not all have experienced catch-up growth in regards to diaphyseal length. Whereas, the significant improvement in diaphyseal length observed in adolescent individuals (9.0-12.49 years) indicates that catch-up growth likely occurred. Catch-up growth is characterized by an increase in growth velocity to the original or maximum growth trajectory following a period of growth disruption (Agarwal, 2016;

Cameron, 2002; Stinson, 2000; Temple, 2008; Wit & Boersma, 2002). The ability to attain catch-up growth depends on a various factors including: the degree of nutrient deprivation, severity or duration of disease episodes, and whether nutrition improved during the post-deprivation period (Pinhasi et al., 2006; Weaver & Fuchs, 2014). However, catch-up growth is difficult to identify in cross-sectional bioarchaeological studies since the study cannot examine the growth of an individual over time (Timmins, 2016). Moreover, because catch-up growth may obliterate evidence of previous growth disruptions (Watts, 2013), interpretations of catch-up growth for individuals displaying normal growth trajectories in cross-sectional studies should be made with caution, as these individuals may not have previously experienced growth delays that required catch-up growth to occur. Taking these issues into consideration, the significant improvement in body mass, femoral length, and %CA occurring in the adolescents (9.0-12.49 years) does indicate an improvement in nutritional input and/or lack of disease load (See Tables 4.2, 4.8, & 4.12). Moreover, because older subadults were likely experiencing the adolescent growth spurt (Moncrieff et al., 1973; Szulc et al., 2000), which results in an increased need for calories, protein, and minerals such as calcium (Christian & Smith, 2018; Spear, 2002), their improvement in diaphyseal length and body mass points to adequate nutritional intakes during this period of growth. Additionally, periods of high bone turnover, such as during the pubertal growth spurt, may increase the response rate to skeletal growth recovery (Weaver & Fuchs, 2014). Other bioarchaeological researchers have established similar trends regarding the amelioration of femoral stunting occurring after the age of four (Wall, 1991) as well as in older children and adolescents (Dori et al.,

2020). Therefore, the onset of puberty may be a critical period for growth recovery when adequate energy is available.

Some clinical and archaeological studies have found catch-up growth to occur longitudinally at the expense of cortical bone accrual (Garn et al., 1964; Hummert, 1983; Huss-Ashmore et al., 1982; McEwan et al., 2005), whereas other studies have found catch-up growth to occur more rapidly for cortical thickness compared to longitudinal growth (Barr et al., 1972). The variability in findings between these studies could, in part, be due to the age categories assessed, type of sample examined (archaeological vs. contemporary), as well as the element used; as the studies mentioned above have examined various elements including: metacarpals, tibiae, femora, and radii. Additionally, population differences in mobility and mechanical loading have been shown to affect appositional growth and cortical thickness (Ruff, 1994). When considering individuals from St. Étienne, both linear and appositional growth have largely recovered to expected values by adolescence (9.0-12.49 years). Whereas other archaeological samples, such as Wharram Percy, do not exhibit the same degree of growth recovery during later childhood (Mays, 1999; Mays, 2010). After the cessation of breastfeeding (approximately 1.0-2.0 years of age), individuals at Wharram Percy were consistently smaller than the modern Denver sample when considering both linear growth and cortical thickness. Unlike in the current study, individuals at Wharram Percy continued to have small-for-age cortical thickness well into late childhood and adolescence, indicating that individuals at Wharram Percy were unable to catch-up to modern expectations. Mays (1999, 2010) suggests that their inability to achieve modern expectations is likely due to insufficient

resources. While studies have found catch-up growth in both long bone length and cortical thickness to occur, cortical thickness has been considered a more reliable indicator of stress in past populations when compared to diaphyseal length.

Bioarchaeological studies suggest that cortical thickness is a sensitive indicator of environmental stress and growth disruption in children. McEwan et al. (2005) found positive correlations between linear growth, dental age, and total cortical width (appositional growth) in the Wharran Percy subadult collection. However, none of these variables were correlated with cortical index (CI). McEwan et al. (2005) suggest that this result indicates that CI is a more sensitive indicator of environmental stress. Mays et al. (2009) likewise found cortical thickness to be a more sensitive indicator of environmental stress in the St. Martin's churchyard collection. This thesis supports these findings, as while body mass and femoral length did not differ significantly from the Denver reference sample, %CA was significantly reduced. This study, as well as the studies of McEwan et al. (2005) and Mays et al. (2009) represent different temporal and socio-cultural backgrounds, yet have produced similar results, indicating a fundamental pattern. The pattern is, that while total area increases with age as the periosteal surface expands, bone is resorbed at the endosteal surface at an accelerated rate, causing a comparatively reduced %CA in the population, especially in infants and young children (0.0-3.99 years). The increase in %CA observed in the older children (4.0-8.99 years) and adolescents (9.0-12.49 years) at St. Étienne suggests a reversal to net deposition at the endosteal surface, leading to the contraction in the medullary cavity (Goldman et al., 2009). It has been suggested that the change from net endosteal resorption to net endosteal formation that

occurs during adolescence is influenced by age-related hormonal changes (Ruff et al., 1994, p. 52). Therefore, it is likely that both hormonal changes resulting from the start of puberty and reduced environmental stressors contributed to the increase in %CA present in the older age categories at St. Étienne.

5.1.2 Reference Population and Mortality Bias

The individuals at St. Étienne were consistently smaller than the Denver reference sample as the total midshaft area and %CA values were found to differ significantly (See Tables 4.14 & 4.15), indicating that St. Étienne individuals were unable to achieve the same level of periosteal expansion and cortical thickness at the midshaft. However, while both femoral length and body mass were also smaller in the St. Étienne individuals, these results did not reach statistical significance (See Tables 4.3 & 4.9). While the results of this study reveal that subadults from St. Étienne are smaller for their age when compared to the modern Denver reference sample, it could be suggested that some of the growth disruption is partially the result of the mortality bias, since the Denver population is derived from healthy living children and the St. Étienne sample consists of non-survivors. However, Saunders and Hoppa (1993) examined the effect of the mortality bias in subadult individuals and found that while archaeological individuals had consistently smaller diaphyseal lengths, thereby creating the potential for the bias to exist, that the effect should be too small to detect. Therefore, while some of the interpretations may have been minorly influenced by the mortality bias, it is likely that the effect of this bias is insignificant to the overall results of this thesis.

5.2 Geometric Properties

5.2.1 Midshaft Shape

The St. Étienne sample generally conforms to the ontogenetic changes in midshaft shape described by previous researchers (e.g Cowgill et al., 2010; Goldman et al., 2009; Gosman et al., 2013; Swan et al., 2020). Individuals at St. Étienne exhibit a femoral midshaft shape that is mediolaterally reinforced until approximately four years of age, after which their midshaft shape becomes progressively more reinforced in the anteroposterior plane. The results of this study provide information regarding the influence of different biomechanical behaviours on midshaft shape change, as well as highlights the high intra- and inter-population variability that exists during development, which may be influenced by cultural norms and the seasonal environment.

During development, the immature femur changes morphologically based on transitions in mechanical loading and locomotion (Cowgill et al., 2010; Swan et al., 2020). One of the most notable changes is the femoral midshaft shape (See Figure 5.1), which can be inferred and compared using second moment of area ratios such as I_x/I_y. Cowgill et al. (2010) was one of the first publications to examine shape changes in the femoral midshaft of subadults using a large sample from seven different modern human skeletal collections. When comparing the St. Étienne sample to Cowgill et al. (2010), the mean I_x/I_y ratio of infants and young children (0.0-1.99 years) is similar, with the mean I_x/I_y ratios being 0.898 and 0.879 respectively. Though, when comparing the St. Étienne sample to that of the 18^{th}-19^{th} century archaeological samples from London, UK, analyzed by Swan et al. (2020), there are significant differences at certain ages and stages

of development. The current study exhibits a significantly more mediolaterally reinforced shape when considering infants aged 0.0-0.49 years, and a more circular shape when considering children aged 1.0-1.99 years (See Table 4.16). While both studies exhibit similar ranges in I_x/I_y ratios for infants aged 0.0-0.49 years and children aged 1.0-1.99 years, the differences in midshaft shape were statistically significant (See Table 4.11; See Swan et al., 2020, Table 4). The significant differences observed between these two studies could be due to high intra- and inter-population midshaft shape variability during infancy. It is also possible that differences could be the result of modalities used and methods of aging, as Swan et al. (2020) used micro-CT data to acquire a 50% midshaft image and documented-age-at death, while the current study used destructive histology and age estimation methods. Additionally, significant differences in midshaft shape between the two study samples could also be due to physiological and cultural factors influencing locomotor behaviour.

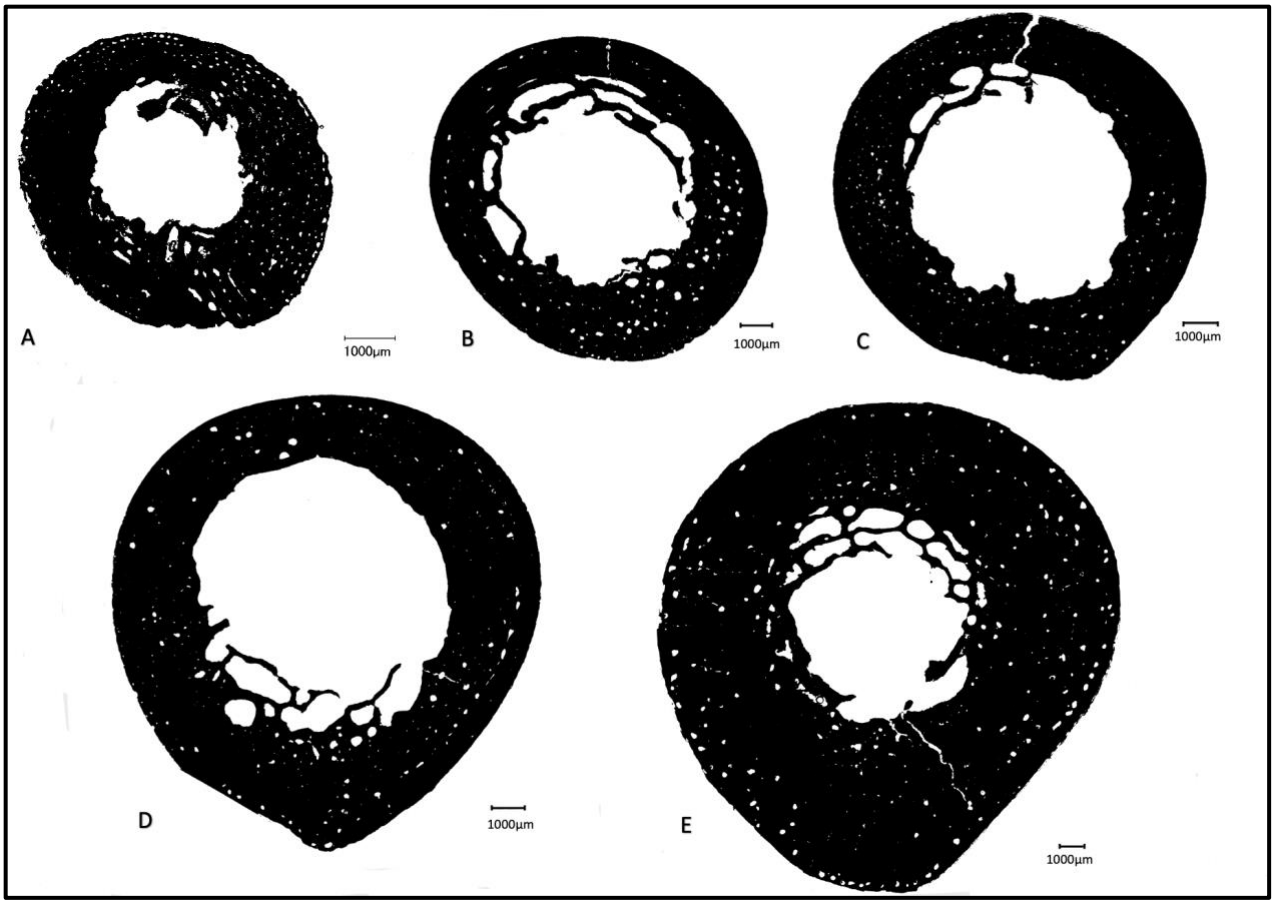

Figure 5. 1 *Displays the changes in femoral shape across the five age categories. Midshaft shape transitions from being more mediolaterally reinforced to being more anteroposteriorly reinforced with age. A) Individual BN-91 represents individuals fetal-0.99 B) Individual BN-103 represents individual 1.0-1.99 C) Individual BN-40 represents individuals aged 2.0-3.99 D) Individual BN-10 represent individuals aged 4.0-8.99 E) Individuals BN-158a represents individuals aged 9.0-12.49. All individuals are oriented medial=left and posterior=down.*

While little research has been conducted to examine the physiological factors influencing variation in infant midshaft shape, variability may, in part, result from differences in locomotor activity and hip abduction. At approximately 11 weeks gestation sporadic muscle contractions cause intrauterine punching and kicking (Acquaah et al., 2015; Reissis & Abel, 2012). Intrauterine kicking is often a clinical sign of fetal well-being (Rauch & Schoeneau, 2001b) and may be considered a form of pre-weight bearing resistance training for the lower limbs (Acquaah et al., 2015). However, the amount of

force imposed on the fetal skeleton during intrauterine movement is not known (Rauch & Schoenau, 2001b). Variation in fetal activity levels may provide an explanation for the variation observed in midshaft shape for young infants at St. Étienne. While, variation in pre- and post-natal non-weight bearing lower limb movement may influence variation in midshaft shape, the immature bipedal gait is known to significantly increase mediolateral reinforcement. Children under four years of age often use a wide abducted stance and appear to have a waddling gait when walking (Cowgill et al., 2010). Gait matures with age as the femora become adducted, and more force is placed anteroposteriorly, causing the midshaft to become more reinforced in the anteroposterior plane (Cowgill et al., 2010). Waddling and/or abducted gaits are associated with high mediolateral forces in the lower limbs of children (Cowgill et al., 2010), obese adults (Agostini & Ross, 2011), as well as other animals such as penguins (Griffin & Kram, 2000) and non-human primates (Nakatsukasa et al, 1995). Additionally, increased bi-iliac breadth is associated with femoral diaphyses that are strengthened in the mediolateral plane (Shaw & Stock, 2011). Therefore, differences in fetal movement, limb abduction, and bi-iliac breadth during infancy and early childhood may contribute to midshaft shape variability.

Cultural norms influencing infant clothing may also affect infant locomotion and femoral shape variability. Diaper wearing has been shown to affect infant walking by increasing step width, thereby decreasing infant stability and exacerbating their already abducted immature gait (Cole et al., 2012). This effect is intensified by old fashioned cloth diapers (Cole et al., 2012), which would likely be similar to the diaper option available to infants in medieval Europe (Levin, 1970). Additionally, the season in which

an infant is born has also been shown to affect the attainment of motor milestones (Atun-Einy et al., 2013; Benson, 1993). When examining 7-month old infants, Atun-Einy et al. (2013) found that individuals born during winter-spring months attained locomotor skills, such as crawling, sooner than those born during summer-fall months. However, this finding is also likely linked to heavier clothes worn during cold months, as Hayashi (1992) found that infants wearing heavy bedclothes and long-sleeved jackets or rompers did not attain certain motor milestones as quickly as infants wearing lighter clothes due to restricted movement. Additionally, the frequent use of straight leg swaddling, which adducts and restricts movement of the lower limb (Nowlan, 2015), may also influence midshaft development in pre-weight bearing (<6-months of age) infants; as bones only subjected to torsion, rather than loading, would likely exhibit a more circular shape (Ruff & Hayes, 1983). Thus, cultural and temporal differences in swaddling, diaper use, as well as cultural and climatic influences on clothing choices could be contributing to the midshaft shape variability observed among different archaeological samples of young infants, such as that observed among the St. Étienne and Swan et al. (2020) samples, by altering gait stance and restricting lower limb movement.

In regards to St. Étienne, it is unlikely that children would have been restricted by heavy bedclothing as paleoclimate data suggests that a warming phase occurred in Southern France from approximately the 11th-13th centuries (Lüning et al., 2019). Correspondingly, no subadults displayed evidence of vitamin D deficiency macro- or micro-structurally; the presence of which would suggest that individuals may be wearing concealing clothing and/or spending little time outdoors (Brickley et al., 2014).

Therefore, the increased mediolateral reinforcement observed in the infants (0.0-0.49 years) from the St. Étienne sample could indicate increased fetal activity levels and reduced use of swaddling, especially when compared to the Swan et al. (2020) sample. The high variability in midshaft shape during infancy (0.0-0.49 years) could also indicate that some infants were swaddled while others were not, which is supported by historical literature (Hanawalt, 2002; See Section 2.2.2). Therefore, some infants at St. Étienne may have experienced lower limb restriction during infancy, while others did not. The increase in anteroposterior reinforcement, resulting in a more circular midshaft shape, observed in the children 1.0-1.99 years of age at St. Étienne could indicate increased femoral adduction and reduction in waddling gait, compared to the children in the Swan et al. (2020) sample. Reduction in waddling gait in children 1.0-1.99 years of age may represent an earlier attainment of a more mature gait or the use of a thinner diaper fabric.

5.3 Harris Lines

5.3.1 Harris Line Frequency and Relationship to Skeletal Growth

Harris lines were found to be common in the St. Étienne collection with approximately half of individuals aged 1.0-12.49 years having at least one observable Harris line. The results of the current study contributes to the ongoing debate regarding the etiology of Harris line formation.

Harris lines were only observed to be present on the distal portion of the femur. This finding is congruent with the literature, as Harris lines have been found to be more common at the distal end of long bones (Goodman & Clark, 1981; Hughes, 1996). Harris lines are likely more common in the distal end of the femur because the distal end grows

more rapidly compared to the proximal end (Scheuer & Black, 2000, p. 385). The majority of the Harris lines formed between 1-2 (n=43) and 2-3 (n=36) years of age (See Table 4.17). The individuals presenting with Harris lines were predominantly young children aged approximately 1.0-3.99 years; indicating that these individuals had suffered and recovered from one or more episodes of growth disruption in the months and/or years leading up to their death. The interpretation that individuals aged 1.0-3.99 years had suffered from growth disruption is supported by the high prevalence of stunted and underweight-for-age individuals in these age categories (See Section 5.1). None of the older children from St. Étienne (7.0-12.49 years) display Harris lines that formed earlier than five years of age. This finding could indicate that those who lived to a later age did not undergo significant episodes of growth disruption earlier in life, or that potential Harris lines were resorbed due to bone remodelling (Alfonso et al., 2005; Alfonso-Durruty, 2011; Geber, 2014; McHenry & Schultz, 1976; Ribot & Roberts, 1996).

Studying the etiology of Harris lines is important for exploring growth disruption in the past. The presence or absence of Harris lines can provide meaningful interpretations for disrupted growth, especially at an individual level, when combined with other indicators of growth disruption, such as delayed linear and appositional growth (See Figure 5.2). When considering the entire sample of individuals aged 1.0-12.49 years, those displaying the presence of Harris lines are smaller in terms of linear and appositional femoral growth measurements as well as body mass compared to individuals without Harris lines; though this finding was not statistically significant (See Tables 4.18-4.19). However, this finding is likely attributed to the higher frequency of individuals

displaying Harris lines in the younger age groups (ages 1.0-4.99 years) compared to the older age groups (ages 5.0-12.49 years); thereby skewing the distribution (See Figure 5.3). When only considering individuals aged 1.0-3.99 years these findings are reversed for some of the growth variables. While still not statistically significant, young children (1.0-3.99 years) who exhibit the presence of Harris lines are larger in terms of femoral growth and body mass compared to those without Harris lines (See Tables 4.20-4.21). This is not an unexpected result when considering the etiology of Harris lines. Harris lines form due to the resumption of growth (Park, 1964; Zapala et al., 2016); therefore, individuals who have recovered from growth disruptions, as indicated by the presence of Harris lines, would have had a greater opportunity to resume linear and appositional growth compared to those without Harris lines. Similarly, severely stunted individuals likely would not have had the opportunity to recover from growth disruption and form a Harris line prior to death. There are examples of this at St. Étienne, as individuals BN-320 and BN-82-87 are severely stunted linearly with both being approximately -9 SDs from their respective means for femoral length and nearly -5 SDs from their respective means for total midshaft area (See Appendix III). Neither of these individuals present with femoral Harris lines (See Appendix V), indicating that they did not have the opportunity to resume linear growth and form recovery (Harris) lines prior to their death.

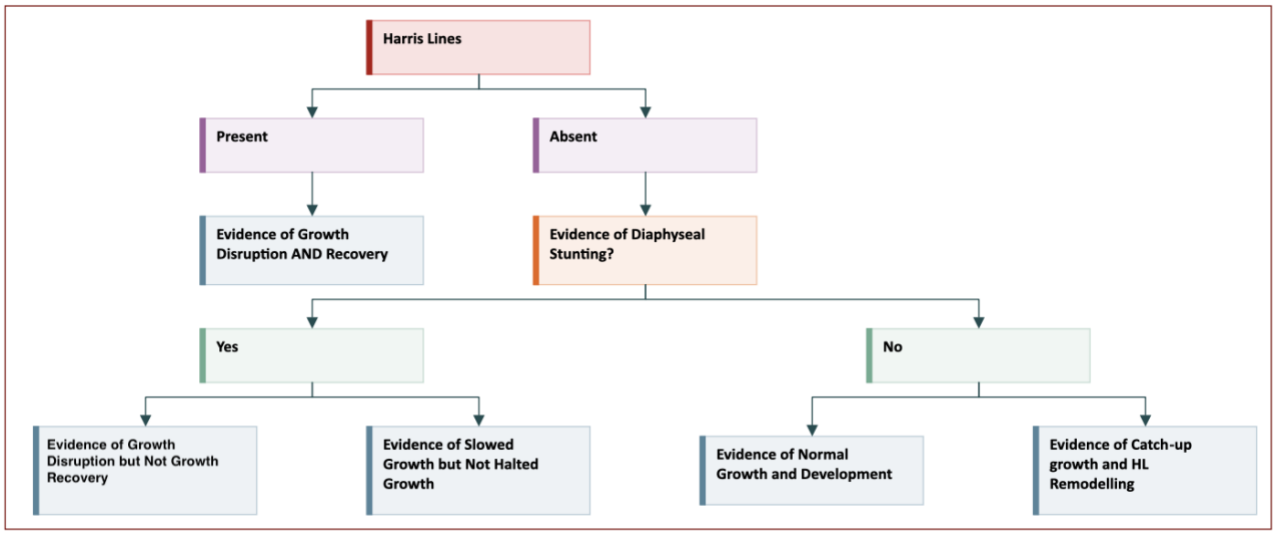

Figure 5. 2 *Flow chart presents possible interpretations when examining the presence and absence of Harris Lines.*

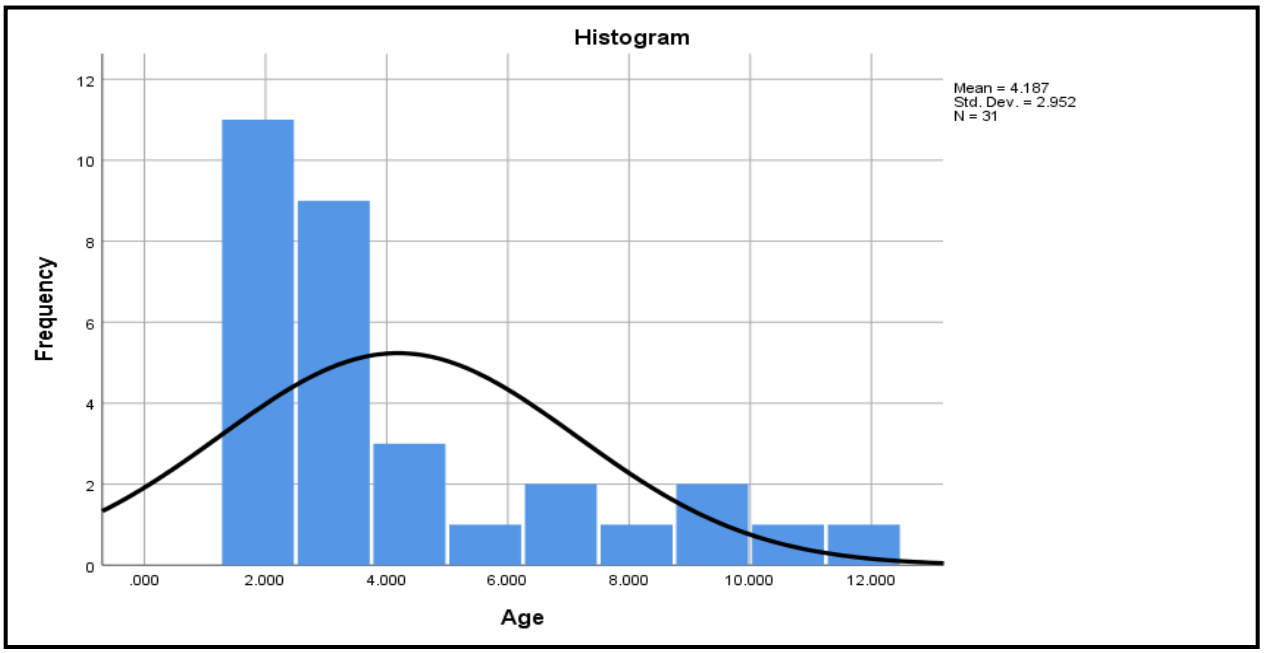

Figure 5. 3 *Histogram exhibits a slight skew towards individuals aged 2.0-4.99 years, demonstrating that younger individuals have higher frequencies of Harris lines compared to older individuals.*

The current data supports the pathological thesis for Harris line formation. As described above (See Section 5.1), poor maternal nutrition and inadequate infant feeding most likely contributed to the high prevalence of stunted and underweight-for-age children aged 1.0-3.99 years. This growth disruption is reflected in the high prevalence of

Harris lines in the same age categories. Therefore, it is likely these Harris lines formed due to growth disruptions from nutritional and/or disease stress, rather than solely accelerated growth, as suggested by the physiological thesis of HL formation (Alfonso-Durruty, 2011). Other bioarchaeological and contemporary studies have found comparable trends in Harris line age-at-formation to the current study (Ameen et al., 2005; Dittman & Grupe, 2000; Goodman & Clark, 1981; Ribot & Roberts, 1996), many of which have likewise attributed the growth disruption to infant feeding practices (Ameen et al., 2005; Dittman & Grupe, 2000; Goodman & Clark, 1981). Several studies have also found a second HL peak occurring between approximately 8 and 14 years of age (Ameen et al., 2005; Goodman & Clark, 1981; Hughes et al., 1996; Nowak & Piontek, 2002; Papageorgopoulou et al., 2011; Piontek et al., 2001), likely resulting from the increased nutritional demands of the pubertal growth spurt. No significant relationship was found between Harris line age-at-formation and the pubertal growth spurt in the current study; however, this is likely due to the small number of individuals who may have begun puberty, with only n=11 individuals aged between 9.0 and 12.49 years. Examination of older adolescents and adults would be required to confirm a second peak occurring around the pubertal growth spurt in this collection. Based on the data presented earlier in this chapter as well as the previous Harris line literature, it is likely that inadequate infant feeding practices and increased nutritional demands following periods of increased growth velocity are responsible for the peak in Harris line formation occurring between the ages of 1.0-2.99 years of age.

5.3.2 Previous Investigation of Harris Line Frequency at St. Étienne

This thesis is not the first to examine the prevalence of Harris line formation in the St. Étienne collection. Grolleau-Raoux et al. (1997) examined Harris line frequency in the distal tibia using a subadult and adult sample from the St. Étienne collection. Most studies use the tibia because even though Harris lines can occur in any long bone, they occur most frequently in the distal tibia (Garn et al. 1968; Park, 1964). Studies examining Harris line formation in both elements have found that the tibia often produces more Harris lines compared to the femur in both children (Spiller et al., 2020) and adults (Hughes, 1996).

The absence of Harris lines in individuals below the age of 1.0 year is consistent with Grolleau-Raoux et al. (1997); as they found the presence of Harris lines in this age category to be rare. Additionally, while both studies have found individuals aged 1.0-9.9 years to have observable HLs, the proportions of individuals experiencing them differ. Grolleau-Raoux et al. (1997) found 83.3% of individuals aged 1.0-4.9 years to have at least one Harris line and 100% of individuals 5.0-9.9 years have at least one Harris line. In the current study only 57.5% of individuals aged 1.0-4.9 have at least one Harris line and 37.5% individuals aged 5.0-9.9 have at least one Harris line. Grolleau-Raoux et al. (1997) did not make an attempt to age the tibial Harris lines; therefore, no direct comparison between Harris line age-at-formation can be made. The differences in Harris line proportions observed between the two studies could be associated with different individuals sampled from the collection as well as differing growth velocities between the

femur and tibia at different age stages. These results indicate that researchers should be cautious when comparing the HL frequencies when different elements are studied.

5.4 Cortical Porosity and Trabecularization

The cortical porosity results of this thesis produced an unanticipated outcome. Originally, it was hypothesized that pore volume would be higher in small individuals (stunted and underweight-for-age) when compared to average individuals (those who met growth expectations). However, porosity did not differ significantly based on femoral length or body mass, but on age. The individuals exhibiting increased midshaft porosity were almost exclusively confined to those aged approximately 0.5 to 1.49 years of age. The interpretation for this result is discussed below.

The increased porosity observed in individuals aged 0.5-1.49 years results from the trabecularization of pores close to the endosteal surface (See Figure 5.4). Trabecularized cortical bone at the endosteal surface mainly results from the remodelling, enlargement, and coalescence of existing canals (pores) (Andreasen et al. 2020, p. 8; Lerebours et al., 2015). This type of trabecularization of enlarged pores at the endosteal surface occurs due to excessive bone resorption and is commonly associated with age-related bone loss and osteoporosis (Andreasen et al., 2020; Bala et al., 2015; Bossy et al., 2004; Cooper et al., 2016; Zebaze et al., 2010). However, while in older adults the increase in trabecularized bone is associated with reduced elemental loading or hormonal imbalances, it is more likely that the increase observed in the St. Étienne infants and young children results from the reorganization and redistribution of bone stimulated by the onset of weight-bearing activities and increased infant growth velocity.

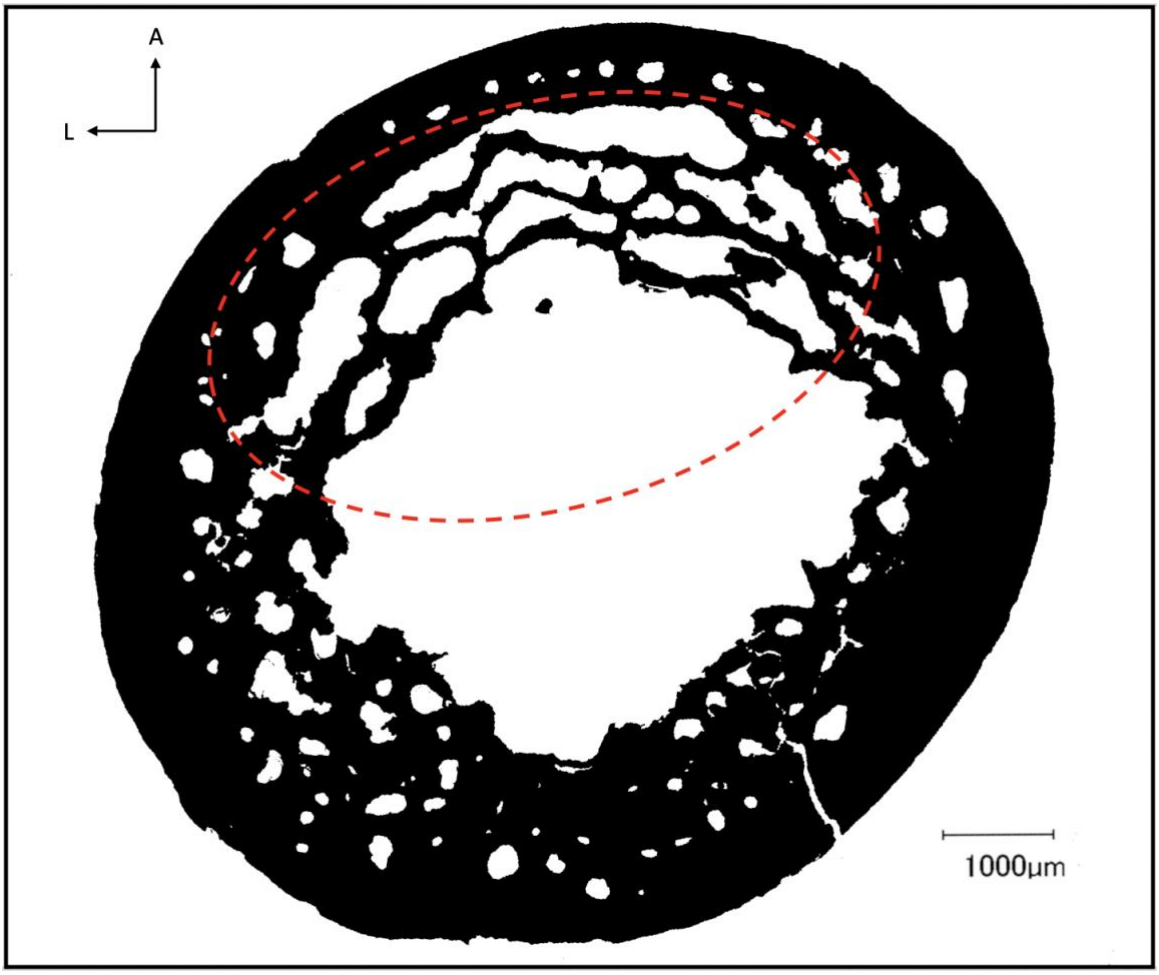

Figure 5. 4 *Displays the femoral midshaft cross-section of individual BN-352. This individual was approximately 0.7 years of age-at-death and exhibits a %pore of 16.24%. The red dashed oval indicates an area of increased trabecularization and large coalesced pores at the endosteal surface.*

Infants aged fetal to 6 months of age have one of the lowest mean %pore of the six age categories defined for this analysis, with a mean %pore of 4.33%. During this period, infants are unable to independently locomote, resulting in minimal loading to the femur (Swan et al., 2020). Individuals in this age category also experienced similar %CA as modern healthy children of the same age category. The high %CA at birth is thought to serve as a calcium reservoir for maintaining mineral homeostasis and for responding to loading demands during post-natal development (Acquaah et al., 2015). The mean %pore

increases significantly to 13.55% around approximately 6-months to 1 year of age. This increase coincides with the onset of regular femoral loading as behaviours such as sitting, hand-and-knees crawling, and standing develop between approximately 6-9 months of age (Bayley, 1969; Frankenburg et al., 1992; Martorell et al., 2006; Sutherland, 1997). During this period the total area of the midshaft nearly doubles from a mean of 33.9mm^2 in the fetal-0.49 age category to 62.3mm^2 in the 0.5-0.99 age category. Cortical area, however, does not increase at the same rate, as it only increases from a mean of 25.1mm^2 in the fetal-0.49 age cateogry to a mean of 38.6mm^2 in the 0.5-0.99 age category. Therefore, the majority of new bone appears to have been added to the periosteal surface rather than to the endosteal surface. Periosteal apposition is thought to be highly influenced by mechanical loading (Ruff, 1994). The results of this study support this hypothesis, since the significant increase in periosteal expansion corresponds with the onset of weight-bearing activity. Diaphyseal length also increases from a mean of 78.9cm in the fetal-0.49 individuals to a mean of 102.7cm in the 0.5-0.99 individuals (increase of 23.2%). These results suggest that cortical bone at the endosteal surface may be sacrificed to achieve normal appositional and endochondral development.

After 1 year of age, children begin walking without assistance (Bayley, 1969; Frankenburg et al., 1992; Martorell et al., 2006; Sutherland, 1997). The mean %pore for the 1.0-1.49 age category remains high with a mean of 10.96% (See Figure 5.5). Diaphyseal growth also remains high with a mean of 127.6 cm (increase of 19.3%). Though, compared to the 0.5-0.99 infants, the rate of periosteal expansion has slowed. The maintained high %pore and diaphyseal growth suggests that bone tissue is still being

relocated from the endosteal surface to other areas of the growing femora during this stage of development.

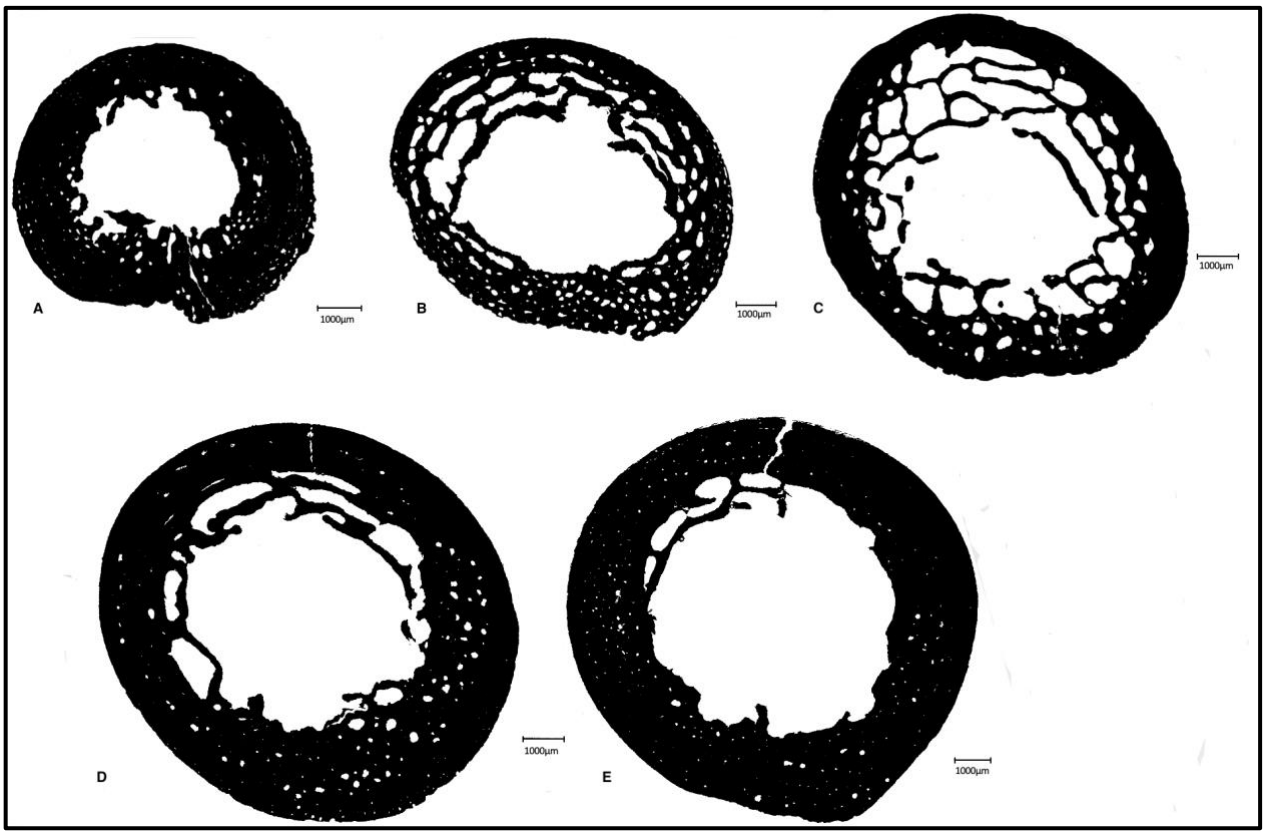

Figure 5. 5 *Displays the porosity exhibited by individuals in each age category. A) Individual BN-365b represents individuals aged fetal-0.49 with a pore% of 3.17% B) Individual BN-142 represents individuals aged 0.5-0.99 with a pore% of 18.67% C) Individual BN-365a represents individuals aged 1.0-1.49 with a pore% of 20.18% D) Individuals BN-103 represents individuals aged 1.5-1.99 with a pore% of 6.95% E) Individual BN-40 represent individuals 2.0-2.99 with a pore% of 3.78. All individuals are oriented medial=left and posterior=down*

In individuals aged 2.0-3.99 years, the immature gait becomes more mature, representing an intermediate stage in gait development (Swan et al., 2020). Correspondingly, the mean %pore and presence of trabecularized cortical bone in individuals 1.5-2.99 years of age decreases significantly from the 0.5-0.99 and 1.0-1.49 year values, indicating that the individuals are approaching some sort of homeostasis as their femora adapt to consistent mechanical loading and growth velocity slows.

Therefore, the increase in cortical porosity most likely results from the trabecularization of large coalesced pores, as cortical bone is redistributed from the endosteal surface to the periosteal margins (Swan et al., 2020) and diaphyseal ends. Ontogenetic patterns in bone tissue reorganization have likewise been observed in other areas of the lower limb corresponding with changes in locomotor behaviour (Gosman & Ketcham, 2009; Milovanovic et al., 2017; Ryan & Krovitz, 2006; Saers et al. 2020).

Calcium requirements are also higher in the first year of life compared to any other time during the life cycle (Matkovic, 1991), as the postnatal period is characterized by extremely high growth velocity of the skeleton (Lovejoy et al., 1990; Ruff, 2003). During periods of heightened calcium requirements, such as egg production, breastfeeding, or puberty in vertebrates, the midshaft of long bones act as calcium reservoirs and may become more porous and less dense as calcium is metabolized and used by other areas of the body (Parfitt, 1994; Prentice et al., 1995; Wink et al., 1987). Therefore, intensified calcium requirements needed for increased appositional and endochondral growth during infancy is likely another major contributor for the heightened endosteal porosity and redistribution of bone tissue in individuals aged 0.5-1.49 years.

Few studies have examined cortical porosity in infants and young children. Previously, research by Robbins Schug and Goldman (2014) examined the cortical porosity in a sample of subadults aged perinatal to 13-months from Inamgaon. Inamgaon was a village in prehistoric India and the individuals examined from this site date to 1400-700 BC. Their study found that subadults classified as small for their age (below -2

SDs for stature and BMI) had significantly higher %pore compared to individuals who met the expectations for stature and BMI. However, the current study did not detect a significant relationship between femoral length or body mass and pore volume. The discrepancies in the findings of the two studies can likely be attributed to sample size; as the Robbins Schug and Goldman (2014) study only had a sample of 11 subadults, while the current study had a total sample size of n=44 individuals, and more than double (n=25) the number of individuals in the same age category examined in the Robbins Schug and Goldman study. Additionally, while pore volume is not quantified in the Swan et al. (2020) publication, based on the comparative midshaft cross-sectional image in Figure 7b, individuals 0.5-0.99 years of age appear to have a larger pore area, and increased trabecularized bone, compared to the other age categories. Increased cortical porosity has been associated with increased fracture risk in both adolescents and adults (Cooper et al., 2016; Parfitt, 1994), as adolescents have similarly demonstrated phases of transient porosity during rapid periods of growth (Wang et al., 2010). Therefore, understanding the mechanisms that cause transient increases in cortical porosity during infancy could be useful for understanding skeletal fragility in both modern and archaeological infants and young children. Additionally, in order to recognize bone pathology in infants and young children for paleopathological and bioarchaeological studies, we must first understand what expected development looks like.

5.5 Children in Bioarchaeology and Life in Medieval Toulouse

Human skeletal remains are an important primary source of evidence for past societies. Unfortunately, the importance of the archaeological child was previously

neglected, and only over the last few decades has it begun to be acknowledged (Kamp, 2015). Previously, children were not viewed as social actors, capable of contributing to society in a meaningful way and were often disregarded in both archaeology and history (Orme, 2009). Additionally, when children were considered in bioarchaeological research the focus frequently fell on how childhood growth deficits could be used to provide information regarding the health of the adult population. In doing so, these studies often overlooked and negated the life experiences of the children themselves. This study highlights how both the maternal nutrition and infant feeding practices affected infant and early childhood health in medieval Toulouse.

Based on the linear, appositional, and Harris line data infants and young children aged fetal-3.99 years suffered from frequent periods of malnutrition and/or disease. Throughout the medieval period, individuals in this region of Europe frequently suffered from malnutrition due to frequent episodes of famine and food insecurity. During the period in which the cemetery was in use, France suffered from numerous famines, with approximately 48 famines occurring between the 10th and 11th centuries (Graves, 1917). Various ailments were also common during the medieval period in France including, but not limited to, bubonic plague, smallpox, tuberculosis, typhoid, measles, and various parasitic infections (Kacki et al., 2011; Kibler et al., 1995; p. 566; Mitchel, 2015; Roberts & Buikstra, 2020; Tran et al., 2011). The French city of Toulouse also suffered from numerous outbreaks of war and invasion (Benjamin, 2017; Chisholm, 1911; Mundy, 1954) and its population consumed primarily cereal crops (Duby & Mandrou, 1964, p. 7), thereby predisposing them to food insecurity and malnutrition. Frequent episodes of

malnutrition as well as disease were likely prevalent in the subadult population, thereby synergistically contributing to childhood stunting and mortality in medieval Toulouse, France.

5.6 Future Research

The explanation of maternal malnutrition and inadequate infant feeding practices was used to interpret the growth deficits observed in infants and children fetal-3.99 years of age. Further research using isotope data is required to confirm this hypothesis in the St. Étienne collection. Additionally, studies examining the health of women of childbearing age from the St. Étienne collection would likely aid in understanding infant growth deficits in the population. Thus, using adult health to aid in interpreting infant and early childhood health.

Moreover, because few studies have quantified midshaft cortical porosity in subadults using adequate sample sizes, further research is required to validate the findings of this thesis. Additional research is also required to examine the mechanisms behind variability in midshaft shape during ontogeny and how that can be used to infer locomotor behaviours in bioarchaeological studies.

5.7 Limitations

This study has several limitations, the first being its inherently cross-sectional design. Cross-sectional studies do not allow for the growth of an individual to be monitored over time. We can only infer growth trends based on differences observed at various developmental stages. Cross-sectional studies are especially limiting when considering interpretations such as catch-up growth and when considering normal

changes in cortical porosity. Z-score results may have also been affected as they were originally created using individuals of known sex. Since sex cannot be reliably estimated from subadult remains (Lamer et al., 2021; Saunders, 2008), z-scores were created using combined means for body mass and femoral measurements. Growth differences between males and females would be especially pronounced after puberty and could have affected z-score values in the older children and adolescents.

Another limitation of this study is the prevalence of post-depositional midshaft damage and bone diagenesis found in the collection. Individuals experiencing significant midshaft damage were excluded from cross-sectional analysis and individuals experiencing significant midshaft damage or diagenetic alterations were excluded from pore volume analysis. It is likely that individuals with midshafts who have less dense bone and higher pore volume may be at an increased risk for damage and diagenesis (Welsh et al., 2020) when compared to individuals with denser bone. Therefore, damage and diagenesis may have disproportionately affected thin, porous bone, excluding them from observation.

There are also limitations to the use of Harris lines. There is a high level of inter- and intra-observer disagreement and error when considering Harris line estimates from radiographs (Grolleau-Raoux et al., 1997; MacChiarelli et al., 1994). Additionally, the fact that HLs may disappear as bone remodels, makes it impossible to know with certainty the correct number of HLs an individual incurred during growth (Papgeorgopoulou et al., 2011).

Chapter 6: Conclusion

6.0 Conclusion

Individuals living in medieval France experienced multiple insults of war, famine, and disease epidemics. Political instability, malnutrition, and disease would have likely affected the health outcomes of individuals living during this time in history, with children being a particularly vulnerable group in the population. The aim of this thesis was to identify and evaluate skeletal development and growth disruption in a sample of subadults from 10^{th}-13^{th} century Toulouse, France using femoral growth, body mass, and Harris line data. The current study also examined age related changes in midshaft cross-sectional geometry and porosity. Through analyzing subadult femora from Toulouse, this study was able to investigate how growth and development may have been affected by the sociocultural environment.

A large proportion of infants and young children from this sample experienced growth disruption based on the diaphyseal growth stunting, reduced cortical expansion, cortical thinning, and Harris line results. Femoral linear and appositional growth disruption and stunting was most prevalent in individuals below four years of age and the majority of Harris lines were found to have formed between 1.0-2.99 years of age. The high rates of growth disruption and stunting indicate that many children from Toulouse were suffering from mild to severe forms of malnutrition. The adverse health outcomes experienced by infants and young children in this sample are likely linked to the health women in the community. Femoral growth stunting among infants suggests that individuals in this sample may have experienced intrauterine growth restriction due to

mothers suffering from malnutrition or disease during pregnancy. Similarly, young children who experienced stunting likely received inadequate nutrition from suboptimal breastmilk provided by malnourished mothers as well as nutritionally poor complementary foods, such as gruel. During the period in which these individuals lived, medieval Toulouse was experiencing sociopolitical change, disease, and a heavy reliance on cereal crops, which may have predisposed both women of childbearing age and children to malnutrition. The weaning process and cessation of breastfeeding can also increase the risk of disease due to a reduction in transmitted passive and collaborative immunity, which may have also contributed to the high prevalence of stunting and mortality observed in the young children from St. Étienne. Therefore, examining infant growth and evidence of stunting may be useful for not only considering childhood health but also when investigating the mother-infant nexus in the past.

Older children and adolescents in this sample appeared to be in better health compared to the younger individuals examined. The interpretation that older children and adolescents were experiencing better health outcomes was made based on the lack of individuals in these life stages classified as underweight-for-age as well as the comparatively minimal prevalence of stunting observed in these age groups. Individuals in these life stages also demonstrate increased total midshaft areas and cortical thickness, comparable to that of modern children. Improvements in all growth variables suggest that individuals who died during these life stages likely experienced superior nutritional intake and/or reduced disease load compared to the younger individuals. Therefore, older children likely either achieved catch-up growth following periods of growth disruption

that occurred earlier in life or had never experienced growth disruption to the same extent as the younger infants and children in this sample.

Harris lines, while prevalent in the sample, were not found to be significantly associated with femoral growth variables. However, through assessing multiple aspects of growth and development it became evident that interpretations regarding the presence and, especially, the absence of Harris lines require a more nuanced approach than previously considered in the bioarchaeological literature. The presence of a Harris line suggests that an individual experienced and recovered from a period of growth disruption; however, more consideration is required when considering individuals who lack Harris lines. In the community investigated, individuals experiencing the most severe growth stunting lacked the presence of Harris lines, indicating that they experienced growth disruption without evidence of recovery. Therefore, it is suggested that multiple measures of growth disruption be used in tandem with Harris lines in order to provide a more holistic view of disrupted growth in the past.

Ontogenetic changes in femoral midshaft geometry were also examined in the St. Étienne subadults. While high intra- and inter-population variability in ontogenetic femoral midshaft changes were observed in the subadults of this collection, this sample generally follows the age related midshaft shape changes reported by previous studies (e.g., Cowgill et al., 2010; Goldman et al., 2009; Gosman et al., 2013; Swan et al., 2020). In young individuals (<4 years of age) the femoral midshaft is reinforced mediolaterally. Mediolateral reinforcement is associated with limb abduction and waddling locomotor behaviour. Leg abduction can be influenced and exacerbated by culturally prescribed

diaper choices, such as thickness of diaper material (Cole et al., 2012). Locomotor behaviour and, as a proxy, midshaft shape is also influenced by clothing choices, such as swaddling and heavy bed clothes, which restrict limb movement (Hayashi, 1992). Therefore, changes in the femoral midshaft may be able to aid in inferring infant locomotor behaviour and clothing choices in past populations. The mediolateral reinforcement observed in the infants at St. Étienne suggests that many of the children were likely not swaddled and that some individuals may have worn cloth diapers.

Increased midshaft porosity was expected to be found in individuals who did not meet growth expectations, as found by Robbins Schug and Goldman (2014). However, this expectation was not supported by the results, as no statistically significant relationship was found between body size variables and midshaft porosity. The observed increase in midshaft porosity was largely the result of the trabecularization of large coalesced pores close to the endosteal surface. Pore trabecularization was found to be linked to age and the typical onset of weight-bearing activities such as sitting, crawling, standing, and walking; as individuals experiencing increased porosity were largely confined to those between the ages of six months and 1.49 years. This transient period of increased porosity is interpreted to be the result of cortical redistribution from the endosteal surface to the periosteal surface and diaphyseal ends due to increased mechanical loading and femoral growth. Future studies are required to support this interpretation of increased femoral porosity during infancy. Understanding transient periods of cortical thinning and cortical porosity during development may aid in

understanding skeletal fragility of certain age groups in the archaeological record as well as understanding how skeletal fragility may influence fracture risk in growing children.

References

Abarca-Gómez, L., Abdeen, Z. A., Hamid, Z. A., Abu-Rmeileh, N. M., Acosta-Cazares, B., Acuin, C., ... & Cho, Y. (2017). Worldwide trends in body-mass index, underweight, overweight, and obesity from 1975 to 2016: a pooled analysis of 2416 population-based measurement studies in 128· 9 million children, adolescents, and adults. *The Lancet*, *390*, 2627-2642.

Acquaah, F., Robson Brown, K. A., Ahmed, F., Jeffery, N., & Abel, R. L. (2015). Early trabecular development in human vertebrae: overproduction, constructive regression, and refinement. *Frontiers in Endocrinology*, *6*, 67.

Adams, A. B., Halcrow, S. E., King, C. L., Miller, M. J., Vlok, M., Millard, A. R., ... & Oxenham, M. F. (2021). We're all in this together: accessing the maternal-infant relationship in prehistoric Vietnam. In E. J. Kendall, & R. Kendall (Eds.), *The Family in Past Perspective* (p. 191-221). London: Routledge.

Agarwal, S. C. (2016). Bone morphologies and histories: Life course approaches in bioarchaeology. *American Journal of Physical Anthropology*, *159*, 130-149.

Agostini, G. M., & Ross, A. H. (2011). The effect of weight on the femur: a cross-sectional analysis. *Journal of Forensic Sciences*, *56*, 339-343.

Alfonso, M. P., Jennifer, A., Thompson, L., & Standen, V. G. (2005). Reevaluating Harris Lines–A comparison between Harris Lines and enamel hypoplasia. *Collegium Antropologicum*, *29*, 393-408.

Alfonso-Durruty, M. P. (2011). Experimental assessment of nutrition and bone growth's velocity effects on Harris lines formation. *American Journal of Physical Anthropology*, *145*, 169-180.

Ali, A. I., Verma, A., & Paul, V. (2018). Assessment of prevailing supplementary and weaning practices in the selected area of Allahabad. *Journal of Pharmacognosy and Phytochemistry*, *7*, 180-186.

Allen, L. H. (2005). Multiple micronutrients in pregnancy and lactation: an overview. *The American Journal of Clinical Nutrition*, *81*, 1206S-1212S.

Ameen, S., Staub, L., Ulrich, S., Vock, P., Ballmer, F., & Anderson, S. E. (2005). Harris lines of the tibia across centuries: a comparison of two populations, medieval and contemporary in Central Europe. *Skeletal Radiology*, *34*, 279-284.

Andreasen, C. M., Bakalova, L. P., Brüel, A., Hauge, E. M., Kiil, B. J., Delaisse, J. M., Kersh, M. E., Thomsen, J. S., & Andersen, T. L. (2020). The generation of enlarged eroded pores upon existing intracortical canals is a major contributor to endocortical trabecularization. *Bone*, *130*, 115127.

Andreasen, C. M., Delaisse, J. M., van der Eerden, B. C., van Leeuwen, J. P., Ding, M., & Andersen, T. L. (2018). Understanding age-induced cortical porosity in women: the accumulation and coalescence of eroded cavities upon existing intracortical canals is the main contributor. *Journal of Bone and Mineral Research*, *33*, 606-620.

Ariès, P. (1962). *Centuries of Childhood: A Social History of Family Life* (R. Baldick, Trans.). New York: Vintage Books.

Assis, A. M. D. O., Prado, M. S., Barreto, M. L., Reis, M. G. D., Pinheiro, S. C., Parraga, I. M., & Blanton, R. E. (2004). Childhood stunting in Northeast Brazil: the role of Schistosoma mansoni infection and inadequate dietary intake. *European Journal of Clinical Nutrition*, *58*, 1022-1029.

Atun-Einy, O., Cohen, D., Samuel, M., & Scher, A. (2013). Season of birth, crawling onset, and motor development in 7-month-old infants. *Journal of Reproductive and Infant Psychology*, *31*, 342-351.

Bala, Y., Zebaze, R., & Seeman, E. (2015). Role of cortical bone in bone fragility. *Current Opinion in Rheumatology*, *27*, 406-413.

Barker, D. J., Eriksson, J. G., Forsén, T., & Osmond, C. (2002). Fetal origins of adult disease: strength of effects and biological basis. *International Journal of Epidemiology*, *31*, 1235-1239.

Barr, D. G. D., Shmerling, D. H., & Prader, A. (1972). Catch-up growth in malnutrition, studied in celiac disease after institution of gluten-free diet. *Pediatric Research, 6*, 521-527.

Bayley, N. (1969). *Bayley scales of infant development*. New York: The Psychological Corporation.

Beaumont, J., Montgomery, J., Buckberry, J., & Jay, M. (2015). Infant mortality and isotopic complexity: New approaches to stress, maternal health, and weaning. *American Journal of Physical Anthropology*, *157*, 441-457.

Belkacemi, L., Nelson, D. M., Desai, M., & Ross, M. G. (2010). Maternal undernutrition influences placental-fetal development. *Biology of Reproduction*, *83*, 325-331.

Bener, A., Ehlayel, M. S., & Abdulrahman, H. M. (2011). Exclusive breast feeding and prevention of diarrheal diseases: a study in Qatar. *Revista Brasileira de Saúde Materno Infantil, 11*, 83-87.

Benjamin, R. (2017). A Forty Years War: Toulouse and the Plantagenets, 1156-96. In J. France (Ed.), *Medieval Warfare 1000–1300* (p. 323-338). New York: Routledge.

Benson, J. B. (1993). Season of birth and onset of locomotion: Theoretical and methodological implications. *Infant Behavior and Development*, *16*, 69-81.

Besbes, L. G., Haddad, S., Meriem, C. B., Golli, M., Najjar, M. F., & Guediche, M. N. (2010). Infantile scurvy: two case reports. *International Journal of Pediatrics, 2010*, 1-4.

Bjørnerem, Å., Bui, Q. M., Ghasem-Zadeh, A., Hopper, J. L., Zebaze, R., & Seeman, E. (2013). Fracture risk and height: an association partly accounted for by cortical porosity of relatively thinner cortices. *Journal of Bone and Mineral Research, 28,* 2017-2026.

Bjørnerem, Å., Wang, X., Bui, M., Ghasem-Zadeh, A., Hopper, J. L., Zebaze, R., & Seeman, E. (2018). Menopause-related appendicular bone loss is mainly cortical

and results in increased cortical porosity. *Journal of Bone and Mineral Research*, *33*, 598-605.

Black, R. E., Allen, L. H., Bhutta, Z. A., Caulfield, L. E., De Onis, M., Ezzati, M., ... & Maternal and Child Undernutrition Study Group. (2008). Maternal and child undernutrition: global and regional exposures and health consequences. *The Lancet*, *371*, 243-260.

Blanco, R. A., Acheson, R. M., Canosa, C., & Salomon, J. B. (1974). Height, weight, and lines of arrested growth in young Guatemalan children. *American Journal of Physical Anthropology*, *40*, 39-47.

Blaydes, L., & Paik, C. (2016). The impact of Holy Land Crusades on state formation: war mobilization, trade integration, and political development in medieval Europe. *International Organization*, *70*, 551-586.

Bloomfield, F. H., Oliver, M. H., Giannoulias, C. D., Gluckman, P. D., Harding, J. E., & Challis, J. R. (2003). Brief undernutrition in late-gestation sheep programs the hypothalamic- pituitary-adrenal axis in adult offspring. *Endocrinology*, *144*, 2933-2940.

Bogin, B. (2020). *Patterns of Human Growth* (Third Edition). Cambridge: Cambridge University Press.

Borah, B., Dufresne, T., Nurre, J., Phipps, R., Chmielewski, P., Wagner, L., ... & Seeman, E. (2009). Risedronate reduces intracortical porosity in women with osteoporosis. *Journal of Bone and Mineral Research*, *25*, 41-47.

Bossy, E., Talmant, M., & Laugier, P. (2004). Three-dimensional simulations of ultrasonic axial transmission velocity measurement on cortical bone models. *The Journal of the Acoustical Society of America*, *115*, 2314-2324.

Bourbou, C., Fuller, B. T., Garvie-Lok, S. J., & Richards, M. P. (2013). Nursing mothers and feeding bottles: reconstructing breastfeeding and weaning patterns in Greek Byzantine populations (6th–15th centuries AD) using carbon and nitrogen stable isotope ratios. *Journal of Archaeological Science, 40*, 3903-3913.

Bourin-Derruau, M. (1987). Villages médiévaux en Bas-Langue- doc. Genèse d'une sociabilité (Xe-XIVe siècle). Paris: L'Harmattan.

Briana, D. D., Gourgiotis, D., Boutsikou, M., Baka, S., Hassiakos, D., Vraila, V. M., ... & Malamitsi-Puchner, A. (2008). Perinatal bone turnover in term pregnancies: the influence of intrauterine growth restriction. *Bone*, *42*, 307-313.

Brickley, M. B., & Ives, R. (2006). Skeletal manifestations of infantile scurvy. *American Journal of Physical Anthropology*, *129*, 163-172.

Brickley, M. B., Ives, R., & Mays, S. (2020a). *The Bioarchaeology of Metabolic Bone Disease Second Edition)*. San Diego: Academic Press.

Brickley, M. B., Kahlon, B., & D'Ortenzio, L. (2020b). Using teeth as tools: Investigating the mother–infant dyad and developmental origins of health and disease hypothesis using vitamin D deficiency. *American Journal of Physical Anthropology*, *171*, 342-353.

Brickley, M. B., Moffat, T., & Watamaniuk, L. (2014). Biocultural perspectives of vitamin D deficiency in the past. *Journal of Anthropological Archaeology, 36,* 48-59.

Brnić, M., Hurrell, R. F., Songré-Ouattara, L. T., Diawara, B., Kalmogho-Zan, A., Tapsoba, C., ... & Wegmüller, R. (2017). Effect of phytase on zinc absorption from a millet-based porridge fed to young Burkinabe children. *European Journal of Clinical Nutrition, 71,* 137-141.

Buikstra, J. E., Ubelaker, D. (1994). Standards for data collection from human skeletal remains. *Arkansas Archaeological Survey Research Series, 44*.

Burgio, G. R., Lanzavecchia, A., Plebani, A., Jayakar, S., & Ugazio, A. G. (1980). Ontogeny of secretory immunity: levels of secretory IgA and natural antibodies in saliva. *Pediatric Research, 14,* 1111-1114.

Cameron, N. (2002). Human growth curve, canalization, and catch-up growth. In N. Cameron (Ed.), *Human Growth and Development* (p. 1-20). Amsterdam: Academic Press.

Cameron, M. E., & Stock, J. T. (2018). Ecological variation in Later Stone Age southern African biomechanical properties. *Journal of Archaeological Science: Reports, 17,* 125-136.

Cardoso, H. F. (2005). *Patterns of Growth and Development of the Human Skeleton and Dentition in Relation to Environmental Quality.* Unpublished PhD thesis in Anthropology. McMaster University: Hamilton, Ontario.

Cardoso, H. F. (2007). Environmental effects on skeletal versus dental development: using a documented subadult skeletal sample to test a basic assumption in human osteological research. *American Journal of Physical Anthropology*, *132*, 223-233.

Cardoso, H. F., & Magalhães, T. (2011). Evidence of neglect from immature human skeletal remains: an auxological approach from bones and teeth. In A. H. Ross, & S. M. Abel (Eds.), *The Juvenile Skeleton in Forensic Abuse Investigations* (p. 125-150). New York: Humana Press.

Cetin, I., Mando, C., & Calabrese, S. (2013). Maternal predictors of intrauterine growth restriction. *Current Opinion in Clinical Nutrition & Metabolic Care*, *16*, 310-319.

Chadio, S. E., Kotsampasi, B., Papadomichelakis, G., Deligeorgis, S., Kalogiannis, D., Menegatos, I., & Zervas, G. (2007). Impact of maternal undernutrition on the hypothalamic–pituitary–adrenal axis responsiveness in sheep at different ages postnatal. *Journal of Endocrinology, 192*, 495-503.

Checkley, W., Epstein, L. D., Gilman, R. H., Black, R. E., Cabrera, L., & Sterling, C. R. (1998). Effects of Cryptosporidium parvum infection in Peruvian children: growth faltering and subsequent catch-up growth. *American Journal of Epidemiology*, *148*, 497-506.

Chisholm, H. (1911). Toulouse. In *Encyclopedia Britannica (Eleventh Edition, 27, p. 99-101).* Cambridge: Cambridge University Press.

Christian, P., & Smith, E. R. (2018). Adolescent undernutrition: global burden, physiology, and nutritional risks. *Annals of Nutrition and Metabolism*, *72*, 316-328.

Clarke, S. K. (1982). The association of early childhood enamel hypoplasias and radiopaque transverse lines in a culturally diverse prehistoric skeletal sample. *Human Biology*, *54*, 77-84.

Cogill, B. (2003). *Anthropometric Indicators Measurement Guide*. Food and Nutrition Technical Assistance Project, Academy for Educational Development, Washington DC.

Cole, W. G., Lingeman, J. M., & Adolph, K. E. (2012). Go naked: Diapers affect infant `walking. *Developmental Science*, *15*, 783-790.

Conceição, E. L. N., & Cardoso, H. F. V. (2011). Environmental effects on skeletal versus dental development II: further testing of a basic assumption in human osteological research. *American Journal of Physical Anthropology*, *144*, 463-470.

Cooper, C., Westlake, S., Harvey, N., Javaid, K., Dennison, E., & Hanson, M. (2006a). Developmental origins of osteoporotic fracture. *Osteoporosis International*, *17*, 337-347.

Cooper, D. M. L., Kawalilak, C. E., Harrison, K., Johnston, B. D., & Johnston, J. D. (2016). Cortical bone porosity: what is it, why is it important, and how can we detect it? *Current Osteoporosis Reports*, *14*, 187-198.

Cooper, D. M., Thomas, C. D. L., Clement, J. G., & Hallgrímsson, B. (2006b). Three-dimensional microcomputed tomography imaging of basic multicellular unit-

related resorption spaces in human cortical bone. *The Anatomical Record Part A*, *288*, 806-816.

Corruccini, R. S., Handler, J. S., & Jacobi, K. P. (1985). Chronological distribution of enamel hypoplasias and weaning in a Caribbean slave population. *Human Biology*, *57*, 699-711.

Cowgill, L. W., & Johnston, R. A. (2018). Biomechanical implications of the onset of walking. *Journal of Human Evolution*, *122*, 133-145.

Cowgill, L. W., Warrener, A., Pontzer, H., & Ocobock, C. (2010). Waddling and toddling: the biomechanical effects of an immature gait. *American Journal of Physical Anthropology*, *143*, 52-61.

de Boer, H. H., Aarents, M. J., & Maat, G. J. R. (2013). Manual for the preparation and staining of embedded natural dry bone tissue sections for microscopy. *International Journal of Osteoarchaeology*, *23*, 83-93.

De Filippo, R., Peixoto, X., & Sauvage, C. (1988). *Toulouse Place Saint-Étienne*. Archaeological excavation report.

de Rooij, S. R., Painter, R. C., Phillips, D. I., Osmond, C., Michels, R. P., Bossuyt, P. M., ... & Roseboom, T. J. (2006). Hypothalamic–pituitary–adrenal axis activity in adults who were prenatally exposed to the Dutch famine. *European Journal of Endocrinology*, *155*, 153-160.

Dewey, K. G., & Adu-Afarwuah, S. (2008). Systematic review of the efficacy and effectiveness of complementary feeding interventions in developing countries. *Maternal & Child Nutrition, 4*, 24-85.

Dittmann, K., & Grupe, G. (2000). Biochemical and palaeopathological investigations on weaning and infant mortality in the early Middle Ages. *Anthropologischer Anzeiger, 58*, 345-355.

Dobrova-Krol, N. A., van IJzendoorn, M. H., Bakermans-Kranenburg, M. J., Cyr, C., & Juffer, F. (2008). Physical growth delays and stress dysregulation in stunted and non-stunted Ukrainian institution-reared children. *Infant Behavior and Development, 31*, 539-553.

Dori, I., Varalli, A., Seghi, F., Moggi-Cecchi, J., & Sparacello, V. S. (2020). Environmental correlates of growth patterns in Neolithic Liguria (northwestern Italy). *International Journal of Paleopathology, 28*, 112-122.

Duby, G. (1991). France in the Middle Ages, 987-1460: From Hugh Capet to Joan of Arc (J. Vale, Trans.). Oxford: Basil Blackwell.

Duby, G., & Mandrou, R. (1964). *A History of French Civilization* (J. B. Atkinson, Trans.). New York: Random House.

Dupras, T. L., & Tocheri, M. W. (2007). Reconstructing infant weaning histories at Roman period Kellis, Egypt using stable isotope analysis of dentition. *American Journal of Physical Anthropology, 134*, 63-74.

Durand, A. (1998). Paysages, terroirs et peuplement dans les campages du Bas-Languedoc (Xe-XIIe siècle). Collection Tempus, Presses Universitaires du Mirail, Toulouse.

Doube, M., Kłosowski, M. M., Arganda-Carreras, I., Cordelières, F. P., Dougherty, R. P., Jackson, J. S., ... & Shefelbine, S. J. (2010). BoneJ: free and extensible bone image analysis in ImageJ. *Bone*, *47*, 1076-1079.

Du Plessis, A., Broeckhoven, C., Guelpa, A., & Le Roux, S. G. (2017). Laboratory x-ray micro-computed tomography: a user guideline for biological samples. *Giga Science*, *6*, 1-11.

Elamin, F., & Liversidge, H. M. (2013). Malnutrition has no effect on the timing of human tooth formation. *PloS One*, *8*, e72274.

Eleazer, C. D., & Jankauskas, R. (2016). Mechanical and metabolic interactions in cortical bone development. *American Journal of Physical Anthropology*, *160*, 317-333.

Enlow, D. H. (1963). *Principles of Bone Remodeling: An Account of Post-Natal Growth and Remodeling Processes in Long Bones and the Mandible*. Springfield: Thomas.

Enlow, D. H. (1976). The remodeling of bone. *Yearbook of Physical Anthropology, 20*, 19–34.

Espo, M., Kulmala, T., Maleta, K., Cullinan, T., Salin, M. L., & Ashorn, P. (2002). Determinants of linear growth and predictors of severe stunting during infancy in rural Malawi. *Acta Paediatrica*, *91*, 1364-1370.

Farr, J. N., & Khosla, S. (2015). Skeletal changes through the lifespan—from growth to senescence. *Nature Reviews Endocrinology, 11*, 513.

Fildes, V. A. (1986). *Breasts, Bottles, and Babies: A History of Infant Feeding*. Edinburgh: Edinburgh University Press.

Fildes, V. (1995). The culture and biology of breastfeeding: an historical review of Western Europe. In P. Stuart-Macadam, & K. A. Dettwyler, *Breastfeeding* (p. 101-126). New York: Routledge.

Fiscella, G. N., Bennike, P., & Lynnerup, N. (2008). Transverse-" Harris"-Lines in a Skeletal Population from the 1711 Danish Plague Site. *Anthropologischer Anzeiger*, *66*, 129-138.

Fisk, C. M., Crozier, S. R., Inskip, H. M., Godfrey, K. M., Cooper, C., Roberts, G. C., ... & Southampton Women's Survey Study Group. (2011). Breastfeeding and reported morbidity during infancy: findings from the Southampton Women's Survey. *Maternal & Child Nutrition*, *7*, 61-70.

Frankenburg, W.K., Dodds, J., Archer, P., Bresnick, B., Maschka, P., Edelman, N., & Shapiro, H. (1992). *Denver II Sceening Manual*. Denver: Denver Developmental Materials, Inc.

Frost, H. M. (1958). Preparation of thin undecalcified bone sections by rapid manual method. *Stain Technology, 33*, 273-277.

Frost H. M. (1973). *Bone Remodeling and its Relationship to Metabolic Bone Diseases*. Springfield: Charles C. Thomas.

Gardner, D. S., Van Bon, B. W. M., Dandrea, J., Goddard, P. J., May, S. F., Wilson, V., ... & Symonds, M. E. (2006). Effect of periconceptional undernutrition and gender on hypothalamic– pituitary–adrenal axis function in young adult sheep. *Journal of Endocrinology*, *190*, 203-212.

Garn, S. M., Guzmán, M. A., & Wagner, B. (1969). Subperiosteal gain and endosteal loss in protein-calorie malnutrition. *American Journal of Physical Anthropology*, *30*, 153-155.

Garn, S. M., Rohmann, C. G., Béhar, M., Viteri, F., Guzman, M. A. (1964). Compact bone deficiency in protein-calorie malnutrition. *American Association for the Advancement of Science, 145,* 1444-1445.

Garn, S. M, Silverman, F., Hertzog, K., Rohman, C. (1968). Lines and bands of increased densitiy: their implication to growth and development. *Medical Radiography and Photography, 33,* 58–89.

Gasser, T., Kneip, A., Binding, A., Prader, A., & Molinari, L. (1991). The dynamics of linear growth in distance, velocity and acceleration. *Annals of Human Biology*, *18*, 187-205.

Geber, J. (2014). Skeletal manifestations of stress in child victims of the Great Irish Famine (1845–1852): Prevalence of enamel hypoplasia, Harris lines, and growth retardation. *American Journal of Physical Anthropology*, *155*, 149-161.

Goldman, H. M., McFarlin, S. C., Cooper, D. M. L., Thomas, C. D. L., & Clement, J. G. (2009). Ontogenetic patterning of cortical bone microstructure and geometry at

the human mid-shaft femur. *The Anatomical Record: Advances in Integrative Anatomy and Evolutionary Biology*, *292*, 48-64.

González-Reimers, E., Pérez-Ramírez, A., Santolaria-Fernández, F., Rodríguez-Rodríguez, E., Martínez-Riera, A., del Carmen Durán-Castellón, M., ... & Gaspar, M. R. (2007). Association of Harris lines and shorter stature with ethanol consumption during growth. *Alcohol*, *41*, 511-515.

Gooderham, E., Matias, A., Liberato, M., Santos, H., Walshaw, S., Albanese, J., & Cardoso, H. F. (2019). Linear and appositional growth in children as indicators of social and economic change during the Medieval Islamic to Christian transition in Santarém, Portugal. *International Journal of Osteoarchaeology*, *29*, 736-746.

Goodman, A. H., & Clark, G. A. (1981). Harris lines as indicators of stress in prehistoric Illinois populations. *Biocultural Adaption Comprehensive Approaches to Skeletal Analysis. Research Report*, *20*, 35-46.

Gosman, J. H., Hubbell, Z. R., Shaw, C. N., & Ryan, T. M. (2013). Development of cortical bone geometry in the human femoral and tibial diaphysis. *The Anatomical Record*, *296*, 774-787.

Gosman, J. H., & Ketcham, R. A. (2009). Patterns in ontogeny of human trabecular bone from SunWatch Village in the Prehistoric Ohio Valley: General features of microarchitectural change. *American Journal of Physical Anthropology*, *138*, 318-332.

Gowland, R. L. (2015). Entangled lives: Implications of the developmental origins of health and disease hypothesis for bioarchaeology and the life course. *American Journal of Physical Anthropology, 158*, 530-540.

Gowland, R. L., & Halcrow, S. (2020). Introduction: the mother-infant nexus in archaeology and anthropology. In R. L. Gowland, & S. Halcrow (Eds.), *The Mother-Infant Nexus in Anthropology* (p. 1-15). Cham: Springer.

Graves, R. A. (1917). Fearful Famines of the Past. *The National Geographic Magazine, 32*, 69-90.

Griffin, T. M., & Kram, R. (2000). Penguin waddling is not wasteful. *Nature, 408*, 929-929.

Grolleau-Raoux, J. L., Crubézy, E., Rouge, D., Brugne, J. F., & Saunders, S. R. (1997). Harris lines: A study of age-associated bias in counting and interpretation. *American Journal of Physical Anthropology, 103*, 209-217.

Gurven, M. (2012). Infant and fetal mortality among a high fertility and mortality population in the Bolivian Amazon. *Social Science & Medicine, 75*, 2493-2502.

Hadley, C., & Hruschka, D. J. (2014). Population level differences in adult body mass emerge in infancy and early childhood: evidence from a global sample of low and lower-income countries. *American Journal of Physical Anthropology, 154*, 232-238.

Hajeebhoy, N., Nguyen, P. H., Mannava, P., Nguyen, T. T., & Mai, L. T. (2014). Suboptimal breastfeeding practices are associated with infant illness in Vietnam. *International Breastfeeding Journal, 9*, 1-7.

Halcrow, S. (2020). Infants in the bioarchaeological past: Who cares? In R. L. Gowland, & S. Halcrow (Eds.), *The Mother-Infant Nexus in Anthropology* (p. 19-38). Cham: Springer.

Halcrow, S. E., Tayles, N., Elliott, G. E., Han, S., Betsinger, T. K., & Scott, A. B. (2017). The bioarchaeology of fetuses. In S. Han, T. K. Betsinger, & A. B. Scott (Eds.), *The Anthropology of the Fetus: Biology, Culture, and Society* (p. 83-111). New York: Berghahan Books.

Hanawalt, B. A. (2002). Medievalists and the Study of Childhood. *Speculum, 77*, 440-460.

Hansman, C. (1970). Anthropometry and Related Data, Anthropometry Skinfold Thickness Measurements. In R.W. McCammon (Ed.), *Human Growth and Development* (pp. 101-154). Springfield: Charles C . Thomas.

Hanson, L. Å., & Korotkova, M. (2002). The role of breastfeeding in prevention of neonatal infection. *Seminars in Neonatology, 7*, 275-281.

Hanson, L. Å., Korotkova, M., Lundin, S., Håversen, L., Silfverdal, S. A., Mattsby-Baltzer, I. N. G. E. R., ... & Telemo, E. (2003). The transfer of immunity from mother to child. *Annals of the New York Academy of Sciences, 987*, 199-206.

Hanson, L., Silfverdal, S. A., Hahn-Zoric, M., Håversen, L., Baltzer, I. M., Moisei, M., & Motas, C. (2009). Immune function. In G. R. Goldberg, A. Prentice, A. Prentice, S. Filteau, & K. Simondon (Eds.), *Breast-feeding: Early Influences on Later Health* (p. 97–111). Dordrecht: Springer Science.

Harris, H. A. (1931). Lines of arrested growth in the long bones in childhood: the correlation of histological and radiographic appearances in clinical and experimental conditions. *The British Journal of Radiology*, *4*, 561-588.

Hatch, J. W., Willey, P. S., & Hunt Jr, E. E. (1983). Indicators of status-related stress in Dallas society: transverse lines and cortical thickness in long bones. *Midcontinental Journal of Archaeology*, *8*, 49-71.

Hayashi, K. (1992). The influence of clothes and bedclothes on infants' gross motor development. *Developmental Medicine & Child Neurology*, *34*, 557-558.

Herrscher, E. (2003). Diet of a historic population: analysis of isotopic data from the necropolis of Saint-Laurent de Grenoble (13th to 15th century, France). *Bulletins et Mémoires de la Société d'Anthropologie de Paris*, *15*, 149-269.

Himes, J. H., Martorell, R., Habicht, J. P., Yarbrough, C., Malina, R. M., & Klein, R. E. (1975). Patterns of cortical bone growth in moderately malnourished preschool children. *Human Biology*, *47*, 337-350.

Hodson, C. M., & Gowland, R. (2020). Like mother, like child: Investigating perinatal and maternal health stress in Post-medieval London. In R. L. Gowland, & S.

Halcrow (Eds.), *The Mother-Infant Nexus in Anthropology* (p. 39-64). Cham: Springer.

Horocholyn, K., & Brickley, M. B. (2017). Pursuit of famine: Investigating famine in bioarchaeological literature. *Bioarchaeology International*, *1*, 101-115.

Hughes, C., Heylings, D. J. A., & Power, C. (1996). Transverse (Harris) lines in Irish archaeological remains. *American Journal of Physical Anthropology*, *101*, 115-131.

Hummert, J. R. (1983). Cortical bone growth and dietary stress among subadults from Nubia's Batn El Hajar. *American Journal of Physical Anthropology*, *62*, 167-176.

Hurrell, R. F. (2003). Influence of vegetable protein sources on trace element and mineral bioavailability. *The Journal of Nutrition*, *133*, 2973S-2977S.

Huss-Ashmore, R., Goodman, A. H., & Armelagos, G. J. (1982). Nutritional inference from paleopathology. In M. B. Schiffer (Ed.), *Advances in Archaeological Method and Theory* (p. 395-474). New York: Academic Press.

Ives, R., & Brickley, M. B. (2004). A procedural guide to metacarpal radiogrammetry in archaeology. *International Journal of Osteoarchaeology*, *14*, 7-17.

Ives, R., & Humphrey, L. (2017). Patterns of long bone growth in a mid-19th century documented sample of the urban poor from Bethnal Green, London, UK. *American Journal of Physical Anthropology*, *163*, 173-186.

Ives, R., & Humphrey, L. (2018). Endochondral growth disruption during vitamin D deficiency rickets in a mid-19th century series from Bethnal Green, London, UK. *American Journal of Physical Anthropology*, *167*, 585-601.

Jenkins, E. E. (2008). The Interplay of Financial and Political Conflicts Connected to Toulouse during the Late Twelfth and Early Thirteenth Centuries. *Mediterranean Studies*, *17*, 46-61.

Johnsen, L., Kongsted, A. H., & Nielsen, M. O. (2013). Prenatal undernutrition and postnatal overnutrition alter thyroid hormone axis function in sheep. *Journal of Endocrinology*, *216*, 389-402.

Jilka, R. L. (2003). Biology of the basic multicellular unit and the pathophysiology of osteoporosis. *Medical and Pediatric Oncology*, *41*, 182-185.

Kacki, S. (2016). *Influences de L'état Sanitaire des Populations Anciennes sur la Mortalité en Temps de Peste: Contribution à la Paléoépidémiologie*. Unpublished PhD thesis in Anthropology. Université de Bordeaux: Bordeaux.

Kacki, S., Rahalison, L., Rajerison, M., Ferroglio, E., & Bianucci, R. (2011). Black Death in the rural cemetery of Saint-Laurent-de-la-Cabrerisse Aude-Languedoc, southern France, 14th century: immunological evidence. *Journal of Archaeological Science*, *38*, 581-587.

Kamp, K. A. (2001). Where have all the children gone?: the archaeology of childhood. *Journal of Archaeological Method and Theory*, *8*, 1-34.

Kamp, K. A. (2015). Children and their childhoods: Retrospectives and prospectives. *Childhood in the Past*, *8*, 161-169.

Kaur, R., Kim, T., Casey, J. R., & Pichichero, M. E. (2012). Antibody in middle ear fluid of children originates predominantly from sera and nasopharyngeal secretions. *Clinical and Vaccine Immunology*, *19*, 1593-1596.

Kendall, E., Millard, A., & Beaumont, J. (2021). The "weanling's dilemma" revisited: Evolving bodies of evidence and the problem of infant paleodietary interpretation. *American Journal of Physical Anthropology*, *175*, 57-78.

Khan, S., Zaheer, S., & Safdar, N. F. (2019). Determinants of stunting, underweight and wasting among children< 5 years of age: evidence from 2012-2013 Pakistan demographic and health survey. *BMC Public Health*, *19*, 1-15.

Kibler, W. W., Zinn, G. A., & Earp, L. (1995). *Medieval France: An Encyclopedia*. New York: Garland Publishing, Inc.

Klopp, A., Vehling, L., Becker, A. B., Subbarao, P., Mandhane, P. J., Turvey, S. E., ... & Azad, M. B. (2017). Modes of infant feeding and the risk of childhood asthma: a prospective birth cohort study. *The Journal of Pediatrics*, *190*, 192-199.

Kulus, M. J., Cebulski, K., Kmiecik, P., & Dabrowski, P. (Submitted Manuscript). Non-linear equations and easy-to-use calculator for age at Harris Lines formation estimation. *International Journal of Molecular Sciences.*

Kulus, M. J., & Dąbrowski, P. (2019). How to calculate the age at formation of Harris lines? A step-by-step review of current methods and a proposal for modifications to Byers' formulas. *Archaeological and Anthropological Sciences*, *11*, 1169-1185.

Kuralkar, P., & Kuralkar, S. V. (2010). Nutritional and Immunological Importance of Colostrum for the new born. *Veterinary World*, *3*, 46.

Lamberti, L. M., Walker, C. L. F., Noiman, A., Victora, C., & Black, R. E. (2011). Breastfeeding and the risk for diarrhea morbidity and mortality. *BMC Public Health*, *11*, 1-12.

Lamer, M., Spake, L., & Cardoso, H. F. (2021). Testing the cross-applicability of juvenile sex estimation from diaphyseal dimensions. *Forensic Science International*, *321*, 110739.

Lampl, M., & Schoen, M. (2017). How long bones grow children: Mechanistic paths to variation in human height growth. *American Journal of Human Biology*, *29*, e22983.

Lausman, A., Kingdom, J., Gagnon, R., Basso, M., Bos, H., Crane, J., ... & Sanderson, F. (2013). Intrauterine growth restriction: screening, diagnosis, and management. *Journal of Obstetrics and Gynaecology Canada*, *35*, 741-748.

Lempicki, M., Rothenbuhler, A., Merzoug, V., Franchi-Abella, S., Chaussain, C., Adamsbaum, C., & Linglart, A. (2017). Magnetic resonance imaging features as surrogate markers of X-linked hypophosphatemic rickets activity. *Hormone Research in Paediatrics*, *87*, 244-253

Leonard, W. R., Dewalt, K. M., Stansbury, J. P., & McCaston, M. K. (2000). Influence of dietary quality on the growth of highland and coastal Ecuadorian children. *American Journal of Human Biology*, *12*, 825-837.

Leonard, W. R., Snodgrass, J. J., & Robertson, M. L. (2012). Comparative and evolutionary perspectives on human brain growth. In N. Cameron & B. Bogin (Eds.), *Human Growth and Development* (p. 397-413). San Diego: Elsevier Inc.

Lerebours, C., Thomas, C. D. L., Clement, J. G., Buenzli, P. R., & Pivonka, P. (2015). The relationship between porosity and specific surface in human cortical bone is subject specific. *Bone, 72*, 109-117.

Lett, D. (1997). *L'enfant des miracles: Enfance et société au moyen âge, XIIe-XIIIe siècle*. Paris: Aubier.

Levin, S. (1970). Diapers. *South African Medical Journal, 44*, 256-263.

Lewis, M. E. (2007). *The Bioarchaeology of Children: Perspectives from Biological and Forensic Anthropology*. Cambridge: Cambridge University Press.

Lewis, M. E. (2017). Fetal paleopathology: An impossible discipline? In S. Han, T. K. Betsinger, & A. B. Scott (Eds.), *The Anthropology of the Fetus: Biology, Culture, and Society* (p. 112–131). New York: Berghan Books.

Li, Y., Jin, L., & Chen, T. (2020). The effects of secretory IgA in the mucosal immune system. *BioMed Research International, 2020,* 1-6.

Lillehammer, G. (2015). 25 Years with the 'Child' and the Archaeology of Childhood. *Childhood in the Past, 8*, 78-86.

Lovejoy, C. O., Russell, K. F., & Harrison, M. L. (1990). Long bone growth velocity in the Libben population. *American Journal of Human Biology, 2*, 533-541.

Lucassen, P. J., Naninck, E. F., van Goudoever, J. B., Fitzsimons, C., Joels, M., & Korosi, A. (2013). Perinatal programming of adult hippocampal structure and function; emerging roles of stress, nutrition and epigenetics. *Trends in Neurosciences, 36*, 621-631.

Lüning, S., Schulte, L., Garcés-Pastor, S., Danladi, I. B., & Gałka, M. (2019). The Medieval climate anomaly in the Mediterranean region. *Paleoceanography and Paleoclimatology, 34*, 1625-1649.

MacChiarelli, R., Bondioli, L., Censi, L., Hernaez, M. K., Salvadei, L., & Sperduti, A. (1994). Intra-and interobserver concordance in scoring Harris lines: A test on bone sections and radiographs. *American Journal of Physical Anthropology*, *95*, 77-83.

Manuel-Apolinar, L., Rocha, L., Damasio, L., Tesoro-Cruz, E., & Zarate, A. (2014). Role of prenatal undernutrition in the expression of serotonin, dopamine and leptin receptors in adult mice: implications of food intake. *Molecular Medicine Reports*, *9*, 407-412.

Maresh, M. M. (1970). Measurements from roentgenograms. In R.W. McCammon (Ed.), *Human Growth and Development* (p. 155-199). Springfield: Charles C . Thomas.

Martorell, R. (2017). Improved nutrition in the first 1000 days and adult human capital and health. *American Journal of Human Biology*, *29*, e22952.

Martorell, R., de Onis, M., Martines, J., Black, M., Onyango, A., & Dewey, K. G. (2006). WHO motor development study: Windows of achievement for six gross motor development milestones. *Acta Paediatrica, 95*, 86–95.

Matkovic, V. (1991). Calcium metabolism and calcium requirements during skeletal modeling and consolidation of bone mass. *The American Journal of Clinical Nutrition, 54*, 245S-260S.

Mays, S. (1985). The relationship between Harris line formation and bone growth and development. *Journal of Archaeological Science, 12*, 207-220.

Mays, S. (1995). The relationship between Harris lines and other aspects of skeletal development in adults and juveniles. *Journal of Archaeological Science*, *22*, 511-520.

Mays, S. (1999). Linear and appositional long bone growth in earlier human populations: a case study from Mediaeval England. In R. D. Hoppa, & C. M. Fitzgerald (Eds.), *Human Growth in the Past: Studies Using Bones and Teeth* (p. 290-312). Cambridge: Cambridge University Press.

Mays, S. (2001). Effects of age and occupation on cortical bone in a group of 18th–19th century British men. *American Journal of Physical Anthropology, 116*, 34-44.

Mays, S. (2010). The effects of infant feeding practices on infant and maternal health in a medieval community. *Childhood in the Past*, *3*, 63-78.

Mays, S. (2013). A discussion of some recent methodological developments in the osteoarchaeology of childhood. *Childhood in the Past*, *6*, 4-21.

Mays, S. (2018a). Micronutrient deficiency diseases: Anemia, scurvy, and rickets. *The International Encyclopedia of Biological Anthropology*, 1-5.

Mays, S. (2018b). The study of growth in skeletal populations. In S. Crawford, D. Hadley, & G. Shepherd (Eds.), *The Oxford Handbook of the Archaeology of Childhood* (p. 71-89). Oxford: Oxford University Press.

Mays, S., & Brickley, M. B. (2018). Vitamin D deficiency in bioarchaeology and beyond: the study of rickets and osteomalacia in the past. *International Journal of Paleopathology*, *23*, 1-5.

Mays, S., Brickley, M., & Ives, R. (2008). Growth in an English population from the Industrial Revolution. *American Journal of Physical Anthropology*, *136*, 85-92.

Mays, S., Gowland, R., Halcrow, S., & Murphy, E. (2017). Child bioarchaeology: Perspectives on the past 10 years. *Childhood in the Past*, *10*, 38-56.

Mays, S., Ives, R., & Brickley, M. (2009). The effects of socioeconomic status on endochondral and appositional bone growth, and acquisition of cortical bone in children from 19th century Birmingham, England. *American Journal of Physical Anthropology*, *140*, 410-416.

McDade, T. W. (2003). Life history theory and the immune system: steps toward a human ecological immunology. *American Journal of Physical Anthropology*, *122*, 100-125.

McEwan, J. M., Mays, S., & Blake, G. M. (2005). The relationship of bone mineral density and other growth parameters to stress indicators in a medieval juvenile population. *International Journal of Osteoarchaeology*, *15*, 155-163.

McHenry, H. M., & Schulz, P. D. (1976). The association between Harris lines and enamel hypoplasia in prehistoric California Indians. *American Journal of Physical Anthropology, 44,* 507-511.

Michaelsen, K. F., & Friis, H. (1998). Complementary feeding: a global perspective, *Nutrition, 14,* 763-766.

Miller, E. M. (2020). The ecology of breastfeeding and mother-infant immune functions. In R. L. Gowland, & S. Halcrow (Eds.), *The Mother-Infant Nexus in Anthropology*, 85-101. Cham: Springer.

Millward, D. J. (2017). Nutrition, infection and stunting: the roles of deficiencies of individual nutrients and foods, and of inflammation, as determinants of reduced linear growth of children. *Nutrition Research Reviews*, *30*, 50-72.

Milovanovic, P., Djonic, D., Hahn, M., Amling, M., Busse, B., & Djuric, M. (2017). Region-dependent patterns of trabecular bone growth in the human proximal femur: A study of 3D bone microarchitecture from early postnatal to late childhood period. *American Journal of Physical Anthropology, 164,* 281-291.

Miszkiewicz, J. J. (2015). Histology of a Harris line in a human distal tibia. *Journal of Bone and Mineral Metabolism, 33,* 462-466.

Mitchell, P. D. (2015). Human parasites in medieval Europe: lifestyle, sanitation and medical treatment. *Advances in Parasitology, 90,* 389-420.

Mkhize, M., & Sibanda, M. (2020). A review of selected studies on the factors associated with the nutrition status of children under the age of five years in South

Africa. *International Journal of Environmental Research and Public Health*, *17*, 7973.

Moncrieff, M. W., Lunt, H. R. W., & Arthur, L. J. H. (1973). Nutritional rickets at puberty. *Archives of Disease in Childhood*, *48*, 221-224.

Moorrees, C. F., Fanning, E. A., & Hunt Jr, E. E. (1963a). Age variation of formation stages for ten permanent teeth. *Journal of Dental Research, 42*, 1490-1502.

Moorrees, C. F., Fanning, E. A., & Hunt Jr, E. E. (1963b). Formation and resorption of three deciduous teeth in children. *American Journal of Physical Anthropology*, *21*, 205-213.

Moossavi, S., Sepehri, S., Robertson, B., Bode, L., Goruk, S., Field, C. J., ... & Azad, M. B. (2019). Composition and variation of the human milk microbiota are influenced by maternal and early-life factors. *Cell Host & Microbe*, *25*, 324-335.

Mundy, J. H. (1954). *Liberty and Political Power in Toulouse: 1050-1230* . New York: Columbia University Press.

Murail, P. (1991). Apport de L'anthropolgie a L'etude du Recrutement et de L'organisation d'un Espace Funeraire: le Cimetiere Saint-Etienne à Toulouse. Unpublished M. A. thesis in Anthropology. Université de Bordeaux: Bordeaux.

Nakatsukasa, M., Hayama, S., & Preuschoft, H. (1995). Postcranial skeleton of a macaque trained for bipedal standing and walking and implications for functional adaptation. *Folia Primatologica*, *64*, 1-29.

Newman, S. L., Gowland, R. L., & Caffell, A. C. (2019). North and south: A comprehensive analysis of non-adult growth and health in the industrial revolution

(AD 18th–19th C), England. *American Journal of Physical Anthropology, 169*, 104-121.

Nitsch, E. K., Humphrey, L. T., & Hedges, R. E. (2011). Using stable isotope analysis to examine the effect of economic change on breastfeeding practices in Spitalfields, London, UK. *American Journal of Physical Anthropology*, *146*, 619-628.

Nowak, O., & Piontek, J. (2002). The frequency of appearance of transverse (Harris) lines in the tibia in relationship to age at death. *Annals of Human Biology*, *29*, 314-325.

Nowlan, N. C. (2015). Biomechanics of foetal movement. *European Cells and Materials, 29*, 1-21.

Oliver, H., Jameson, K. A., Sayer, A. A., Cooper, C., Dennison, E. M., & Hertfordshire Cohort Study Group. (2007). Growth in early life predicts bone strength in late adulthood: the Hertfordshire Cohort Study. *Bone, 41*, 400-405.

O'Neill, M. C., & Ruff, C. B. (2004). Estimating human long bone cross-sectional geometric properties: a comparison of noninvasive methods. *Journal of Human Evolution, 47*, 221-235.

Orme, N. (2009). Medieval childhood: challenge, change and achievement. *Childhood in the Past, 1*, 106-119.

Osima, M., Borgen, T. T., Lukic, M., Grimnes, G., Joakimsen, R. M., Eriksen, E. F., & Bjørnerem, Å. (2018). Serum parathyroid hormone is associated with increased cortical porosity of the inner transitional zone at the proximal femur in

postmenopausal women: the Tromsø study. *Osteoporosis International, 29*, 421-431.

Paccou, J., Ward, K. A., Jameson, K. A., Dennison, E. M., Cooper, C., & Edwards, M. H. (2016). Bone microarchitecture in men and women with diabetes: the importance of cortical porosity. *Calcified Tissue International, 98*, 465-473.

Padmadas, S. S., Hutter, I., & Willekens, F. (2002). Weaning initiation patterns and subsequent linear growth progression among children aged 2–4 years in India. *International Journal of Epidemiology*, *31*, 855-863.

Palmquist, A. E. (2017). Consuming immunities: Milk sharing and the social life of passive immunity. In C. Tomori, A. E. L. Palmquist, & E. A. Quinn (Eds.), *Breastfeeding* (p. 40-54). London: Routledge.

Papageorgopoulou, C., Suter, S. K., Rühli, F. J., & Siegmund, F. (2011). Harris lines revisited: prevalence, comorbidities, and possible etiologies. *American Journal of Human Biology*, *23*, 381-391.

Papathakis, P. C., Singh, L. N., & Manary, M. J. (2016). How maternal malnutrition affects linear growth and development in the offspring. *Molecular and Cellular Endocrinology*, *435*, 40-47.

Parfitt, A. M. (1994). The two faces of growth: benefits and risks to bone integrity. *Osteoporosis International, 4*, 382-398.

Park, E. A. (1964). The imprinting of nutritional disturbances on the growing bone. *Pediatrics*, *33*, 815-861.

Peacock, T., Bourbou, C., D'Ortenzio, L., Kahlon, B., Prowse, T., & Brickley, M. B. (2019). Mobility and rickets: Investigating Vitamin D deficiency and regional mobility in Aventicum, Roman Switzerland (first to third century CE). *International Journal of Osteoarchaeology*, *29*, 654-664.

Pearson, O. M., & Lieberman, D. E. (2004). The aging of Wolff's "law": ontogeny and responses to mechanical loading in cortical bone. *American Journal of Physical Anthropology*, *125*, 63-99.

Pérez-Escamilla, R., Buccini, G. S., Segura-Pérez, S., & Piwoz, E. (2019). Perspective: should exclusive breastfeeding still be recommended for 6 months? *Advances in Nutrition*, *10*, 931-943.

Pinhasi, R., Shaw, P., White, B., & Ogden, A. R. (2006). Morbidity, rickets and long-bone growth in post-medieval Britain—a cross-population analysis. *Annals of Human Biology*, *33*, 372-389.

Piontek, J., Jerszynska, B., & Nowak, O. S. K. A. R. (2001). Harris lines in subadult and adult skeletons from the mediaeval cemetery in Cedynia, Poland. *Variability and Evolution*, *9*, 33-43.

Pomeroy, E. (2013). Biomechanical insights into activity and long distance trade in the south-central Andes (AD 500–1450). *Journal of Archaeological Science*, *40*, 3129-3140.

Pratt, I. V., Johnston, J. D., Walker, E., & Cooper, D. M. (2018). Interpreting the three-dimensional orientation of vascular canals and cross-sectional geometry of cortical bone in birds and bats. *Journal of Anatomy, 232*, 931-942.

Prentice, A., Jarjou, L. M., Cole, T. J., Stirling, D. M., Dibba, B., & Fairweather-Tait, S. (1995). Calcium requirements of lactating Gambian mothers: effects of a calcium supplement on breast-milk calcium concentration, maternal bone mineral content, and urinary calcium excretion. *The American Journal of Clinical Nutrition, 62*, 58-67.

Rauch, F., & Schoenau, E. (2001a). Changes in bone density during childhood and adolescence: an approach based on bone's biological organization. *Journal of Bone and Mineral Research, 16*, 597-604.

Rauch, F., & Schoenau, E. (2001b). The developing bone: slave or master of its cells and molecules? *Pediatric Research, 50*, 309-314.

Recker, R. R., & Moreira, C. A. (2019). In J. P. Bilezikian (Ed.), *Primer on the Metabolic Bone Diseases and Disorders of Mineral Metabolism* (p. 310-318). Hoboken: John Wiley & Sons, Inc.

Reissis, D., & Abel, R. L. (2012). Development of fetal trabecular micro-architecture in the humerus and femur. *Journal of Anatomy, 220*, 496-503.

Rewekant, A. (2001). Do environmental disturbances of an individual's growth and development influence the later bone involution processes? A study of two mediaeval populations. *International Journal of Osteoarchaeology, 11*, 433-443.

Ribot, I., & Roberts, C. (1996). A study of non-specific stress indicators and skeletal growth in two mediaeval subadult populations. *Journal of Archaeological Science, 23*, 67-79.

Riché, P., & Alexandre-Bidon, D. (1994). *L'enfance au moyen âge*. Paris: Biliothèque Nationale de France.

Riskin, A., Almog, M., Peri, R., Halasz, K., Srugo, I., & Kessel, A. (2012). Changes in immunomodulatory constituents of human milk in response to active infection in the nursing infant. *Pediatric Research, 71*, 220-225.

Robbins, G., Sciulli, P. W., & Blatt, S. H. (2010). Estimating body mass in subadult human skeletons. *American Journal of Physical Anthropology, 143*, 146-150.

Robbins Schug, G., & Goldman, H. M. (2014). Birth is but our death begun: A bioarchaeological assessment of skeletal emaciation in immature human skeletons in the context of environmental, social, and subsistence transition. *American Journal of Physical Anthropology, 155*, 243-259.

Roberts, C. A., & Buikstra, J. E. (2020). The history of tuberculosis from earliest times to the development of drugs. In L. N. Friedman, M. Dedicoat, & P. D. O. Davies (Eds.), *Clinical Tuberculosis* (pp. 3-15). Boca Raton: CRC Press.

Rogol, A. D., & Hayden, G. F. (2014). Etiologies and early diagnosis of short stature and growth failure in children and adolescents. *The Journal of Pediatrics, 164*, S1-S14.

Rolian, C. (2020). Endochondral ossification and the evolution of limb proportions. *Wiley Interdisciplinary Reviews: Developmental Biology*, *9*, e373.

Ros, J., & Ruas, M. P. (2013, June). Agriculture, food and products from Antiquity to Middle Age in Northern Catalonia (Pyrénées-Orientales, France). In *16th Conference of the International Work Group for Palaeoethnobotany*.

Rousham, E. K., & Humphrey, L. T. (2002). The dynamics of child survival. In H. Macbeth, & P. Collinson (Eds.), *Human Population Dynamics: Cross-Disciplinary Perspectives* (p. 124-140). Cambridge: Cambridge University Press.

Ruas, M. P. (2005). Aspects of early medieval farming from sites in Mediterranean France. *Vegetation History and Archaeobotany*, *14*, 400-415.

Ruff, C. (2003). Ontogenetic adaptation to bipedalism: age changes in femoral to humeral length and strength proportions in humans, with a comparison to baboons. *Journal of Human Evolution*, *45*, 317-349.

Ruff, C. (2007). Body size prediction from juvenile skeletal remains. *American Journal of Physical Anthropology*, *133*, 698-716.

Ruff, C. (2019). Biomechanical analyses of Archaeological Human Skeletons. In M. A. Katzenberg, & A. L. Grauer (Eds.), *Biological Anthropology of the Human Skeleton* (p. 189-224). Oxford: John Wiley & Sons, Inc.

Ruff, C. B., Garofalo, E., & Holmes, M. A. (2013). Interpreting skeletal growth in the past from a functional and physiological perspective. *American Journal of Physical Anthropology*, *150*, 29-37.

Ruff, C. B., & Hayes, W. C. (1983). Cross-sectional geometry of Pecos Pueblo femora and tibiae—A biomechanical investigation: I. Method and general patterns of variation. *American Journal of Physical Anthropology*, *60*, 359-381.

Ruff, C. B., Walker, A., & Trinkaus, E. (1994). Postcranial robusticity in Homo. III: ontogeny. *American Journal of Physical Anthropology*, *93*, 35-54.

Russell, C., & Russell, W. M. S. (2000). Population crises and population cycles. *Medicine, Conflict and Survival*, *16*, 383-410.

Ryan, T. M., & Krovitz, G. E. (2006). Trabecular bone ontogeny in the human proximal femur. *Journal of Human Evolution*, *51*, 591-602.

Saers, J. P., Ryan, T. M., & Stock, J. T. (2020). Baby steps towards linking calcaneal trabecular bone ontogeny and the development of bipedal human gait. *Journal of Anatomy*, *236*, 474-492.

Said-Mohamed, R., Pettifor, J. M., & Norris, S. A. (2018). Life History theory hypotheses on child growth: Potential implications for short and long-term child growth, development and health. *American Journal of Physical Anthropology*, *165*, 4-19.

Salam, R. A., Das, J. K., & Bhutta, Z. A. (2014). Impact of intrauterine growth restriction on long-term health. *Current Opinion in Clinical Nutrition & Metabolic Care*, *17*, 249-254.

Sandberg, P. A., Sponheimer, M., Lee-Thorp, J., & Van Gerven, D. (2014). Intra-tooth stable isotope analysis of dentine: A step toward addressing selective mortality in

the reconstruction of life history in the archaeological record. *American Journal of Physical Anthropology*, *155*, 281-293.

Sankar, M. J., Sinha, B., Chowdhury, R., Bhandari, N., Taneja, S., Martines, J., & Bahl, R. (2015). Optimal breastfeeding practices and infant and child mortality: a systematic review and meta-analysis. *Acta Paediatrica*, *104*, 3-13.

Saunders, S. (2008). Juvenile skeletons and growth-related studies. In M. A. Katzenberg, & S. R. Saunders (Eds.), *Biological Anthropology of the Human Skeleton* (Second Edition) (pp. 117–147). Hoboken: John Wiley & Sons, Inc.

Saunders, S., Crubezy, E., & Zammit, J. (1994). A report on the sub-adult skeletal sample from the St. Etienne Cathedral cemetery site, Toulouse, France. Unpublished manuscript, McMaster University.

Saunders, S., Hoppa, R., & Southern, R. (1993). Diaphyseal growth in a nineteenth century skeletal sample of subadults from St Thomas' Church, Belleville, Ontario. *International Journal of Osteoarchaeology*, *3*, 265-281.

Seckler, D. (1980). "Malnutrition": An Intellectual Odyssey. *Western Journal of Agricultural Economics*, *5*, 219-227.

Scheuer, L., & Black, S. (2000). *Developmental Juvenile Osteology*. London: Elsevier Academic Press.

Scheuer, L., & Black, S. (2004). *The Juvenile Skeleton*. London: Elsevier Academic Press.

Schillaci, M. A., Nikitovic, D., Akins, N. J., Tripp, L., & Palkovich, A. M. (2011). Infant and juvenile growth in ancestral Pueblo Indians. *American Journal of Physical Anthropology*, *145*, 318-326.

Schillaci, M. A., Sachdev, H. P. S., & Bhargava, S. K. (2012). Comparison of the Maresh Reference Data with the WHO International Standard for normal growth in healthy children. *American Journal of Physical Anthropology*, *147*, 493-498.

Schindelin, J., Arganda-Carreras, I., Frise, E., Kaynig, V., Longair, M., Pietzsch, T., ... & Cardona, A. (2012). Fiji: an open-source platform for biological-image analysis. *Nature Methods*, *9*, 676-682.

Schlemmer, U., Frølich, W., Prieto, R. M., & Grases, F. (2009). Phytate in foods and significance for humans: food sources, intake, processing, bioavailability, protective role and analysis. *Molecular Nutrition & Food Research*, *53*, S330-S375.

Shang, Y. U., Tang, L. H., Zhou, S. S., Chen, Y. D., Yang, Y. C., & Lin, S. X. (2010). Stunting and soil-transmitted-helminth infections among school-age pupils in rural areas of southern China. *Parasites & Vectors*, *3*, 1-6.

Sharma, D., Shastri, S., & Sharma, P. (2016). Intrauterine growth restriction: antenatal and postnatal aspects. *Clinical Medicine Insights: Pediatrics*, *10*, CMPed-S40070.

Shaw, C. N., & Stock, J. T. (2009). Intensity, repetitiveness, and directionality of habitual adolescent mobility patterns influence the tibial diaphysis morphology of athletes. *American Journal of Physical Anthropology*, *140*, 149-159.

Shaw, C. N., & Stock, J. T. (2011). The influence of body proportions on femoral and tibial midshaft shape in hunter-gatherers. *American Journal of Physical Anthropology*, *144*, 22-29.

Sims, N. A., & Martin, T. J. (2014). Coupling the activities of bone formation and resorption: a multitude of signals within the basic multicellular unit. *BoneKEy Reports*, *3*, 1-10.

Slavin, P. (2010). Crusaders in Crisis: Towards the Re-assessment of the Origins and Nature of the" People's Crusade" of 1095-1096. *Imago Temporis: Medium Aevum*, *2010*, 175-199.

Smith, S. L., & Buschang, P. H. (2004). Variation in longitudinal diaphyseal long bone growth in children three to ten years of age. *American Journal of Human Biology*, *16*, 648-657.

Snoddy, A. M. E., Buckley, H. R., & Halcrow, S. E. (2016). More than metabolic: considering the broader paleoepidemiological impact of vitamin D deficiency in bioarchaeology. *American Journal of Physical Anthropology*, *160*, 183-196.

Snoddy, A. M. E., Halcrow, S. E., Buckley, H. R., Standen, V. G., & Arriaza, B. T. (2017). Scurvy at the agricultural transition in the Atacama desert (ca 3600–3200 BP): nutritional stress at the maternal-foetal interface? *International Journal of Paleopathology*, *18*, 108-120.

Spear, B. A. (2002). Adolescent growth and development. *Journal of the Academy of Nutrition and Dietetics*, *102*, S23-S29.

Spiller, L. R., Kellogg, N. D., Mercado-Deane, M. G., Zarka, A. I., & Gelfond, J. A. (2020). Growth recovery lines: a specific indicator of child abuse and neglect? *Pediatric Radiology*, *50*, 207-215.

Stinson, S. (2000). Growth variation: biological and cultural factors. In S. Stinson, B. Bogin, R. Huss-Ashmore, & D. O'Rourke (Eds.), *Human Biology: An Evolutionary and Biocultural Perspective* (p. 425-464). New York: Wiley-Liss.

Stock, J. T., & Macintosh, A. A. (2016). Lower limb biomechanics and habitual mobility among mid-Holocene populations of the Cis-Baikal. *Quaternary International*, *405*, 200-209.

Sumner, D. R., & Andriacchi, T. P. (1996). Adaptation to differential loading: comparison of growth-related changes in cross-sectional properties of the human femur and humerus. *Bone*, *19*, 121-126.

Sundh, D., Mellström, D., Ljunggren, Ö., Karlsson, M. K., Ohlsson, C., Nilsson, M., ... & Lorentzon, M. (2016). Low serum vitamin D is associated with higher cortical porosity in elderly men. *Journal of Internal Medicine*, *280*, 496-508.

Sutherland, D. H., Olshen, R. I. C. H. A. R. D., Cooper, L., & Woo, S. L. (1980). The development of mature gait. *Journal of Bone and Joint Surgery American Volume*, *62*, 336-353.

Swan, K. R., Ives, R., Wilson, L. A., & Humphrey, L. T. (2020). Ontogenetic changes in femoral cross-sectional geometry during childhood locomotor development. *American Journal of Physical Anthropology*, *173*, 80-95.

Szulc, P., Seeman, E., & Delmas, P. D. (2000). Biochemical measurements of bone turnover in children and adolescents. *Osteoporosis International*, *11*, 281-294.

Teele, R. L., Abbott, G. D., Mogridge, N., & Teele, D. W. (1999). Femoral growth lines: bony birthmarks in infants. *AJR. American Journal of Roentgenology*, *173*, 719-722.

Telmon, N., Rougé, D., Brugne, J. F., Sevin, A., Larrouy, G., & Arbus, L. (1993). Critères ostéoscopiques d'exploration du vieillissement. L'exemple de la nécropole médiévale de Saint-Étienne de Toulouse. *Bulletins et Mémoires de la Société d'Anthropologie de Paris*, *5*, 293-300.

Temple, D. H. (2008). What can variation in stature reveal about environmental differences between prehistoric Jomon foragers? Understanding the impact of systemic stress on developmental stability. *American Journal of Human Biology*, *20*, 431-439.

Temple, D. H. (2018). Exploring linear enamel hypoplasia as an embodied indicator product of childhood stress among Late/Final Jomon period foragers. In S. C. Agarwal, & P. Beauchesne (Eds.), *Children and Childhood in the Past* (p. 239–261). Gainesville: University Press of Florida.

Thacher, T. D., Aliu, O., Griffin, I. J., Pam, S. D., O'Brien, K. O., Imade, G. E., & Abrams, S. A. (2009). Meals and dephytinization affect calcium and zinc absorption in Nigerian children with rickets. *The Journal of Nutrition*, *139*, 926-932.

The GIMP Development Team. (2019). *GIMP*. Retrieved from https://www.gimp.org

Thompson, D. D. (1980). Age changes in bone mineralization, cortical thickness, and haversian canal area. *Calcified Tissue International, 31*, 5-11.

Thompson, J. W. (1959). *Economic and Social History of the Middle Ages, 300-1300*. New York: Ungar.

Timmins, S. (2016). *Subadult Growth and Rickets from a Late Roman and Merovingian Period Context in Lisieux, France*. Unpublished MA thesis in Anthropology. McMaster University: Hamilton, Ontario.

Tran, T. N. N., Forestier, C. L., Drancourt, M., Raoult, D., & Aboudharam, G. (2011). Brief communication: Co-detection of Bartonella quintana and Yersinia pestis in an 11th–15th burial site in Bondy, France. *American Journal of Physical Anthropology*, *145*, 489-494.

Tranchant, M. (2012). Risk" Culture" in Populations Using the Sea and Coast of Western France (11th-16th Centuries). *Journal of Maritime Research*, *9*, 45-60.

Trinkaus, E., & Ruff, C. B. (1996). Early modern human remains from eastern Asia: the Yamashita-cho 1 immature postcrania. *Journal of Human Evolution*, *30*, 299-314.

Turner, R. V. (1988). Eleanor of Aquitaine and her children: an inquiry into medieval family attachment. *Journal of Medieval History, 14*, 321-335.

van Gerven, D. P., Hummert, J. R., & Burr, D. B. (1985). Cortical bone maintenance and geometry of the tibia in prehistoric children from Nubia's Batn el Hajar. *American Journal of Physical Anthropology, 66*, 275-280.

Veselka, B., Brickley, M. B., D'Ortenzio, L., Kahlon, B., Hoogland, M. L., & Waters-Rist, A. L. (2019). Micro-CT assessment of dental mineralization defects indicative of vitamin D deficiency in two 17th–19th century Dutch communities. *American Journal of Physical Anthropology*, *169*, 122-131.

Victora, C. G., Bahl, R., Barros, A. J., França, G. V., Horton, S., Krasevec, J., ... & Group, T. L. B. S. (2016). Breastfeeding in the 21st century: epidemiology, mechanisms, and lifelong effect. *The Lancet*, *387*, 475-490.

Vieau, D. (2011). Perinatal nutritional programming of health and metabolic adult disease. *World Journal of Diabetes*, *2*, 133.

Vu, T. D., Wang, X. F., Wang, Q., Cusano, N. E., Irani, D., Silva, B. C., ... & Seeman, E. (2013). New insights into the effects of primary hyperparathyroidism on the cortical and trabecular compartments of bone. *Bone*, *55*, 57-63.

Walford, C. (1878). The famines of the world: past and present. *Journal of the Statistical Society of London*, *41*, 433-535.

Wall, C. E. (1991). Evidence of weaning stress and catch-up growth in the long bones of a central California Amerindian sample. *Annals of Human Biology*, *18*, 9-22.

Wallace, I. J., Tommasini, S. M., Judex, S., Garland Jr, T., & Demes, B. (2012). Genetic variations and physical activity as determinants of limb bone morphology: an experimental approach using a mouse model. *American Journal of Physical Anthropology*, *148*, 24-35.

Wang, Q., Alén, M., Nicholson, P. H., Halleen, J. M., Alatalo, S. L., Ohlsson, C., ... & Cheng, S. (2006). Differential effects of sex hormones on peri-and endocortical bone surfaces in pubertal girls. *The Journal of Clinical Endocrinology & Metabolism*, *91*, 277-282.

Wang, Q., Wang, X. F., Iuliano-Burns, S., Ghasem-Zadeh, A., Zebaze, R., & Seeman, E. (2010). Rapid growth produces transient cortical weakness: a risk factor for metaphyseal fractures during puberty. *Journal of Bone and Mineral Research*, *25*, 1521-1526.

Watts, R. (2013). Childhood development and adult longevity in an archaeological population from Barton-upon-Humber, Lincolnshire, England. *International Journal of Paleopathology*, *3*, 95-104.

Weaver, C. M., & Fuchs, R. K. (2014). Skeletal growth and development. In D. B. Burr, & M. R. Allen (Eds.), *Basic and Applied Bone Biology* (p. 245-260). New York: Academic Press.

Weemaes, C., Klasen, I., Göertz, J., Beldhuis-Valkis, M., Olafsson, O., & Haraldsson, A. (2003). Development of immunoglobulin A in infancy and childhood. *Scandinavian Journal of Immunology*, *58*, 642-648.

Welsh, H., Nelson, A. J., van der Merwe, A. E., de Boer, H. H., & Brickley, M. B. (2020). An Investigation of Micro-CT Analysis of Bone as a New Diagnostic Method forPaleopathological Cases of Osteomalacia. *International Journal of Paleopathology*, *31*, 23-33.

Wink, C. S., Elsey, R. M., & Hill, E. M. (1987). Changes in femoral robusticity and porosity during the reproductive cycle of the female alligator (Alligator mississippiensis). *Journal of Morphology*, *193*, 317-321.

Wit, J. M., & Boersma, B. (2002). Catch-up growth: definition, mechanisms, and models. *Journal of Pediatric Endocrinology and Metabolism*, *15*, 1229-1242

Wölfel, E. M., Jähn-Rickert, K., Schmidt, F. N., Wulff, B., Mushumba, H., Sroga, G. E., ... & Busse, B. (2020). Individuals with type 2 diabetes mellitus show dimorphic and heterogeneous patterns of loss in femoral bone quality. *Bone*, *140*, 115556.

Wollmann, H. A. (1998). Intrauterine growth restriction: definition and etiology. *Hormone Research in Paediatrics*, *49*, 1-6.

World Health Organization (WHO). (2009). *Infant and Young Child Feeding: Model Chapter for Textbooks for Medical Students and Allied Health Professionals*. Geneva: World Health Organization.

Zapala, M. A., Tsai, A., & Kleinman, P. K. (2016). Growth recovery lines are more common in infants at high vs. low risk for abuse. *Pediatric Radiology*, *46*, 1275-1281.

Zebaze, R. M., Ghasem-Zadeh, A., Bohte, A., Iuliano-Burns, S., Mirams, M., Price, R. I., Mackie, E. J., & Seeman, E. (2010). Intracortical remodelling and porosity in the distal radius and post-mortem femurs of women: a cross-sectional study. *The Lancet*, *375*, 1729-1736.

Zebaze, R., & Seeman, E. (2015). Cortical bone: a challenging geography. *Journal of Bone and Mineral Research*, *30*, 24-29.

Zuckerman, M. K., Kamnikar, K. R., & Mathena, S. A. (2014). Recovering the 'body politic': A relational ethics of meaning for bioarchaeology. *Cambridge Archaeological Journal*, *24*, 513-522.

Appendices

Appendix I: Ages estimates by Saunders' Research Team using Dentition and Diaphyseal Lengths*

Burial Number	Deciduous Mean Age	Permanent Mean Age	Mean Dental Age	Gen age
2	1.76	2.28	1.98	1.98
7	-	-	-	0-.25
9	0.61	-	0.61	.61
10	-	-	-	6.50
11	-	-	-	fetal
12	2.56	6.02	4.63	4.63
15	1.52	3.70	3.03	3.03
16	1.00	2.17	1.39	1.39
18	-	-	-	8.50
18a	-	-	-	0-.25
18b	-	-	-	fetal
19	6.11	5.01	5.38	5.38
23-86	6.75	6.99	6.95	6.95
23-87	-	-	-	0-.25
25	-	-	-	2.50
28	2.23	5.09	3.45	3.45
29-86	1.30	2.67	1.81	1.81
30	1.77	2.97	2.49	2.49
32	-	-	-	8.5-10.5
33	-	9.68	9.68	9.68
35	1.87	3.17	2.61	2.61
37	-	-	-	.75
40	2.11	2.92	2.60	2.60
43	1.33	2.00	1.60	1.60
45	0.40	-	0.40	.40
49	-	-	-	0-.25
53	2.16	3.86	3.41	3.41
57	1.92	3.65	2.95	2.95
60	-	-	-	0-.25
64	-	-	-	3.50
65	-	-	-	1.50
67b	0.23	-	0.23	.23

74	1.21	2.17	1.45	1.45
82-87	-	3.77	3.77	3.77
83	1.84	3.39	2.87	2.87
85	2.08	4.50	3.69	3.69
86	0.30	0.63	0.46	.46
87	2.04	2.63	2.39	2.39
87i	-	-	-	0-.25
88	6.11	8.79	8.34	8.34
89	0.48	-	0.48	.48
90	0.48	-	0.48	.48
91	-	-	-	0-.25
93	1.33	1.88	1.64	1.64
100	2.01	2.74	2.42	2.42
102	1.91	3.07	2.69	2.69
103	1.21	1.67	1.51	1.51
105	1.36	2.14	1.70	1.70
114	7.16	8.15	7.93	7.93
122	-	-	-	9.50
125	-	9.42	9.42	9.42
128	-	2.54	2.54	2.54
129b	-	-	-	0-.25
132	0.60	0.63	0.61	.61
135	-	-	-	9.50
142	-	-	-	.75
144	-	-	-	0-.25
145	-	-	-	4.50
154	-	10.62	10.62	10.62
155	3.81	5.47	5.09	5.09
158a	-	11.47	11.47	11.47
162	-	-	-	fetal
167	1.44	2.14	1.71	1.71
301	-	-	-	0-.25
302	-	-	-	3.50
304	0.65	0.63	0.65	.65
306	-	-	-	.75
307	0.23		0.23	.23
311	2.45	5.59	4.70	4.70

312	1.91	4.15	3.59	3.59
314	2.11	3.74	3.13	3.13
316	1.62	2.85	2.15	2.15
319	-	10.33	10.33	10.33
320	1.33	4.25	2.31	2.31
321	1.27	2.09	1.68	1.68
323	-	-	-	0-.25
324	1.84	2.81	2.33	2.33
325-1	1.08	1.78	1.32	1.32
326	2.15	2.57	2.38	2.38
327	1.84	3.63	2.83	2.83
329	6.88	7.75	7.46	7.46
334	-	-	-	0-.25
336	4.71	7.41	6.45	6.45
337	-	12.42	12.42	12.42
339	-	10.29	10.29	10.29
343	-	9.53	9.53	9.53
347	2.50	4.10	3.50	3.50
352	0.72	0.63	0.70	.70
357	7.76	7.87	7.84	7.84
365a	1.08	1.33	1.15	1.15
365b	-	-	-	0-.25
367	-	10.68	10.68	10.68
371	-	-	-	.75
5226	-	-	-	0-.25

**The distribution of diaphyseal lengths from the dentally aged sample were then used to create age estimates for the individuals without ageable dentition (Saunders et al., 1994).*

Appendix II: St. Étienne Femoral Lengths and Body Mass Estimations

Burial Number	Side (L or R)	Femoral Length* (cm)	Distal Metaphysis (mm)	Femoral Head Diameter (mm)	*J*	Body Mass (kg)
162	L	62.9	-	-	83.08	4.05
11	L	63.4	-	-	20.14	3.86
18b	L	62.4	-	-	52.26	3.96
67b	L	73.6	-	-	77.60	4.03
307	L	77.0	-	-	147.07	4.24
7	L	80.6	-	-	145.94	4.24
49	L	74.5	-	-	124.30	4.17
60	L	74.7	-	-	154.28	4.26
87i	L	66.0	-	-	46.03	3.94
91	Unsideable	74.0	-	-	117.60	4.15
144	L	81.2	-	-	156.89	4.27
301	L	74.6	-	-	165.51	4.30
323	L	71.1	-	-	190.24	4.37
334	L	75.0	-	-	130.95	4.19
365b	L	75.1	-	-	181.49	4.34
5226	L	73.8	-	-	144.83	4.23
18a	L	73.0	-	-	90.45	4.07
23-87	L	77.0	-	-	125.15	4.18
129b	L	75.0	-	-	157.62	4.27
45	L	92.0	-	-	276.05	4.63
86	L	136.0	-	-	1262.53	7.59
89	L	107.0	-	-	511.80	5.34
90	L	95.0	-	-	276.61	4.63
9	L	100.0	-	-	236.44	7.57
132	L	104.0	-	-	266.66	7.63
304	R	106.0	-	-	475.98	8.05
352	L	n/a	-	-	395.32	7.89
37	L	93.0	-	-	1560.59	10.22
142	L	120.0	-	-	294.30	7.69
306	L	101.0	-	-	584.53	8.27
371	L	95.0	-	-	586.29	8.27
365a	L	120.0	-	-	478.83	8.06
325-1	L	135.0	-	-	709.16	8.52
16	L	118.0	-	-	618.70	8.34

74	L	136.0	-	-	1042.26	9.18
65	L	120.0	-	-	920.45	9.94
103	L	141.0	33.4	-	-	9.10
43	L	130.0	-	-	455.96	9.01
93	L	141.0	34.99	-	-	9.53
321	L	129.0	33.27	-	-	9.07
105	L	138.0	-	-	1180.4	10.46
167	L	149.0	-	-	1160.06	10.42
29-86	R	134.0	31.53	-	-	8.60
2	L	140.0	31.96	-	-	8.71
316	L	152.0	36.6	-	-	9.97
320	R	111.0	-	-	330.99	8.76
324	L	156.0	39.88	-	-	10.86
326	L	158.0	42.67	-	-	11.61
87	L	167.0	-	-	1553.85	11.21
100	L	161.0	40.64	-	-	11.06
30	L	148.0	35.81	-	-	9.76
25	L	152.0	-	-	-	11.44
128	L	141.0	33.78	-	-	10.04
40	L	165.0	41.91	-	-	12.19
35	L	143.0	37.08	-	-	10.92
102	L	151.0	38.35	-	-	11.25
327	L	146.0	32.26	-	-	9.63
83	L	158.0	31.24	-	-	9.36
57	L	168.0	35.81	-	-	10.58
15	L	171.0	-	-	1429.88	11.93
314	L	161.0	-	-	1310.43	11.81
53	L	180.0	40.89	-	-	11.91
28	L	221.0	51.05	-	-	14.52
302	L	175.0	38.68	-	-	11.97
64	L	165.0	44.45	-	-	9.49
347	L	168.0	30.99	-	-	13.85
312	L	135.0	-	-	1044.53	12.44
85	L	165.0	38.35	-	-	11.87
82-87	L	124.0	28.70	-	-	8.76
145	R	206.0	-	-	2851.08	15.65
12	L	215.0	-	-	2359.22	15.16

311	L	209.0	-	-	2011.03	14.81
155	L	237.0	-	-	4509.92	17.31
19	L	202.0	-	-	3227.75	16.03
336	L	264.0	-	-	4998.99	19.20
10	L	243.0	-	26.42	-	21.08
23-86	L	245.0	-	23.95	-	19.86
329	L	262.0	-	27.64	-	22.46
357	L	266.0	-	-	5106.20	21.11
114	L	284.0	-	-	6267.22	22.27
88	L	270.0	-	-	6741.24	22.74
18	L	272.0	-	29.71	-	25.72
125	L	287.0	-	30.23	-	27.44
32	L	338.0	-	32.51	-	29.45
122	L	299.0	-	28.7	-	24.81
135	L	288.0	-	32.26	-	23.91
343	L	297.0	-	29.72	-	26.03
33	L	301.0	-	32.26	-	29.14
339	L	339.0	-	31.75	-	28.51
319	L	313.0	-	33.27	-	30.40
154	L	364.0	-	33.27	-	31.35
367	L	405.0	-	38.05	-	38.77
158a	L	247.0	-	32.26	-	29.86
337	L	380.0	-	35.56	-	34.80

Legend – L = Left; R = Right; J = Polar Moment of Inertia.
[*]Femoral length measurements recorded by Dr. Shelley Saunders' research team (Saunders et al., 1994).

Appendix III: Z-Score Results Femoral Length, Body Mass, and Geometric Variables

Burial Number	Z-score (FL)	Z-score (BM)	Z-score (TA)	Z-score (CA)	Z-score (MA)	Z-score (CA/MA)	Z-score (%CA)
162	-	1.79	-	-	-	-	-
11	-	1.39	-	-	-	-	-
18b	-	1.59	-	-	-	-	-
67b	-2.04	-2.59	-4.75	-3.82	-2.16	0.39	0.31
307	-1.34	-2.25	-3.08	-1.58	-2.59	4.63	2.20
7	-0.60	-1.01	-3.14	-1.29	-2.98	8.74	2.99
49	-1.86	-1.13	-3.49	-2.50	-2.12	1.56	0.92
60	-1.81	-0.97	-2.96	-1.15	-3.06	10.30	2.89
87i	-3.61	-1.55	-5.92	-4.74	-2.63	0.67	0.61
91	-1.96	-1.17	-3.57	-2.77	-1.92	0.79	0.42
144	-0.47	-0.95	-2.89	-1.32	-2.57	4.88	2.37
301	-1.84	-0.91	-2.74	-0.90	-2.96	9.19	2.95
323	-2.56	-0.77	-2.10	-1.09	-1.76	1.79	1.26
334	-1.75	-1.09	-3.10	-2.90	-1.14	-0.56	-0.78
365b	-1.73	-0.82	-2.04	-1.79	-0.95	-0.12	-0.21
5226	-2.00	-1.02	-3.05	-1.76	-2.51	3.95	1.71
18a	-2.16	-1.31	-4.37	-3.24	-2.32	1.42	1.04
23-87	-1.34	-1.13	-3.69	-1.61	-3.41	18.75	3.59
129b	-1.75	-0.95	-2.71	-1.57	-2.30	3.11	1.42
45	-1.31	-3.05	-1.77	-1.59	-1.08	-0.02	-0.12
86	5.73	0.11	4.12	1.10	3.65	-1.71	-3.37
89	-0.31	-2.66	-0.47	-2.44	1.25	-1.90	-3.74
90	-2.81	-3.52	-2.35	-4.59	1.53	-2.69	-5.68
9	-1.77	0.09	-2.82	-4.67	1.30	-2.67	-5.21
132	-0.94	0.16	-2.58	-4.50	0.69	-2.44	-5.13
304	-0.52	-0.73	-1.12	-2.12	0.01	-1.15	-2.17
352	-	-0.90	-1.69	-2.89	-0.45	-1.18	-2.84
37	-7.10	1.54	0.52	0.88	-1.49	3.49	0.64
142	-2.06	-1.11	-2.66	-3.23	-1.02	-1.27	-2.56
306	-5.61	-0.50	-1.58	-2.16	-0.43	-1.04	-1.75
371	-6.73	-0.50	-1.60	-1.96	-1.09	-0.20	-1.19
365a	-2.06	-1.56	-1.83	-2.66	-0.57	-1.23	-2.59
325-1	-2.20	-1.95	-3.11	-3.47	-1.71	-0.69	-1.58
16	-4.77	-2.09	-3.36	-4.03	-1.50	-1.39	-2.86
74	-2.05	-1.42	-1.87	-2.99	0.30	-2.00	-3.41
65	-4.47	-0.83	-1.72	-3.78	1.22	-2.76	-5.99
103	-1.29	-1.49	-2.10	-2.83	-0.59	-1.33	-2.37
43	-2.95	-1.56	-3.57	-5.26	0.45	-3.24	-7.04
93	-1.29	-1.15	-1.56	-3.03	0.91	-2.31	-4.21
321	-3.11	-1.52	-1.78	-3.03	0.21	-1.97	-3.71
105	-1.74	-0.42	-1.34	-2.64	0.82	-2.08	-3.61

167	-0.08	-0.45	-1.77	-2.27	-0.35	-1.17	-1.57
29-86	-4.44	-2.88	-4.49	-2.18	-0.38	-1.78	0.91
2	-3.61	-2.79	-4.59	-1.98	-0.56	-1.26	-0.44
316	-1.94	-1.78	-2.42	-1.25	-0.19	-1.23	-0.48
320	-8.90	-3.44	-6.23	-10.59	-0.79	-2.16	-5.52
324	-3.10	-1.81	-	-	-	-	-
326	-2.84	-1.23	-3.22	-5.35	-0.45	-1.06	-1.55
87	-1.68	-1.54	-2.11	-5.04	0.33	-1.36	-2.66
100	-2.45	-1.66	-	-	-	-	-
30	-4.13	-2.67	-4.42	-8.48	-0.28	-1.82	-4.30
25	-3.61	-1.36	-4.22	-7.05	-0.70	-1.32	-2.37
128	-5.03	-2.45	-	-	-	-	-
40	-1.94	-0.79	-3.22	-5.42	-0.59	-0.99	-1.63
35	-4.77	-1.77	-	-	-	-	-
102	-3.74	-1.51	-3.63	-7.07	0.09	-1.66	-3.29
327	-5.47	-3.29	-4.97	-7.32	-1.27	-1.46	-2.48
83	-4.07	-3.48	-4.32	-6.49	-1.06	-1.30	-2.15
57	-2.91	-2.61	-3.41	-4.48	-1.36	-0.30	-0.33
15	-2.56	-1.65	-2.83	-5.52	0.33	-1.69	-3.08
314	-3.72	-1.74	-3.21	-5.45	-0.37	-1.39	-2.37
53	-2.29	-2.31	-3.27	-4.97	-0.81	-1.12	-0.10
28	1.54	-0.51	-0.40	-1.36	0.49	-0.97	-0.08
302	-2.76	-2.27	-2.90	-4.52	-0.55	-1.17	-0.10
64	-3.69	-3.98	-	-	-	-	-
347	-3.41	-0.97	-	-	-	-	-
312	-6.50	-1.94	-4.11	-7.10	-0.45	-2.12	-0.27
85	-3.69	-2.34	-3.60	-6.17	-0.53	-1.75	-0.21
82-87	-9.25	-4.77	-	-	-	-	-
145R	-2.01	-1.01	-1.28	-4.57	0.91	-2.07	-4.34
12	-1.19	-1.30	-2.65	-3.46	-1.39	0.11	0.20
311	-1.74	-1.51	-2.87	-5.24	-0.39	-1.63	-2.64
155	-0.22	-0.62	-0.60	-1.12	-0.53	-0.05	-0.53
19	-3.97	-1.73	-2.07	-3.03	-0.47	-1.05	-1.08
336	-0.49	-1.14	-1.43	-2.88	0.39	-1.29	-1.86
10	-2.08	-0.38	-2.18	-3.76	-0.25	-1.18	-1.98
23-86	-2.68	-1.14	-3.66	-5.41	-0.39	-1.68	-2.52
329	-2.68	-0.75	-3.26	-4.41	-0.44	-0.72	-1.48
357	-2.32	-1.49	-2.94	-2.99	-1.25	0.00	-0.18
114	-1.13	-1.17	-2.07	-2.47	-0.38	-0.62	-0.70
88	-2.63	-1.30	-1.95	-3.04	0.20	-1.11	-1.53
18	-2.50	-0.52	-1.82	-2.90	0.14	-1.05	-1.50
125	-2.41	-0.76	-2.24	-4.84	0.63	-1.71	-3.01
32	0.55	-0.31	-0.95	-2.77	0.80	-1.36	-1.96
122	-1.72	-1.34	-2.10	-3.55	-0.10	-1.10	-1.37
135	-2.35	-1.54	-2.36	-3.84	-0.29	-1.05	-1.36

343	-1.83	-1.07	-2.65	-4.63	-0.08	-1.38	-2.10
33	-1.60	-0.38	-1.24	-1.67	-0.45	-0.30	-0.21
339	-0.35	-1.18	-0.38	-1.31	0.83	-1.13	-1.49
319	-1.73	-0.84	-0.56	-0.52	-0.47	-0.02	-0.02
154	0.98	-0.67	-0.41	-1.14	0.59	-0.98	-1.20
367	3.16	0.64	2.01	1.34	1.11	-0.60	-0.68
158a	-5.69	-1.30	-0.61	0.15	-1.46	2.34	1.11
337	0.26	-1.12	-1.46	-1.85	-0.02	-0.89	-1.02

Notes – Z-scores highlighted in red represent scores below -2 standard deviations from the mean. Legend – FL = Femoral Length; BM = Body Mass; TA = Total Area; CA = Cortical Area; MA = Medullary Area; CA/MA = Cortical Area/Medullary Area; %CA = Cortical Area/Total Area.

Appendix IV: Cross-Sectional Geometry Data

Burial Number	TA	CA	MA	PA	%CA	CA/MA	%pore	Imax/Imin	Ix/Iy	*J*
162	23.54	18.92	3.97	0.65	0.80	4.77	-	1.23	1.01	83.08
11	11.71	8.63	3.04	0.04	0.74	2.84	-	1.40	0.83	20.14
18b	18.48	15.83	2.20	0.45	0.86	7.21	2.76	1.32	0.77	52.26
67b	22.79	17.06	5.40	0.34	0.75	3.16	1.94	1.40	0.77	77.60
307	30.59	26.30	4.06	0.23	0.86	6.48	0.86	1.45	1.14	147.07
7	30.30	27.46	2.84	-	0.91	9.68	-		0.78	145.94
49	28.67	22.48	5.51	0.68	0.78	4.08	2.95	1.30	0.92	124.30
60	31.18	28.07	2.58	0.54	0.90	10.90	1.87	1.35	0.81	154.28
87i	17.35	13.28	3.93	0.14	0.77	3.38	-	1.66	0.61	46.03
91	28.32	21.37	6.15	0.80	0.75	3.47	3.60	1.30	0.86	117.60
144	31.47	27.36	4.10	-	0.87	6.67	-	-	0.72	156.89
301	32.16	29.08	2.90	0.19	0.90	10.03	0.65	1.44	0.72	165.51
323	35.16	28.28	6.65	0.23	0.80	4.25	0.80	1.27	0.87	190.24
334	30.49	20.85	8.61	1.04	0.68	2.42	4.75	1.29	0.83	130.95
365b	35.44	25.43	9.19	0.83	0.72	2.77	3.16	1.27	0.79	181.49
5226	30.76	25.56	4.30	0.90	0.83	5.94	3.39	1.32	0.79	144.83
18a	24.59	19.46	4.91	0.22	0.79	3.96	1.13	1.04	0.99	90.45
23-87	27.76	26.14	1.50	0.13	0.94	17.49	0.48	1.60	0.63	125.15
129b	32.33	26.31	4.98	1.05	0.81	5.29	3.83	1.16	0.87	157.62
45	43.25	31.33	10.71	1.22	0.72	2.93	3.73	1.42	0.88	276.05
86	99.25	57.94	31.86	9.45	0.58	1.82	14.02	1.26	0.93	1262.53
89	64.53	36.45	21.95	6.12	0.56	1.66	14.37	1.15	0.95	511.80
90	50.26	23.47	23.11	3.69	0.47	1.02	13.59	1.36	1.17	276.61
9	46.72	22.94	22.17	1.62	0.49	1.03	6.61	1.42	0.99	236.44
132	48.53	24.02	19.65	4.86	0.49	1.22	16.83	1.33	1.11	266.66
304	59.62	38.41	16.88	4.33	0.64	2.28	10.13	1.33	0.90	475.98
352	55.30	33.77	14.99	6.55	0.61	2.25	16.24	1.34	0.99	395.32
37	103.01	79.30	12.51	11.20	0.77	6.34	12.38	1.42	0.80	1560.59
142	49.68	26.67	16.88	6.12	0.54	1.58	18.67	1.49	0.83	294.30
306	67.79	40.37	22.33	5.09	0.60	1.81	11.20	1.34	0.90	584.53
371	67.53	42.95	16.20	8.38	0.64	2.65	16.33	1.12	1.01	586.29
365a	63.56	33.97	21.01	8.58	0.53	1.62	20.17	1.32	0.90	478.83
325-1	71.82	48.31	19.72	3.79	0.67	2.45	7.28	1.20	0.91	709.16
16	68.34	42.44	20.99	4.91	0.62	2.02	10.37	1.35	0.75	618.70

74	88.92	53.25	32.25	3.41	0.60	1.65	6.02	1.39	0.86	1042.26
65	90.93	45.04	38.01	7.89	0.50	1.18	14.90	1.34	0.89	920.45
103	85.76	54.97	26.69	4.10	0.64	2.06	6.95	1.28	0.92	1001.35
43	65.42	29.64	33.18	2.60	0.45	0.89	8.07	1.19	1.07	455.96
93	93.19	52.81	36.08	4.31	0.57	1.46	7.54	1.10	1.08	1081.03
321	90.11	52.87	31.67	5.56	0.59	1.67	9.52	1.38	1.07	1036.48
105	96.28	56.90	35.50	3.88	0.59	1.60	6.39	1.23	0.92	1180.30
167	90.38	60.80	28.18	1.40	0.67	2.16	2.24	1.37	0.86	1160.06
29-86	68.30	35.72	31.10	1.47	0.52	1.15	-	1.38	1.09	573.42
2	66.81	40.55	25.82	0.44	0.61	1.57	-	1.21	0.93	595.27
316	97.45	58.54	36.74	2.18	0.60	1.59	3.59	1.36	0.81	1266.74
320	57.45	22.97	32.92	1.56	0.40	0.70	6.37	1.40	1.01	330.99
324	-	-	-	-	-	-	-	-	-	-
326	98.66	61.55	36.74	0.38	0.62	1.68	-	1.19	0.85	1331.84
87	113.85	63.90	45.40	4.55	0.56	1.41	6.65	1.15	0.96	1553.85
100	-	-	-	-	-	-	-	-	-	-
30	82.26	38.52	38.65	5.09	0.47	1.00	11.68	1.22	1.09	757.72
25	84.90	49.02	33.96	1.92	0.58	1.44		1.22	1.02	941.27
128	-	-	-	-	-	-	-	-	-	-
40	98.64	61.08	35.19	2.37	0.62	1.74	3.73	1.12	0.92	1316.42
35	-	-	-	-	-	-	-	-	-	-
102	93.02	48.90	42.76	1.36	0.53	1.14	-	1.27	1.24	1071.83
327	71.00	40.61	29.71	0.68	0.57	1.37	-	1.30	1.00	658.27
83	81.89	48.32	32.29	1.27	0.59	1.50	2.57	1.40	0.82	868.74
57	96.90	67.01	28.67	1.23	0.69	2.34	1.80	1.15	0.91	1346.95
15	106.58	57.39	49.10	0.09	0.54	1.17	-	1.33	0.75	1429.88
314	100.28	57.96	40.69	1.64	0.58	1.42	-	1.29	0.87	1310.43
53	107.74	68.54	37.88	1.32	0.64	1.81	-	1.33	0.80	1603.87
28	156.65	102.68	53.84	0.13	0.66	1.91	-	1.31	1.27	3480.46
302	114.05	72.76	41.02	0.27	0.64	1.77	-	1.07	1.03	1796.29
347	-	-	-	-	-	-	-	-	-	-
64	-	-	-	-	-	-	-	-	-	-
312	93.52	48.31	42.28	2.94	0.52	1.14	-	1.06	1.03	1044.53
85	102.27	57.17	41.24	3.86	0.56	1.39	-	1.23	0.88	1340.61
82-87	-	-	-	-	-		-	-	-	-
145R	156.23	79.05	66.60	10.58	0.51	1.19	-	1.16	1.16	2851.08
12	127.16	91.18	35.29	0.69	0.72	2.58	-	1.16	0.87	2359.22

311	122.70	71.79	48.92	2.00	0.59	1.47	-	1.50	0.69	2011.03
155	179.91	122.17	49.64	8.11	0.68	2.46	-	1.09	0.91	4509.92
19	150.49	101.85	48.64		0.68	2.09	-		1.03	3227.75
336	189.65	121.28	67.91	0.46	0.64	1.79	-	1.38	1.28	4998.99
10	169.78	107.50	57.14	5.14	0.63	1.88	-	1.09	1.06	3924.22
23-86	140.42	82.78	57.13	0.51	0.59	1.45	-	1.30	1.23	2632.32
329	164.56	107.91	55.84	0.81	0.66	1.93	-	1.33	1.32	3794.53
357	186.47	135.11	45.55	5.81	0.72	2.97	-	1.47	0.70	5106.20
114	208.27	144.69	62.12	1.45	0.69	2.33	-	1.15	0.96	6267.22
88	218.18	142.43	74.91	0.84	0.65	1.90	-	1.30	1.14	6741.24
18	221.82	145.21	73.73	2.88	0.65	1.97	-	1.24	1.20	6854.22
125	222.21	118.91	100.28	3.02	0.54	1.19	-	1.07	0.93	6029.38
32	269.71	163.11	105.01	1.59	0.60	1.55	-	1.22	1.19	9922.78
122	227.33	146.32	79.57	1.44	0.64	1.84	-	1.21	1.09	7157.66
135	217.60	140.23	74.23	3.15	0.64	1.89	-	1.14	0.88	6554.24
343	207.01	123.30	80.18	3.53	0.60	1.54	-	1.31	1.26	5734.47
33	259.00	186.58	69.53	2.89	0.72	2.68	-	1.05	1.00	9864.89
339	315.75	201.76	111.19	2.80	0.64	1.81	-	1.10	1.08	13742.62
319	308.43	227.44	74.09	6.90	0.74	3.07	-	1.05	1.05	13836.77
154	314.50	207.07	104.26	3.17	0.66	1.99	-	1.29	1.10	14005.77
367	415.19	287.74	119.32	8.13	0.69	2.41	-	1.57	0.82	24987.64
158a	336.51	275.11	46.68	14.72	0.82	5.89	-	1.22	1.10	17232.35
337	318.77	218.21	98.61	1.94	0.68	2.21	-	1.19	1.19	14726.47

Legend – TA= Total Area; CA= Cortical Area; MA= Medullary Area; PA = Pore Area; %pore= Pore Area/Cortical Area; CA/MA= Cortical Area/Medually Area; I_{max}/I_{min} = Maximum polar moment of Area/Minimum Polar moment of area; I_x/I_y= Polar moment of area about the mediolateral axis/Polar area about the Anteroposterior axis; J= I_x+I_y; %CA= Cortical Area/Total Area

Appendix V: Harris Line Presence/Absence Results

Burial Number	Harris Lines Present (P) or Absent (A)	Number of total observed Harris Lines
162	A	0
11	A	0
18b	A	0
67b	A	0
307	A	0
7	A	0
49	A	0
60	A	0
87i	A	0
91	A	0
144	A	0
301	A	0
323	A	0
334	A	0
365b	A	0
5226	A	0
18a	A	0
23-87	A	0
129b	A	0
45	A	0
86	A	0
89	A	0
90	A	0
9	n/a	-
132	A	0
304	A	0
352	A	0
37	A	0
142	A	0
306	A	0
371	A	0
365a	A	0
325-1	P	2
16	A	0

74	A	0
65	n/a	-
103	P	2
43	n/a	-
93	P	1
321	A	0
105	A	0
167	P	4
29-86	P	4
2	P	2
316	P	5
320	A	0
324	P	3
326	P	6
87	n/a	-
100	P	2
30	P	1
25	P	2
128	P	2
40	P	2
35	P	2
102	P	7
327	P	8
83	P	10
57	A	0
15	P	3
314	n/a	0
53	A	0
28	A	0
64	A	0
302	P	5
347	P	4
312	n/a	-
85	A	0
82-87	A	0
145	A	0
12	P	7

311	P	10
155	P	1
19	A	0
336	P	10
10	n/a	-
23-86	P	1
329	A	0
357	A	0
114	P	1
88	A	0
18	n/a	-
125	A	0
32	A	0
122	P	1
135	A	0
343	P	7
33	A	0
339	P	4
319	A	0
154	n/a	0
367	A	0
158a	A	0
337	P	1

Appendix VI: Harris Line Age-at-Formation Results using the Kulus et al. (Submitted Manuscript) Estimation Tool

Burial Number	FL (cm)	HL Distance from Diaphyseal End (cm)	Distal (D) or Proximal (P)	Age of individual (2-17 years)	Percent (%) of bone growth at HL formation	Percent (%) of "would-be-adult" bone	Estimated age-at-formation (years)
2	14	0.74	D	2	92.44	35.92	1.71
2	14	0.53	D	2	94.56	36.74	1.82
12	21.5	5.72	D	5	61.96	35.59	1.67
12	21.5	5.18	D	5	65.54	37.65	1.94
12	21.5	4.65	D	5	69.08	39.69	2.22
12	21.5	4.22	D	5	71.96	41.34	2.45
12	21.5	3.94	D	5	73.81	42.41	2.60
12	21.5	3.48	D	5	76.86	44.15	2.86
12	21.5	0.91	D	5	93.92	53.96	4.41
15	17.1	4.14	D	3	65.38	29.41	0.90
15	17.1	2.99	D	3	75.00	33.74	1.43
15	17.1	0.79	D	3	93.42	42.03	2.55
25	15.2	0.58	D	3	94.50	42.52	2.62
25	15.2	0.46	D	3	95.70	43.05	2.70
30	14.8	0.69	D	2	93.37	36.29	1.76
35	14.3	0.86	D	3	91.36	41.10	2.42
35	14.3	0.58	D	3	94.16	42.36	2.60
40	16.5	0.61	D	3	94.72	42.61	2.63
40	16.5	0.46	D	3	96.04	43.21	2.72
83	15.8	3.99	D	3	63.91	28.75	0.82
83	15.8	2.11	D	3	80.92	36.41	1.78
83	15.8	1.83	D	3	83.45	37.54	1.93
83	15.8	1.60	D	3	85.52	38.47	2.05
83	15.8	1.30	D	3	88.28	39.72	2.22
83	15.8	1.19	D	3	89.20	40.13	2.28
83	15.8	1.07	D	3	90.34	40.65	2.35
83	15.8	0.91	D	3	91.72	41.27	2.44
83	15.8	0.71	D	3	93.56	42.09	2.56
83	15.8	0.53	D	3	95.17	42.82	2.66
93	14.1	0.81	D	2	91.76	35.66	1.68
100	16.1	0.99	D	2	91.20	35.44	1.65
100	16.1	0.86	D	2	92.33	35.88	1.71

102	15.1	4.55	D	3	56.95	25.62	0.45
102	15.1	3.51	D	3	66.81	30.06	0.97
102	15.1	1.83	D	3	82.68	37.20	1.88
102	15.1	1.04	D	3	90.14	40.55	2.34
102	15.1	0.89	D	3	91.58	41.20	2.43
102	15.1	0.66	D	3	93.75	42.18	2.57
102	15.1	0.51	D	3	95.19	42.83	2.67
103	14.1	1.57	D	2	84.03	32.65	1.29
103	14.1	1.37	D	2	86.09	33.45	1.39
114	28.4	0.41	D	8	97.94	70.89	7.65
122	29.9	0.61	D	10	97.08	78.47	9.37
128	14.1	1.24	D	3	87.38	39.31	2.17
128	14.1	0.58	D	3	94.08	42.32	2.59
155	23.7	1.04	D	5	93.72	53.84	4.39
167	14.9	1.50	D	2	85.61	33.27	1.37
167	14.9	1.19	D	2	88.54	34.41	1.52
167	14.9	0.74	D	2	92.93	36.11	1.74
167	14.9	0.61	D	2	94.15	36.59	1.80
302	17.5	1.83	D	4	85.06	43.10	2.70
302	17.5	1.40	D	4	88.58	44.89	2.97
302	17.5	1.04	D	4	91.49	46.36	3.19
302	17.5	0.76	D	4	93.77	47.51	3.37
302	17.5	0.48	D	4	96.06	48.67	3.55
311	20.9	5.99	D	5	58.99	33.89	1.45
311	20.9	4.29	D	5	70.63	40.58	2.34
311	20.9	3.76	D	5	74.28	42.67	2.64
311	20.9	3.33	D	5	77.23	44.37	2.89
311	20.9	2.72	D	5	81.40	46.77	3.25
311	20.9	1.47	D	5	89.92	51.66	4.03
311	20.9	1.24	D	5	91.48	52.56	4.18
311	20.9	0.97	D	5	93.40	53.66	4.36
311	20.9	0.66	D	5	95.48	54.85	4.56
311	20.9	0.51	D	5	96.52	55.45	4.67
316	15.1	1.19	D	2	88.73	34.48	1.53
316	15.1	1.04	D	2	90.15	35.03	1.60
316	15.1	0.81	D	2	92.30	35.87	1.71
316	15.1	0.64	D	2	93.99	36.52	1.79

316	15.1	0.53	D	2	94.95	36.90	1.84
324	15.6	1.98	D	2	81.84	31.80	1.19
324	15.6	0.99	D	2	90.92	35.33	1.64
324	15.6	0.64	D	2	94.17	36.59	1.80
326	15.8	1.80	D	2	83.68	32.52	1.28
326	15.8	1.47	D	2	86.67	33.68	1.42
326	15.8	0.94	D	2	91.49	35.55	1.66
326	15.8	0.84	D	2	92.41	35.91	1.71
326	15.8	0.79	D	2	92.87	36.09	1.73
326	15.8	0.66	D	2	94.02	36.54	1.79
327	14.6	3.99	D	3	60.94	27.42	0.66
327	14.6	3.28	D	3	67.91	30.55	1.03
327	14.6	1.93	D	3	81.09	36.48	1.79
327	14.6	1.42	D	3	86.07	38.72	2.09
327	14.6	1.17	D	3	88.56	39.84	2.24
327	14.6	0.97	D	3	90.55	40.74	2.37
327	14.6	0.79	D	3	92.29	41.52	2.48
327	14.6	0.53	D	3	94.78	42.64	2.64
336	26.4	9.66	D	6	47.66	29.73	0.93
336	26.4	9.02	D	6	51.16	31.91	1.20
336	26.4	8.15	D	6	55.84	34.83	1.57
336	26.4	7.29	D	6	60.51	37.75	1.96
336	26.4	6.53	D	6	64.64	40.32	2.31
336	26.4	2.74	D	6	85.14	53.11	4.27
336	26.4	2.54	D	6	86.24	53.80	4.38
336	26.4	1.75	D	6	90.51	56.46	4.84
336	26.4	0.97	D	6	94.77	59.12	5.32
336	26.4	0.74	D	6	96.01	59.89	5.46
337	38	5.92	D	12	77.73	69.35	7.32
339	33.9	5.46	D	10	76.96	62.21	5.89
339	33.9	5.00	D	10	78.89	63.77	6.19
339	33.9	3.91	D	10	83.50	67.49	6.94
339	33.9	1.75	D	10	92.61	74.85	8.53
343	29.7	4.27	D	10	79.43	64.20	6.28
343	29.7	2.18	D	10	89.48	72.33	7.96
343	29.7	2.01	D	10	90.34	73.02	8.12
343	29.7	1.07	D	10	94.86	76.68	8.95

343	29.7	0.86	D	10	95.84	77.47	9.13
343	29.7	0.64	D	10	96.94	78.36	9.35
343	29.7	0.48	D	10	97.68	78.95	9.49
347	16.8	3.58	D	4	69.52	35.22	1.62
347	16.8	2.67	D	4	77.30	39.17	2.15
347	16.8	1.07	D	4	90.92	46.07	3.15
347	16.8	0.86	D	4	92.65	46.95	3.28
23-86	24.5	1.07	D	7	93.75	63.00	6.05
29-86	13.4	1.52	D	2	83.74	32.54	1.28
29-87	13.4	1.27	D	2	86.45	33.59	1.41
29-88	13.4	0.79	D	2	91.60	35.59	1.67
29-89	13.4	0.70	D	2	92.57	35.97	1.72
325-1	13.5	3.43	D	2	63.68	24.75	0.35
325-2	13.5	1.91	D	2	79.82	31.02	1.09*

Legend – FL = Femoral Length; HL = Harris Line

*This HL was placed in the 0-1 age at formation category as it was overestimated due to BN-325-1 being estimated to 1.31 years of age.